TR CISPR 18-1

Edition 2.0 2010-06

TECHNICAL REPORT

INTERNATIONAL SPECIAL COMMITTEE ON RADIO INTERFERENCE

Radio interference characteristics of overhead power lines and high-voltage equipment –
Part 1: Description of phenomena

Copyrighted material licensed to BR Demo by Thomson Reuters (Scientific), Inc., subscriptions.techstreet.com, downloaded on Nov-28-2014 by James Madison. No further reproduction or distribution is permitted. Uncontrolled when print

THIS PUBLICATION IS COPYRIGHT PROTECTED

Copyright © 2010 IEC, Geneva, Switzerland

All rights reserved. Unless otherwise specified, no part of this publication may be reproduced or utilized in any form or by any means, electronic or mechanical, including photocopying and microfilm, without permission in writing from either IEC or IEC's member National Committee in the country of the requester.

If you have any questions about IEC copyright or have an enquiry about obtaining additional rights to this publication, please contact the address below or your local IEC member National Committee for further information.

IEC Central Office
3, rue de Varembé
CH-1211 Geneva 20
Switzerland
Email: inmail@iec.ch
Web: www.iec.ch

About the IEC

The International Electrotechnical Commission (IEC) is the leading global organization that prepares and publishes International Standards for all electrical, electronic and related technologies.

About IEC publications

The technical content of IEC publications is kept under constant review by the IEC. Please make sure that you have the latest edition, a corrigenda or an amendment might have been published.

- Catalogue of IEC publications: www.iec.ch/searchpub

The IEC on-line Catalogue enables you to search by a variety of criteria (reference number, text, technical committee,…). It also gives information on projects, withdrawn and replaced publications.

- IEC Just Published: www.iec.ch/online_news/justpub

Stay up to date on all new IEC publications. Just Published details twice a month all new publications released. Available on-line and also by email.

- Electropedia: www.electropedia.org

The world's leading online dictionary of electronic and electrical terms containing more than 20 000 terms and definitions in English and French, with equivalent terms in additional languages. Also known as the International Electrotechnical Vocabulary online.

- Customer Service Centre: www.iec.ch/webstore/custserv

If you wish to give us your feedback on this publication or need further assistance, please visit the Customer Service Centre FAQ or contact us:

Email: csc@iec.ch
Tel.: +41 22 919 02 11
Fax: +41 22 919 03 00

Copyrighted material licensed to BR Demo by Thomson Reuters (Scientific), Inc., subscriptions.techstreet.com, downloaded on Nov-28-2014 by James Madison. No further reproduction or distribution is permitted. Uncontrolled when print

TR CISPR 18-1

Edition 2.0 2010-06

TECHNICAL REPORT

INTERNATIONAL SPECIAL COMMITTEE ON RADIO INTERFERENCE

Radio interference characteristics of overhead power lines and high-voltage equipment –
Part 1: Description of phenomena

INTERNATIONAL
ELECTROTECHNICAL
COMMISSION

PRICE CODE XB

ICS 33.100.01

ISBN 978-2-88912-016-1

® Registered trademark of the International Electrotechnical Commission

Copyrighted material licensed to BR Demo by Thomson Reuters (Scientific), Inc., subscriptions.techstreet.com, downloaded on Nov-28-2014 by James Madison. No further reproduction or distribution is permitted. Uncontrolled when print

CONTENTS

FOREWORD 5
INTRODUCTION 7
1 Scope 8
2 Normative references 8
3 Terms and definitions 8
4 Radio noise from power lines 9
4.1 General 9
4.2 Physical aspects of radio noise 9
4.2.1 Mechanism of formation of a noise field 9
4.2.2 Definition of noise 12
4.2.3 Influence of external parameters 12
4.3 Main characteristics of the noise field resulting from conductor corona 13
4.3.1 General 13
4.3.2 Frequency spectrum 13
4.3.3 Lateral profile 14
4.3.4 Statistical distribution with varying seasons and weather conditions 16
5 Effects of corona from conductors 17
5.1 Physical aspects of corona from conductors 17
5.1.1 General 17
5.1.2 Factors in corona generation 17
5.2 Methods of investigation of corona by cages and test lines 19
5.2.1 General 19
5.2.2 Test cages 19
5.2.3 Test lines 20
5.3 Methods of predetermination 20
5.3.1 General 20
5.3.2 Analytical methods 20
5.3.3 CIGRÉ method 21
5.4 Catalogue of standard profiles 21
5.4.1 General 21
5.4.2 Principle of catalogue presentation 21
6 Radio noise levels due to insulators, hardware and substation equipment (excluding bad contacts) 23
6.1 Physical aspects of radio noise sources 23
6.1.1 General 23
6.1.2 Radio noise due to corona discharges at hardware 23
6.1.3 Radio noise due to insulators 23
6.2 Correlation between radio noise voltage and the corresponding field strength for distributed and individual sources 25
6.2.1 General 25
6.2.2 Semi-empirical approach and formula 25
6.2.3 Analytical methods 27
6.2.4 Example of application 28
6.3 Influence of ambient conditions 28
7 Sparking due to bad contacts 28
7.1 Physical aspects of the radio noise phenomenon 28

Copyrighted material licensed to BR Demo by Thomson Reuters (Scientific), Inc., subscriptions.techstreet.com, downloaded on Nov-28-2014 by James Madison. No further reproduction or distribution is permitted. Uncontrolled when print

7.2 Example of gap sources 29
8 Special d.c. effects 30
8.1 General 30
8.2 Effects of corona from conductors 30
8.3 Radio noise due to insulators, hardware and substation equipment 34
8.4 Valve firing effects 34
9 Figures 36
Annex A (informative) Calculation of the voltage gradient at the surface of a conductor of an overhead line 46
Annex B (informative) Catalogue of profiles of radio noise field due to conductor corona for certain types of power line 50
Annex C (informative) Summary of the catalogue of radio noise profiles according to the recommendations of the CISPR 66
Bibliography 68

Figure 1 – Typical lateral attenuation curves for high voltage lines, normalized to a lateral distance of y_0 = 15 m, distance in linear scale 36
Figure 2 – Typical lateral attenuation curves for high voltage lines, normalized to a direct distance of D_0 = 20 m, distance in logarithmic scale 37
Figure 3 – Examples of statistical yearly distributions of radio-noise levels recorded continuously under various overhead lines 38
Figure 4 – Examples of statistical yearly distributions of radio-noise levels recorded continuously under various overhead lines 39
Figure 5 – Example of statistical yearly distributions of radio-noise levels recorded continuously under various overhead lines 40
Figure 6 – Examples of statistical yearly distributions of radio-noise levels recorded continuously under various overhead lines 41
Figure 7 – Equipotential lines for clean and dry insulation units 42
Figure 8 – Determination of the magnetic field strength from a perpendicular to a section of a line, at a distance *x* from the point of injection of noise current *I* 43
Figure 9 – Longitudinal noise attenuation versus distance from noise source (from test results of various experiments frequencies around 0,5 MHz) 43
Figure 10 – Lateral profile of the radio noise field strength produced by distributed discrete sources on a 420 kV line of infinite length 44
Figure 11 – Example of relative strength of radio noise field as a function of frequency 45
Figure 12 – Example of relative strength of radio noise field as a function of the distance from the line 45
Figure B.1 – Triangular formation (1) 51
Figure B.2 – Triangular formation (2) 52
Figure B.3 – Flat formation 53
Figure B.4 – Arched formation 54
Figure B.5 – Flat wide formation 55
Figure B.6 – Vertical formation (480 (Rail) X 4B) 56
Figure B.7 – Flat formation 57
Figure B.8 – Flat formation 58
Figure B.9 – Arched formation 59
Figure B.10 – Flat formation 60
Figure B.11 – Arched formation 61

Copyrighted material licensed to BR Demo by Thomson Reuters (Scientific), Inc., subscriptions.techstreet.com, downloaded on Nov-28-2014 by James Madison. No further reproduction or distribution is permitted. Uncontrolled when print

Figure B.12 – Flat formation 62
Figure B.13 – Vertical formation (480 (Cardinal) X 6B) 63
Figure B.14 – Typical frequency spectra for the radio noise fields of high voltage power lines 64
Figure B.15 – Prediction of radio noise level of a transmission line for various types of weather 65
Figure C.1 – Examples of transformations of the profiles of Figures B.1 to B.13 using the direct distance of 20 m as reference 67

Table B.1 – List of profiles 50

Copyrighted material licensed to BR Demo by Thomson Reuters (Scientific), Inc., subscriptions.techstreet.com, downloaded on Nov-28-2014 by James Madison. No further reproduction or distribution is permitted. Uncontrolled when print

INTERNATIONAL ELECTROTECHNICAL COMMISSION
INTERNATIONAL SPECIAL COMMITTEE ON RADIO INTERFERENCE

RADIO INTERFERENCE CHARACTERISTICS OF OVERHEAD POWER LINES AND HIGH-VOLTAGE EQUIPMENT –

Part 1: Description of phenomena

FOREWORD

1) The International Electrotechnical Commission (IEC) is a worldwide organization for standardization comprising all national electrotechnical committees (IEC National Committees). The object of IEC is to promote international co-operation on all questions concerning standardization in the electrical and electronic fields. To this end and in addition to other activities, IEC publishes International Standards, Technical Specifications, Technical Reports, Publicly Available Specifications (PAS) and Guides (hereafter referred to as "IEC Publication(s)"). Their preparation is entrusted to technical committees; any IEC National Committee interested in the subject dealt with may participate in this preparatory work. International, governmental and non-governmental organizations liaising with the IEC also participate in this preparation. IEC collaborates closely with the International Organization for Standardization (ISO) in accordance with conditions determined by agreement between the two organizations.
2) The formal decisions or agreements of IEC on technical matters express, as nearly as possible, an international consensus of opinion on the relevant subjects since each technical committee has representation from all interested IEC National Committees.
3) IEC Publications have the form of recommendations for international use and are accepted by IEC National Committees in that sense. While all reasonable efforts are made to ensure that the technical content of IEC Publications is accurate, IEC cannot be held responsible for the way in which they are used or for any misinterpretation by any end user.
4) In order to promote international uniformity, IEC National Committees undertake to apply IEC Publications transparently to the maximum extent possible in their national and regional publications. Any divergence between any IEC Publication and the corresponding national or regional publication shall be clearly indicated in the latter.
5) IEC itself does not provide any attestation of conformity. Independent certification bodies provide conformity assessment services and, in some areas, access to IEC marks of conformity. IEC is not responsible for any services carried out by independent certification bodies.
6) All users should ensure that they have the latest edition of this publication.
7) No liability shall attach to IEC or its directors, employees, servants or agents including individual experts and members of its technical committees and IEC National Committees for any personal injury, property damage or other damage of any nature whatsoever, whether direct or indirect, or for costs (including legal fees) and expenses arising out of the publication, use of, or reliance upon, this IEC Publication or any other IEC Publications.
8) Attention is drawn to the Normative references cited in this publication. Use of the referenced publications is indispensable for the correct application of this publication.
9) Attention is drawn to the possibility that some of the elements of this IEC Publication may be the subject of patent rights. IEC shall not be held responsible for identifying any or all such patent rights.

The main task of IEC technical committees is to prepare International Standards. However, a technical committee may propose the publication of a technical report when it has collected data of a different kind from that which is normally published as an International Standard, for example "state of the art".

CISPR 18-1, which is a technical report, has been prepared by CISPR subcommittee B: Interference relating to industrial, scientific and medical radio-frequency apparatus, to other (heavy) industrial equipment, to overhead power lines, to high voltage equipment and to electric traction.

This second edition cancels and replaces the first edition published in 1982. It is a technical revision.

Copyrighted material licensed to BR Demo by Thomson Reuters (Scientific), Inc., subscriptions.techstreet.com, downloaded on Nov-28-2014 by James Madison. No further reproduction or distribution is permitted. Uncontrolled when print

This edition includes the following significant technical changes with respect to the previous edition: while the first edition of CISPR 18-1 only covered the direct distance D_0 for the establishment of standard profiles for the lateral radio noise field emanating from HV overhead power lines, this second edition now also allows for use of the lateral distance y_0 for these purposes. This way it allows for the establishment of standard profiles for the lateral radio noise field also from modern HV overhead power line constructions with tall suspension towers.

The text of this technical report is based on the following documents:

DTR	Report on voting
CISPR/B/493/DTR	CISPR/B/501/RVC

Full information on the voting for the approval of this technical report can be found in the report on voting indicated in the above table.

This technical report has been drafted in accordance with the ISO/IEC Directives, Part 2.

A list of all parts of the CISPR 18 series can be found, under the general title *Radio interference characteristics of overhead power lines and high-voltage equipment*, on the IEC website.

The committee has decided that the contents of this publication will remain unchanged until the stability date indicated on the IEC web site under "http://webstore.iec.ch" in the data related to the specific publication. At this date, the publication will be

- reconfirmed,
- withdrawn,
- replaced by a revised edition, or
- amended.

A bilingual version of this publication may be issued at a later date.

Copyrighted material licensed to BR Demo by Thomson Reuters (Scientific), Inc., subscriptions.techstreet.com, downloaded on Nov-28-2014 by James Madison. No further reproduction or distribution is permitted. Uncontrolled when print

INTRODUCTION

This technical report forms the first of a three-part publication dealing with radio noise generated by electrical power transmission and distribution facilities (overhead lines and substations). It contains information in relation of the physical phenomena involved in the generation of electromagnetic noise fields. It also includes the main properties of such fields and their numerical values. Its content was adjusted such as to allow for use of the lateral distance *y* for the establishment of standard profiles for the lateral radio noise field emanating from HV overhead power lines.

The technical data given in this part 1 of the CISPR 18 series are intended to be a useful aid to overhead line designers and also to anyone concerned with checking the radio noise performance of a line to ensure satisfactory protection of wanted radio signals. The data should facilitate the use of the recommendations given in its parts 2 and 3 dealing with

– methods of measurement and procedures for determining limits, and a
– code of practice for minimizing the generation of radio noise.

The CISPR 18 series do not deal with biological effects on living matter or any issues related to exposure in electromagnetic fields.

This technical report has been prepared in order to provide information on the many factors involved in protecting the reception of radio and television broadcasting from interference due to high voltage overhead power lines and associated equipment. The information given should be of assistance when means of avoiding or abating radio noise are being considered.

Information is mainly given on the generation and characteristics of radio noise from a.c. power lines and equipment operating at 1 kV and above, in the frequency ranges 0,15 MHz to 30 MHz (a.m. sound broadcasting) and 30 MHz to 300 MHz (f.m. sound broadcasting and television broadcasting). The special aspect of spark discharges due to bad contacts is taken into account. Some information is also given on interference due to d.c. overhead lines for which corona and interference conditions are different from those of a.c. power lines.

The general procedure for establishing the limits of the radio noise from the power lines and equipment is given, together with typical values as examples, and methods of measurement.

The clause on limits concentrates on the low frequency and medium frequency bands as it is only in these where ample evidence, based on established practice, is available. No examples of limits to protect reception in the frequency band 30 MHz to 300 MHz have been given, as measuring methods and certain other aspects of the problems in this band have not yet been fully resolved. Site measurements and service experience have shown that levels of noise from power lines at frequencies higher than 300 MHz are so low that interference is unlikely to be caused to television reception.

The values of limits given as examples are calculated to provide a reasonable degree of protection to the reception of broadcasting at the edges of the recognized service areas of the appropriate transmitters in the a.m. radio frequency bands, in the least favourable conditions likely to be generally encountered. These limits are intended to provide guidance at the planning stage of the line and national standards or other specifications against which the performance of the line may be checked after construction and during its useful life.

Recommendations are made on the design, routing, construction and maintenance of the lines and equipment forming part of the power distribution system to minimize interference and it is hoped that this publication will aid other radio services in the consideration of the problems of interference.

Copyrighted material licensed to BR Demo by Thomson Reuters (Scientific), Inc., subscriptions.techstreet.com, downloaded on Nov-28-2014 by James Madison. No further reproduction or distribution is permitted. Uncontrolled when print

RADIO INTERFERENCE CHARACTERISTICS OF OVERHEAD POWER LINES AND HIGH-VOLTAGE EQUIPMENT –

Part 1: Description of phenomena

1 Scope

This part of CISPR 18, which is a technical report, applies to radio noise from overhead power lines and high-voltage equipment which may cause interference to radio reception. The scope of this publication includes the causes, measurement and effects of radio interference, design aspects in relation to this interference, methods and examples for establishing limits and prediction of tolerable levels of interference from high voltage overhead power lines and associated equipment, to the reception of radio broadcast services.

The frequency range covered is 0,15 MHz to 300 MHz.

Radio frequency interference caused by the pantograph of overhead railway traction systems is not considered in this technical report.

2 Normative references

The following referenced documents are indispensable for the application of this document. For dated references, only the edition cited applies. For undated references, the latest edition of the referenced document (including any amendments) applies.

IEC 60050-161, *International Electrotechnical Vocabulary (IEV) – Chapter 161: Electromagnetic compatibility*

CISPR 16-1-1, *Specification for radio disturbance and immunity measuring apparatus and methods – Part 1-1: Radio disturbance and immunity measuring apparatus – Measuring apparatus*

CISPR/TR 18-2:2010, *Radio interference characteristics of overhead power lines and high-voltage equipment – Part 2: Methods of measurement and procedure for determining limits*

ISO/IEC Guide 99, *International vocabulary of metrology – Basic and general concepts and associated terms (VIM)*

NOTE Informative references are listed in the Bibliography.

3 Terms and definitions

For the purposes of this document, the terms and definitions given in the IEC 60050-161 and the ISO/IEC Guide 99 apply.

Copyrighted material licensed to BR Demo by Thomson Reuters (Scientific), Inc., subscriptions.techstreet.com, downloaded on Nov-28-2014 by James Madison. No further reproduction or distribution is permitted. Uncontrolled when print

4 Radio noise from power lines

4.1 General

Radio noise from high voltage, which is to say above 1 kV, overhead power lines may be generated over a wide band of frequencies by

a) corona discharges in the air at the surfaces of conductors, insulator assemblies and hardware;

b) discharges and sparking at highly stressed areas of insulators;

c) sparking at loose or imperfect contacts of hardware.

The sources of a) and b) are usually distributed along the length of the line, but source c) is usually local. For lines operating above about 100 kV, the electric stress in the air at the surface of conductors and hardware can cause corona discharges. Sparking at bad contacts or broken or cracked insulators can give rise to local sources of radio noise. High voltage apparatus in substations may also generate radio noise which can be propagated along the overhead lines.

If the field strength of the radio noise at the antennas used for receiving broadcast sound and television services is too high, it can cause degradation of the sound output and, in the case of television, the picture also.

The generation of radio noise is affected by weather conditions, for example, conductor corona is more likely to occur in wet weather because of the water droplets which form on the conductors whereas, under these conditions, bad contacts can become bridged with water droplets and the generation of radio noise, by this process, ceases. Consequently, loose or imperfect contacts are more likely to spark in dry weather conditions. Dry, clean insulators may cause interference in fair weather, but prolonged sparking on the surfaces of insulators is more likely to occur when they are polluted, particularly during wet, foggy or icy conditions.

For interference-free reception of radio and television signals it is important that a sufficiently high ratio is available at the input to the receiver between the level of the wanted signal and the level of the unwanted radio noise. Interference may therefore be experienced when the signal strength is low and the weather conditions are conducive to the generation of radio noise.

When investigating radio noise it should be borne in mind that the local field may be caused by a distant source or sources as the noise may be propagated along the line over a considerable distance.

4.2 Physical aspects of radio noise

4.2.1 Mechanism of formation of a noise field

4.2.1.1 General

Corona discharges on conductors, insulators or line hardware or sparking at bad contacts can be the source of radio noise as they inject current pulses into the line conductors. These propagate along the conductors in both directions from the injection point. The various components of the frequency spectrum of these pulses have different effects.

In the frequency range 0,15 MHz to a few megahertz, the noise is largely the result of the effect of propagation along the line. Direct electromagnetic radiation from the pulse sources themselves does not materially contribute to the noise level. In this case the wavelength is long in comparison with the clearances of the conductors and thus the line is not an efficient radiator. However, associated with each spectral voltage and current component, an electric and a magnetic field propagate along the line. In view of the relatively low attenuation of this propagation, the noise field is determined by the aggregation of the effects of all the

Copyrighted material licensed to BR Demo by Thomson Reuters (Scientific), Inc., subscriptions.techstreet.com, downloaded on Nov-28-2014 by James Madison. No further reproduction or distribution is permitted. Uncontrolled when print

discharges spread over many kilometres along the line on either side of the reception point. It should be noted that close to the line the guided field predominates, whereas further from the line the radiated field predominates. The change-over is not abrupt and the phenomenon is not well known. This effect is not important at low frequencies but is apparent at medium frequencies.

However, for spectral components above 30 MHz where the wavelengths are close to or less than the clearance of the line conductors, the noise effects can be largely explained by antenna radiation theory applied to the source of noise, as there is no material propagation along the line.

It should be appreciated, however, that 30 MHz does not represent a clear dividing line between the two different mechanisms producing noise fields.

4.2.1.2 Longitudinal propagation

In the case of a single conductor line mounted above the ground there is a simultaneous propagation of a voltage wave $U(t)$ and a current wave $I(t)$.

For a given frequency the two quantities are related by the expression $U(\omega) = Z(\omega) \times I(\omega)$ where Z, also a function of ω, is the surge impedance of the line.

During propagation the waves are attenuated by a common coefficient α where:

$$U_x = U_0 e^{-\alpha x}$$

$$I_x = I_0 e^{-\alpha x}$$

U_0 and I_0 are the amplitudes at the source and x is the distance of propagation along the line.

In case of multi-phase lines, experience shows that any system of voltages or currents becomes distorted in propagation, that is to say, the attenuation varies with the distance propagated and it differs for each conductor. Theory of propagation and actual measurements on power lines have shown that noise voltages on the phase conductors can be considered as being made up of a number of "modes", each one having components on every conductor. One mode propagates between all conductors in parallel and earth. The others propagate between conductors. Each mode has its own different propagation attenuation. The complete theory of modal propagation is complex and involves matrix equations outside the scope of this publication. Reference is made here to CIGRÉ and other published works. It is important to note that the attenuation of the conductor-to-earth mode propagation is fairly high, that is to say 2 dB/km to 4 dB/km, while the attenuation of the various conductor-to-conductor modes is a small fraction of 1 dB/km at a frequency of 0,5 MHz.

4.2.1.3 Electromagnetic field

The radio noise voltages and currents propagating along the line produce an associated propagating electromagnetic field near the line.

It should be noted here that in free space the electric and magnetic components of the field associated with radiated electromagnetic waves are at right angles both to each other and to the direction of propagation. The ratio of their amplitudes represents a constant value:

$$\frac{E_{(\mathrm{V/m})}}{H_{(\mathrm{A/m})}} = 377\,\Omega$$

and is called the intrinsic impedance or impedance of free space.

Copyrighted material licensed to BR Demo by Thomson Reuters (Scientific), Inc., subscriptions.techstreet.com, downloaded on Nov-28-2014 by James Madison. No further reproduction or distribution is permitted. Uncontrolled when print

On the other hand, the fields near the line are related to the radio frequency voltages and currents propagating along the line and their ratio depends on the surge impedance of the line for the various modes. Furthermore, the directions of the electric and magnetic field components differ from those for radiated fields in free space as they are largely determined by the geometrical arrangements of the line conductors. The matter is further complicated by the fact that soil conditions affect differently the mirror image in the ground of the electric and magnetic field components, respectively.

The electric field strength $E(y)$ at ground level of a single conductor line, which is the vertical component of the total electric field strength, can be predicted by the following empirical formula that has, in a lot of cases, proven to give a good approximation:

$$E(y) = 120\ I \frac{h}{h^2 + y^2}$$

where

I is the radio noise current, in A, propagating in the conductor;

h is the height above ground, in metres, of the conductor;

y is the lateral distance, also in metres, from a point at ground level directly under the conductor to the measuring point; and

E is the electric field strength in V/m.

Furthermore, for an infinitely long single conductor line, the induction zone, or near field, has the same simple ratio of electric and magnetic field strength as the far field from a radio transmitter, that is to say 377 Ω and this is approximately true for all values of ground conductivity.

In the case of a multi-phase line the total electric field strength is the vectorial sum of the individual field strength components associated with each phase conductor. A more comprehensive treatment, together with practical methods of assessing the electromagnetic field, is discussed in 5.2 of CISPR/TR 18-2. The formula given above is a simplified version accurate for a distance of D = 20 m and f = 0,5 MHz where D is the direct distance, in metres, between the measuring antenna and the nearest conductor of the line, and f is the measurement frequency. For conventional power transmission lines (i.e. with a conductor height above ground which is less than 15 m), this direct distance D approximately corresponds to a lateral distance y of 15 m. For a wider range of D and f it would be necessary to take into account all the parameters affecting the formula.

4.2.1.4 Aggregation effect

In the case of uniformly distributed noise sources, the field strength generated by a unit length of a phase conductor can be expressed at any point along the line as a function of the longitudinal distance x and the lateral distance y, that is to say, $E(y,x)$. At a given lateral distance of y,

$$E(y,x) = E_0(y)e^{-\alpha x}$$

The random pulses on a long line with uniformly distributed noise sources combine together to form the total field. The manner in which they combine is not unanimously agreed upon. Some investigators consider that they combine quadratically:

$$E^2(y) = 2\int_0^{\infty} E_0^2(y)\mathrm{e}^{-2\alpha x}\mathrm{d}x$$

Copyrighted material licensed to BR Demo by Thomson Reuters (Scientific), Inc., subscriptions.techstreet.com, downloaded on Nov-28-2014 by James Madison. No further reproduction or distribution is permitted. Uncontrolled when print

or $$E(y) = \frac{E_0}{\sqrt{\alpha}} \ .$$

Other investigators believe that, if a quasi-peak detector is used to measure the field strength, the individual pulses do not add and others have obtained results between the two extremes. This disagreement is only important in analytical prediction methods, the results obtained by the different methods vary by only 1 dB or 2 dB.

In case of multi-phase lines, the calculation follows the sample principle but is complicated by the presence of several modes, each mode having a different attenuation coefficient. A more detailed discussion, with examples of calculation, is given in Clause 6.

4.2.2 Definition of noise

The instantaneous value of the noise varies continuously and in a random manner, but its average power level over a sufficiently long period, for example, 1 s, gives a stationary random quantity which can be measured. Another quantity suitable for measurement is the peak or some weighted peak value of the noise level.

A noise measuring instrument is basically a tuneable selective and sensitive voltmeter with a specified pass-band. When connecting to a suitable rod or loop antenna and properly calibrated, it can measure the electric or magnetic component of the noise field. For measurements of the magnetic component of the noise field in the frequency range up to 30 MHz, normally a loop antenna is used. For measurements of the electric component of the noise field in the frequency range above 30 MHz, use of a biconical antenna is recommended.

Depending on the design of the measuring receiver, the noise level can be measured in terms of r.m.s., peak or quasi-peak values. The r.m.s. value defines the noise in terms of energy. Many types of noise from electrical equipment, as well as noise due to power-line corona, consist of a succession of short pulses with approximately stable repetition frequencies. In such cases the nuisance effect of the noise can be realistically indicated by a quasi-peak type of voltmeter rather than by the r.m.s. type. The quasi-peak value is obtained from a circuit which includes a diode and a capacitor with relatively short charge and long discharge time constants. The voltage on the capacitor floats at a value somewhat below the peak value and depends on the repetition rate, that is to say a weighting feature is included in the response. This principle is adopted in the CISPR measuring receiver, details of which are given in CISPR 16-1-1. The noise level is thus defined by the value measured by such an instrument expressed in microvolts (μV) or microvolts per metre (μV/m). Using the ratio of the electric to magnetic field components, E/H = 377 Ω, the measured values can also be expressed by convention in μV/m even for instruments using a loop antenna responding to the magnetic field component.

4.2.3 Influence of external parameters

To determine the corona inception gradient g_c of a cylindrical conductor with smooth surface, Peek's formula is often used:

$$g_c \text{ (kV/cm)} = 31\ \delta \left(1 + \frac{0{,}308}{\sqrt{\delta r}}\right)$$

For a.c. voltages, g_c is the peak value of the gradient, r is the radius of the conductor in centimetres, $\delta = \frac{0{,}294p}{273+T}$ is the relative air density (δ = 1 for p = 1 013 mbar and T = 25 °C).

However, practical conditions on overhead lines do not agree with these idealized assumptions. Stranding of the conductors, surface imperfections and irregularities lead to local enhancements of the electric field strength and consequently to a lower corona inception

Copyrighted material licensed to BR Demo by Thomson Reuters (Scientific), Inc., subscriptions.techstreet.com, downloaded on Nov-28-2014 by James Madison. No further reproduction or distribution is permitted. Uncontrolled when print

voltage than is obtained from the above formula. This often means that the critical gradient for initiating radio noise has, under foul weather conditions, about half the value given by Peek's formula.

Atmospheric conditions likewise play an important part in occurrence of corona and spark discharges. In conditions of rain, fog, snow or dew, drops of water form on the surface of the conductor and at low temperatures ice can form. This further reduces the corona inception voltage and increases the noise level as shown in Clauses 5 and 6.

With regard to bad contacts and the production of small sparks, the effect of rain and humidity is to bridge the relevant gaps either by water droplets or by humid layers, thus reducing the level of this type of noise.

Rain and humidity thus affect the corona noise from conductors in a way opposite to that due to bad contacts. Hence when interference is observed during rain or fog, it can be concluded that it is caused by corona. On the other hand, when interference is observed during fair weather and disappears or decreases during rain or fog, it is due to bad contacts.

4.3 Main characteristics of the noise field resulting from conductor corona

4.3.1 General

To rationalize the measurement of radio noise from a transmission line and facilitate comparisons between different lines, it is desirable to standardize the conditions under which the measurement is to be carried out.

The main characteristics of the noise field are the frequency spectrum, its lateral field strength profile and the statistical variation of the noise with weather conditions. It is assumed as a first approximation that these characteristics are independent of each other.

4.3.2 Frequency spectrum

The frequency spectrum is the variation of the radio noise measured at a given point in the vicinity of a line, as a function of the measurement frequency. Two phenomena are involved:

a) Current pulses

   The current pulses generated in the conductors by the discharges show a particular spectrum dependent on the pulse shape. For this type of discharge the measured noise level decreases with an increase of the measurement frequency. In the range of broadcasting frequencies, where the positive discharges have a predominant effect, the spectrum is independent of the conductor diameter.

b) Attenuation along the line

   The attenuation of noise propagating along the line increases with frequency. This effect modifies the spectrum by reducing still further the noise level with increase in frequency.

The measured spectra are often fairly irregular because of the standing waves caused by discontinuities such as angle or terminal towers or abrupt ground level variations. In addition, the noise generation might vary whilst the measurements are being made.

To aid prediction calculations, "standard spectra" are used. Experience has shown that all spectra can be put into two families, one applying to horizontal conductor configurations, the other to double-circuit and triangular or vertical conductor configurations. The difference between these two families originates from the phenomenon mentioned in item b) above, the propagation differing slightly according to the type of line. However, as the difference is not material in relation to the accuracy of such calculations, only one standard spectrum is given in relative values, the reference point being taken at 0,5 MHz.

The following formula is a good representation of this spectrum:

Copyrighted material licensed to BR Demo by Thomson Reuters (Scientific), Inc., subscriptions.techstreet.com, downloaded on Nov-28-2014 by James Madison. No further reproduction or distribution is permitted. Uncontrolled when print

$$\Delta E = 5\left[1 - 2(\lg 10 f)^2\right] \text{ in dB}$$

where

ΔE is the deviation of the radio noise level at a given frequency f which is different from the reference frequency of 0,5 MHz; and

f is the numerical value of the given frequency, taken in megahertz, where the formula is valid over the range 0,15 MHz to 4 MHz.

It should be noted that other investigators have developed different formulae which give similar results.

At higher frequencies the noise spectra are more difficult to predict.

4.3.3 Lateral profile

The variation of the noise fields as a function of increasing lateral distance from the line is characterized by a decrease depending on the frequency. Measurements are taken along a perpendicular to a mid-span which is as close as possible to an average span of the line under consideration. The proximity of substations or interconnections, sharp angles, neighbouring lines and great variations in level of terrain shall be avoided.

Lateral profiles of the radio noise field can be determined either using the direct distance D or the lateral distance y.

Conventions

(1) In order to allow for comparison of obtained profiles of the noise field, the profile is determined at a height of 2 m above the ground immediately beneath an outside conductor over a distance D or y not exceeding 200 m. Beyond this distance the noise level of the lines generally becomes negligible. The reference frequency for CISPR measurements is 0,5 MHz.

(2) For the profiles which relate to the direct distance D, this distance is to be taken from the nearest conductor of the line (reference point (x,y,z), i.e. x = place along the line at mid-span in between two towers where the measurements are made, y = 0 m and z = n m corresponding to the height above ground of the outmost sub-conductor) to the centre of the measuring antenna. For comparison purposes it has been agreed that the reference distance through which the profiles eventually converge is the direct distance D_0 of 20 m also referred to later on as the *CISPR position*. Figure 2 shows an example.

(3) For the profiles which relate to the lateral distance y, this distance is to be taken laterally (at ground level) from the vertical projection to ground of the outmost sub-conductor of the transmission line (reference point (x,y,z), i.e. x = place along the line at mid-span in between two towers where the measurements are made, y = 0 m and z = 2 m corresponding to the vertical projection to ground of the outmost sub-conductor) to the centre of the measuring antenna. For comparison purposes it has been agreed that the reference distance through which these profiles eventually converge is the lateral distance y_0 of 15 m.

The standard profiles shown in Annex B, Figures B.1 to B.13, refer to the lateral distance y.

NOTE 1 Care should be taken as to not confuse measurement results obtained from measurements at direct and/or lateral distances.

(4) Normalised and/or standard profiles (for the catalogue) are usually shown with a logarithmic scale of distance.

While the profiles obtained from measurements at direct distances correlate with the considerations on the prediction and predetermination formulae, this is not necessarily the case for the profiles obtained from measurements at lateral distances. In the latter case, such correlation is only given for conventional transmission lines with a conductor height above

Copyrighted material licensed to BR Demo by Thomson Reuters (Scientific), Inc., subscriptions.techstreet.com, downloaded on Nov-28-2014 by James Madison. No further reproduction or distribution is permitted. Uncontrolled when print

ground of up to 15 m. As a rule, future profiles of the noise field will be presented as a function of the lateral distance y in relation to a reference distance y_0 = 15 m, see also Figure 1. Such a presentation is useful for predicting the width of the corridor along the pathway of the transmission line subject to interference. It can be used for any type of modern transmission line regardless of the height of the towers and the conductors above ground. It is quite obvious that in such conditions the classical prediction formulae found elsewhere in this publication may become invalid. If needed, the validity of these formulae should be checked.

The measured profiles are often irregular both because of the continual fluctuations of the radio noise during a series of measurements and because of irregularities such as angle or dead-end towers and terrain variations.

Numerous measurements carried out under some fifty different lines have provided a good experimental knowledge of these profiles, which has been confirmed by theoretical calculations.

An accurate analysis has enabled profiles to be plotted as functions of classes of line voltage and configuration up to distances of about 100 m, beyond which the noise level is normally so low that reliable measurements are not practicable.

In the vicinity of a power line there are two types of noise fields, the direct or guided field and the radiation field. The latter is a result of irregularities in the line such as conductor sag and changes in line direction and imperfect ground conductivity. Both fields contribute to the resulting observed total field strength. The field strength component of the direct field decreases as the square of the increasing lateral distance from the line, while the field strength component of the radiation field decreases directly with the increase of this lateral distance. Close to the line the direct field predominates, whereas at greater distances the radiation field predominates. Based on certain antenna concepts, the magnitudes of the two field strength contributions may be expected to be equal at a distance of around $300/2\pi f$ metres where f is to be taken as the numerical value of the frequency in MHz. In actual fact, the lateral attenuation close to the line falls off less rapidly than the square of the distance. The attenuation factor k for frequencies between 0,5 MHz and 1,6 MHz, for example, is 1,65 (see Annex C). Close to the line the lateral attenuation may be described by:

$$E = f(D) = E_0 + 20k \lg D_0/D \quad \text{in dB(µV/m)}$$

where

E is the level of the electric component of the noise field strength, in dB(µV/m), at a direct distance D;

k is the attenuation factor;

E_0 is the level of the electric component of the noise field strength, in dB(µV/m), at the reference distance D_0 = 20 m.

NOTE 2 For conventional transmission lines, this direct distance D_0 corresponds to a lateral distance y_0 = 15 m.

Further from the line the attenuation factor gradually decreases until it reaches a value of unity. Some investigators consider that the magnitudes of the two field contributions are equal at around $300/2\pi f$ m as discussed above.

Standard profiles are shown with a logarithmic scale of distance referring to a direct distance to the conductor of 20 m. This presentation shows the physical law of the noise field strength decreasing as a function of the distance from the nearest conductor. The profiles can also be presented as a function of the lateral distance. This presentation is useful for predicting the width of the corridor subject to interference.

Copyrighted material licensed to BR Demo by Thomson Reuters (Scientific), Inc., subscriptions.techstreet.com, downloaded on Nov-28-2014 by James Madison. No further reproduction or distribution is permitted. Uncontrolled when print

4.3.4 Statistical distribution with varying seasons and weather conditions

The systematic study of fluctuations in the radio noise level of a line necessitates the continuous recording of the field strength under this line for at least a year at a fixed distance from the line and with a fixed measurement frequency. Numerous researchers, in many countries, have carried out such measurements with the result that there exists fairly reliable data on the annual or seasonal variations in radio noise level. These results are often presented according to statistical analysis methods, which are to say in the form of histograms or as cumulative distributions. The latter express the percentage of time during which the radio noise level was less than a given value.

The most important causes of fluctuations in recorded radio noise level are:

– the random nature of the phenomenon;
– variations of the meteorological conditions, both at the measuring point and along the few tens of kilometres of the line which contributes to the local interference;
– changes in the surface state of the conductors, which is affected not only by weather conditions such as rain and frost, but also by deposits of dust, insects and other particles.

These causes are very difficult to measure systematically. Even variations of the applied line voltage result in fluctuations in the radio noise level, but this cause is possible to measure.

The distribution of the noise levels likewise depends on the type of climate; a very humid climate, a rainy one, or one with abundant snow or frost will increase the percentage of high levels, whereas a very dry climate will reduce it.

The curves in Figures 3 to 6 in a temperate climate show examples of an all weather distribution survey, together with a dry weather distribution and an average heavy-rain distribution. It can be seen that the overall curve is more or less a combination of two or three Gaussian distributions.

On such an all weather distribution, it is customary to define several characteristic radio noise levels:

– The *99 % level* is practically the highest possible level of the line, at a given point.
– The *average heavy-rain level* is the most stable and reproducible and the rainfall is considered to be heavy when it reaches 0,6 mm or more per hour. For this reason the average heavy-rain level is often chosen as the reference level for the calculation of radio noise. Practically, the average heavy-rain level is a 95 % level and is about 5 dB lower than the 99 % level.
– The *average fair weather level*, corresponding to dry conductor conditions. This is important for practical purposes, but, due to the larger dispersion, a greater number of measurements throughout the year are necessary to obtain reliable results. Fortunately, measurements are more easily made in average fair weather than in average heavy rain.
– The *50 % level*, read on the all-weather cumulative curve. This 50 % level shall not be confused with the above defined average fair weather level, since it arises not only from dry weather conditions, but also from the whole range of climatic conditions prevailing during the long term recordings. Both the average fair weather and 50 % levels are furthermore strongly dependent on the surface state of the conductors; these levels can vary over a range of more than 10 dB according to whether or not the conductors are polluted, greasy, etc. Some experts consider that the 50 % level will not vary by more than 10 dB over a relatively long period, say a month or a year, even though individual readings may vary by more than 10 dB.
– The *80 % level*, read on the all-weather distribution curve, is chosen as the characteristic value, to be used as the basis for limits. This 80 % level, intermediate between the fair weather level and the average heavy-rain level, is probably less subject to uncertainties than the 50 % level and for this reason is preferred as the "characteristic level". A survey of numerous cumulative curves shows that the difference between the 95 % and 80 %

Copyrighted material licensed to BR Demo by Thomson Reuters (Scientific), Inc., subscriptions.techstreet.com, downloaded on Nov-28-2014 by James Madison. No further reproduction or distribution is permitted. Uncontrolled when print

levels lies between 5 dB and 12 dB. As mentioned in 4.3.3, it should be remembered that beyond about 100 m to 200 m reliable measurements are normally not practicable.

The above generalized guidelines are illustrated in Figures 3 to 6, related to 400 kV to 765 kV lines, and are valid for lines where the predominant noise source is conductor corona.

5 Effects of corona from conductors

5.1 Physical aspects of corona from conductors

5.1.1 General

The generation of radio noise by conductor corona is by means of the electrical discharge, usually called corona, occurring at or near the conductor surface. Corona is defined as "a discharge with slight luminosity produced in the neighbourhood of a conductor and limited to the region surrounding the conductor in which the electric field strength exceeds a certain value". Many aspects of corona discharge on lines are unknown and undefined; however, the basic physical process is that of electron multiplication or avalanche formation. The electric gradient in the vicinity of the line conductor is the highest gradient and, if this gradient or electric stress is sufficiently high, any free electrons in the air around the conductor will ionize the gas molecules and electrons produced by this ionization will cause an avalanche. If an additional electron is formed in this gradient by some process from the original electron avalanche, a new avalanche is formed by this secondary process and the corona discharge is developed.

In the case of the transmission line conductor, it is believed that the important secondary process is the ejection of electrons from gas molecules by high energy ultra-violet light (photoionization) generated by the original avalanche. It has been found by several investigators that the radio noise level generated when the conductor is positive is significantly greater than it is when the conductor is negative. In the case of a positive overhead line conductor, the cathode is so far away that cathode emission is of no consequence and the secondary process existing in this case is photoionization of the gas.

When streamer corona forms at a point on the conductor, two types of pulse fields will exist. Near the streamer a localized field is formed and along the line the direct field is developed due to the pulses travelling down the line. For the design of extra high voltage lines, only the direct field is considered significant, and the most useful measurements are made at some distance from the streamer locations on the line conductor.

For a more detailed discussion of the theoretical aspects of conductor corona, see [1, 2] [1].

5.1.2 Factors in corona generation

5.1.2.1 General

The possibility of a corona discharge taking place at the surface of a conductor is dependent upon several factors, these include:

a) Theoretical conductor surface voltage gradient which depends on:
   1) system voltage;
   2) conductor diameter;
   3) spacing of the conductor from earth and other phase conductors;
   4) number of conductors per phase or in the bundle.
b) Conductor diameter.
c) Conductor surface conditions.

[1] The figures in square brackets refer to the Bibliography.

Copyrighted material licensed to BR Demo by Thomson Reuters (Scientific), Inc., subscriptions.techstreet.com, downloaded on Nov-28-2014 by James Madison. No further reproduction or distribution is permitted. Uncontrolled when print

d) Atmospheric and weather conditions.

Each of these factors will be considered separately.

5.1.2.2 Conductor surface voltage gradient

One of the most important quantities in determining the radio noise level of a line, especially when conductor corona is dominant, is the strength of the electric field in the air at the surface of the conductor or surface voltage gradient.

Because of the close dependence of conductor corona on the value of this voltage gradient, it is necessary to use a method of calculation which gives the gradient with a precision of about 1 %.

Since conductors are usually stranded, the surface voltage gradient varies about a mean value around the circumference of the conductor. However, it is customary to calculate the surface gradient for a smooth conductor with the same overall diameter, even if an experimental stranding factor has to be introduced.

Formulae for the calculation of the voltage gradient at the surface of a conductor are given in Annex A for the simple case of a single-phase line with earth return or a monopolar d.c. line to the more complex three-phase multicircuit and bipolar d.c. lines. Usually the calculations need a matrix equation and computer programs are used for both single and multicircuit three-phase lines and the more complex high-voltage d.c. lines.

5.1.2.3 Conductor diameter

The radio noise level increases with increasing conductor diameter even if the conductor surface gradient remains the same. This phenomenon is due to the fact that the decay of the electric field strength from the surface of a conductor decreases with increasing conductor diameter. Therefore, the electric field surrounding a large conductor can support longer corona streamers than the electric field around small conductors.

5.1.2.4 Conductor surface conditions

The type of conductor, for example circular or segmental stranding, and the condition of its surface, that is to say the degree of smoothness or roughness, the presence or absence of pollution, water droplets, snow flakes, etc., have a strong influence on the generation of corona. A transmission line conductor when first strung will usually have higher corona activity due to surface irregularities such as aluminium burrs, bird droppings, dust, soil, mud or any other deposits causing corona even in fair weather. However, after a line is energized the corona losses and radio noise will decrease with time.

There are usually two time periods involved; the first period is the first few minutes after the conductor is energized and the corona activity is burning off the dust and other particles that have collected on the conductor before it was energized. The longer time period is needed to blacken completely a conductor which makes it look weathered and also destroys the surface grease on new conductors.

There is also evidence that as the conductor ages the radio noise level, even during rain, will decrease. The surface of a new conductor is hydrophobic, due to the oil that is present on the surface from the manufacturing processes, and water beads form on this oily surface. As the conductor ages, its surface becomes hydrophilic whereby the surface of the conductor draws up the water drops into the strands.

5.1.2.5 Atmospheric and weather conditions

A reduction in the barometric pressure or an increase in the ambient temperature, or both, can reduce the air density which reduces the breakdown strength of air and thereby increases the likelihood of a corona discharge taking place on a conductor. The barometric pressure is

Copyrighted material licensed to BR Demo by Thomson Reuters (Scientific), Inc., subscriptions.techstreet.com, downloaded on Nov-28-2014 by James Madison. No further reproduction or distribution is permitted. Uncontrolled when print

usually important only at altitudes above approximately 1 000 m. In areas that have sufficient rain, fog, frost or falling temperatures which can lead to the formation of ice or water droplets on the conductor, corona discharges are more likely to take place due to these conditions. Rain and snow are the cause of the highest corona activity at the surface of a conductor and can cause the radio noise level to increase by more than 20 dB compared with the noise from the same line under dry conditions. The water droplets or snow which collects on the conductor surface during a storm modify the electric field significantly, creating a large number of corona sources. Discharges may also occur when a snowflake or raindrop passes the conductor and initiates a discharge from the conductor to the particle.

5.2 Methods of investigation of corona by cages and test lines

5.2.1 General

Two basic methods have been used to investigate the corona phenomena from transmission lines. These are test cages and test lines [9, 21, 31].

5.2.2 Test cages

Test cages have been used by many experimenters to determine rapidly the excitation function of a conductor or a bundle of conductors [4 to 6]. The excitation function is related to the current in the bundle by the following:

$$I = \Gamma \frac{C}{2\pi\varepsilon_0} \qquad (1)$$

where

I is the high frequency current injected into the conductor or bundle of conductors in A/m$^{1/2}$,

C is the capacitance in F/m;

Γ is the excitation function in A/m$^{1/2}$: and

ε_0 is the absolute permittivity of the air.

The main advantage of the concept of the excitation functions is that it is a quantity independent of the conductor capacitance per unit length.

The radio noise current in a test cage is measured using measuring instruments complying with CISPR 16-1-1. The current at one end of the conductor or bundle is passed through a high-frequency coupling circuit similar to those described in 4.5 of CISPR/TR 18-2. The equivalent impedance of the resistors and of the measuring instrument used in these circuits is usually made equal to the characteristic impedance of the conductor or bundle to avoid the occurrence of successive reflections.

Test cages have been found to give reproducible radio noise data under heavy rain but, under foul weather conditions, they have proved inadequate because of the relatively small number of sources per unit length of conductor under normal stress. The length of conductor in a cage is generally too short to give a representation of an actual long line. Additionally, the surface condition of the conductor and meteorological conditions surrounding a short line near to the ground are not necessarily the same as the conditions on an operational line.

Application of the excitation function to multi-phase lines requires the use of equation (1) in matrix form [7 to 9].

$$[I] = \frac{1}{2\pi\varepsilon_0} \times [C] \times [\Gamma] \qquad (2)$$

Copyrighted material licensed to BR Demo by Thomson Reuters (Scientific), Inc., subscriptions.techstreet.com, downloaded on Nov-28-2014 by James Madison. No further reproduction or distribution is permitted. Uncontrolled when print

5.2.3 Test lines

Whilst test cages are built for reasons of economy and ease of testing, full-scale test lines are still being built, primarily to study corona phenomena on future ultra high voltage (UHV) lines. There is no standard length for test lines. Test lines, single and three-phase a.c. lines and bipolar d.c. lines, as long as 8 km an as short as 300 m have been built, [10 to 30].

There have been some attempts to measure the excitation function on short test lines and with some success, especially on short d.c. test lines, [28, 29].

For long transmission lines, the radio noise frequency spectrum exhibits a characteristic of a steadily decreasing level with increasing frequency. However, for short test lines this situation does not exist. Due to reflections of the radio noise voltages and currents at the line terminations, a standing-wave pattern in the frequency spectrum is created. This spectrum is characterized by sharp peaks and broad valleys, the exact form being dependent on the length of the line, the type of terminations, and the longitudinal location of the measuring point.

The approach that has been used by most investigators to correct the short-line frequency spectrum to the long-line spectrum is the "Geometric mean method" [12, 14 to 16, 18, 26, 29]. This correction is made by taking the geometric mean in terms of μV/m of the successive maxima and minima of the short line frequency spectrum. In terms of dB(μV/m), the arithmetic mean is used.

This approach, strictly speaking, is only valid for the idealized case of a perfectly horizontal single phase line with terminations that appear as pure open circuits for radio frequencies. However, experimental studies show that, for all practical purposes, this approach is valid for a.c. and d.c. lines [28, 32, 33].

5.3 Methods of predetermination

5.3.1 General

Because of the need for higher transmission voltages, a considerable amount of research has been conducted over the past 50 years, in various parts of the world, to understand the corona process. One of the primary purposes of this research was to develop methods to predetermine radio noise.

Radio noise measurements that have been conducted on short full-scale single and three-phase a.c. test lines, on d.c. test lines, on operational lines, and in the laboratory, have resulted in several empirical and semi-empirical formulae for predicting radio noise. These formulae can be used to predict the radio noise performance of different high-voltage lines, as long as the voltage and the design parameters are known. All the methods rely on experimental data either from test lines, operational lines or test cages. Two basic methods have evolved over the years, the first one being analytical or semi-empirical and the second being empirical or comparative.

5.3.2 Analytical methods

No purely analytical method of predicting transmission line radio noise exists. Two semi-empirical methods have been developed by Electricité de France (EDF) [8] and Project Ultra High Voltage (UHV) [7] in the United States of America. Both of these analytical methods rely on radio noise data from test cages and on highly complex analysis, and they are adequately described in the literature.

The calculation of radio noise from transmission lines using these analytical methods is a two-stage process. The excitation function is obtained from cage tests, the system of line capacitances is established and the injected noise currents per unit conductor length are calculated using equation (2). The theory of modal propagation is applied to obtain the modal currents flowing in a given cross-section of the line. The attenuations of propagation of these modal currents are calculated and these currents are recombined into real high-frequency

Copyrighted material licensed to BR Demo by Thomson Reuters (Scientific), Inc., subscriptions.techstreet.com, downloaded on Nov-28-2014 by James Madison. No further reproduction or distribution is permitted. Uncontrolled when print

currents taking into account the quadratic summation over the whole line length to obtain the total noise currents.

The next step is to calculate the noise field near the line, which is based on the total noise currents through the cross-section of the line, or the noise voltages on the phases. The lateral noise profile can then be obtained (see examples in 5.4).

Computer programs are usually used to perform these complex calculations and such programs have been written at EDF and Project UHV.

5.3.3 CIGRÉ method

The comparative formulae are generally quite simple and easy to use. Some of the best known formulae for a.c. lines are described in a CIGRÉ Publication [1] and the technical literature [34, 35]. There are also several comparative formulae for d.c. lines and these are described in Clause 8.

The highest precision of predetermination, using any of these formulae, is obtained by choosing long-term data from an operational reference line which uses conductors or bundles close to those being studied [36, 37, 38].

CIGRÉ has made a more complete analysis of the different predetermination methods using the data collected by the CIGRÉ/IEEE Survey [6, 34, 35]. From this analysis they developed a new method that can be considered optimal. This method is expressed by a fairly simple formula, which is given in 5.3 of CISPR/TR 18-3 [59].

5.4 Catalogue of standard profiles

5.4.1 General

A large number of measurements on operational lines, together with calculations supported by measurements on cage and test lines, have been carried out and examples of the results for a variety of line designs are given in Annex B. The given values are valid only for lines constructed and maintained according to normal practice and not heavily polluted, as otherwise these conditions can give rise to higher radio noise levels than those due to conductor corona.

Annex B gives the estimated value of the radio noise field which is possible to obtain under certain well-defined conditions. It also includes references which can be used for predetermining the field that a new line may be expected to produce. It also includes, as examples, curves giving the field strength as a function of the lateral distance *y* from the line for certain types of line (see Figures B.1 to B.13).

NOTE The appearance of a given line in the catalogue in Annex B does not mean that this line generates an acceptable radio noise level; it gives only an indication of the order of magnitude to be expected for the given line design.

5.4.2 Principle of catalogue presentation

Radio noise measurements taken both on operational lines and on test lines have indicated that the stability and reproducibility of the field due to conductor corona is most accurate under conditions of heavy and continuous rain. It should be noted that this heavy rain value may not be the maximum foul-weather value, which can be a few dB higher.

Extensive statistical surveys have also indicated that there is a reasonable correlation between the heavy rain radio noise level and the 50 % fair-weather level, though the dispersion under fair-weather conditions is larger. For practical purposes, the 50 % fair-weather level is usually of greater importance, this value being derived from the heavy continuous-rain level by a reduction of between 17 dB and 25 dB, depending upon conductor surface conditions.

Copyrighted material licensed to BR Demo by Thomson Reuters (Scientific), Inc., subscriptions.techstreet.com, downloaded on Nov-28-2014 by James Madison. No further reproduction or distribution is permitted. Uncontrolled when print

It is therefore possible to establish a catalogue of radio noise fields for certain transmission lines. For the practical use of this catalogue, three noise levels are considered, namely the 50 % fair-weather level and, depending on the origin of the profiles, either the heavy-rain level (20 dB higher) or the maximum foul-weather level (24 dB higher). From these reference levels, it is possible to estimate the radio noise levels for other types of weather, if the yearly statistical distribution of levels is known for the geographical area under consideration (see, for example, Figure B.15).

These principles are valid only for radio noise generated by conductor corona. The radio noise currents generated by other components of the line, insulator strings, hardware and so on, are not taken into consideration. These conditions are satisfied when the conductors of the line are subjected to a relatively high surface stress, in excess of, say, 14 kV r.m.s. per centimetre when referred to smooth conductors. However, for lines whose conductors are subjected to a surface stress less than, say 12 kV r.m.s. per centimetre, it is the radio noise from the insulators and other hardware which may, under certain conditions, predominate. Under these conditions it is not possible to use this catalogue to predict the noise level since a good quality of insulators and hardware has been assumed.

The radio noise profiles for the 225 kV, 380 kV and 750 kV lines included in this catalogue were calculated by the Analig method [8].

The profiles for the 362 kV, 525 kV and 765 kV lines were determined from the results of the CIGRÉ/IEEE survey [35, 39].

The radio noise profiles for the 345 kV and 765 kV HV transmission lines included in this catalogue were calculated by the comparative method [56].

The surface gradients have been calculated using the general method of potential coefficients. This method gives, with great accuracy, the electric surface gradient of each conductor of a line. A survey of methods for calculating transmission line surface voltage gradients is given in [40].

The shape of the lateral profiles of the radio noise field is essentially dependent on the conductor configuration. The distance between phases and their height above the ground have a major influence. The type of conductor or the bundle only slightly affects the shape of the profile owing to the structure of the capacitance matrix. When changing from one type of conductor to another with the same geometry, so long as the two matrices are proportional to each other, the profile will not be significantly changed. This assumption is sufficiently true to be applied in practice.

In Annex B, profiles have been assembled for certain types of overhead power line. The influence of the number and arrangements of conductors per phase, their diameter and their voltage gradient, were taken into account merely by applying the appropriate correction to a reference profile. Thus each figure in the catalogue gives such a reference profile and a table of values and corrections applicable to other lines using other conductors and bundles.

The profiles are given for a measurement frequency of 0,5 MHz and the radio noise levels for other frequencies, 0,15 MHz to 4 MHz, can be obtained from Figure B.14.

The variations of the radio noise level, due either to climatic conditions or surface state of the conductors, can also be taken into consideration by estimated corrections to the levels of the basic profiles (see Figure B.15).

Examples of measurements and calculations can be found in [8, 35, 39].

The catalogue is summarized in Annex C according to the conventions agreed so far in CISPR; that is to say the strengths of the radio noise fields are plotted as a function of the direct distance, measured from the centre of the loop antenna to the nearest conductor of the

Copyrighted material licensed to BR Demo by Thomson Reuters (Scientific), Inc., subscriptions.techstreet.com, downloaded on Nov-28-2014 by James Madison. No further reproduction or distribution is permitted. Uncontrolled when print

line, using a logarithmic scale. From Figure C.1, it is seen that substantially straight lines are obtained, and the field strengths at the reference distance of both, D_0 = 20 m (direct distance) and simultaneously y_0 = 15 m (lateral distance) are obtained by interpolation.

The main radio noise levels, given in the catalogue, are listed in the table of Annex C; from this table it is possible to compare the levels of the various lines given in the catalogue and to predict, with sufficient accuracy for practical purposes, the field strength to be expected from a proposed line of similar design, provided the distance between a receiving antenna and the nearest conductor of the line is greater than 20 m.

6 Radio noise levels due to insulators, hardware and substation equipment (excluding bad contacts)

6.1 Physical aspects of radio noise sources

6.1.1 General

Insulators, hardware and substation equipment may be the source of radio noise which may lead to radio and, in some cases, to television interference also. This may be due to various phenomena such as corona discharges in the air at insulators and hardware, surface discharges on insulators and sparks due to bad contacts. Commutation effects in a.c./d.c. converting equipment, which can also be a source of radio noise, are discussed in Clause 8.

This clause examines the phenomena of corona and surface discharges from the physical point of view; sparks due to bad contacts are dealt with in Clause 7.

6.1.2 Radio noise due to corona discharges at hardware

Corona discharges are caused by high potential gradients at certain surfaces of hardware such as suspension clamps, guard-rings or guard-horns, spacers and joints. Assuming that the voltage applied to the hardware is progressively increased, numerous different discharge processes occur. Only some of these are able to generate radio noise, but all are luminous to some extent and contribute to corona losses. The phenomena are similar to those described in 5.1 in respect of conductors. Similarly, in this case, various corona modes occur, depending on the polarity of voltage applied and in the following sequence; onset streamer, glow and pre-breakdown streamer for positive corona; Trichel or negative pulses, glow, and pre-breakdown streamer for negative corona. A glow discharge does not produce radio noise but onset streamer does. Trichel pulses produce low levels of radio noise but pre-breakdown streamers produce very high levels at very high voltages.

The highest noise levels occur with modes corresponding to the pre-breakdown streamer, both positive and negative; however, these phenomena take place at much higher gradients that those corresponding to normal voltages and are therefore of little practical interest.

As in the case of conductors, radio noise from hardware tends to increase in high humidity or rain, as a result of the increase in local gradients due to the presence of drops of water on the surface of the hardware.

6.1.3 Radio noise due to insulators

Insulator noise may be due to various reasons, most of which are associated with phenomena occurring at their surfaces, for example, small discharges due to enhanced local gradients, corona discharges due to unevenness created by dry deposits or drops of water, or sparks across dry bands caused by leakage currents on polluted insulators. Only in special cases, for example defective insulators, is the noise due to phenomena occurring inside the insulator, that is to say sparking in internal voids or punctures. However, radio noise can result from discharges between the cement and porcelain or glass and may occur if small air gaps are present at this margin.

Copyrighted material licensed to BR Demo by Thomson Reuters (Scientific), Inc., subscriptions.techstreet.com, downloaded on Nov-28-2014 by James Madison. No further reproduction or distribution is permitted. Uncontrolled when print

When the surface of an insulator is clean and dry, the current pulses at the origin of the radio noise are caused by discharges in areas of high potential gradient, depending on the geometry and material of the insulator and on the type of bonding to the cap and to the pin. Figure 7 shows, by way of an example, the equipotential lines, expressed as a fraction of the applied voltage, in a cross-section of a clean and dry insulator unit.

It should be noted that these lines are much more concentrated and, therefore, the gradients are higher, near the cap and pin, where the discharges that cause the noise actually occur. The values of local potential gradients in an insulator unit, and therefore the noise levels, depend on the value of the voltage applied to the unit and, in the case of insulators consisting of several units, they also depend on the voltage distribution along the insulator string. This distribution tends to be less uniform as the number of units increases and, consequently, for the longer insulator strings or post insulators, it is necessary to have devices, such as metal rings, to improve the voltage distribution.

The current pulses producing the radio noise on a clean and dry insulator do not differ substantially between positive and negative polarity and, generally, the pulses occur between the zero and peak values of the applied power frequency voltage. The shape of these pulses and, consequently, the cut-off frequency of their spectrum, depend on the self-capacitance of the insulator and the surge impedance of the line to which the insulator is connected. For normal values of these parameters, the cut-off frequency is about 1 MHz. The noise produced by a clean and dry insulator is therefore limited to frequencies up to about 30 MHz and, generally, for insulators with average characteristics, fairly low levels are produced. Bad design and suitable bonding can, however, cause higher levels extending to higher frequencies. As is also the case with corona discharges at hardware, television reception is not usually affected by this type of radio noise.

If the insulator is lightly polluted and reasonably dry, for example in fair weather, the phenomenon described above is accompanied by corona discharges at surface irregularities caused by pollutants on the insulator. Generally this second phenomenon produces less serious effects than the first so that the noise levels, except in the case of certain types of pollution, for example near chemical works, are not significantly different from, or only slightly greater than, those occurring with a dry and clean insulator.

If the surface of the insulator is clean, but damp or wet, the existence of drops of water produces pronounced corona discharges which, generally, produce higher levels of radio noise than are produced by discharges from points of surface pollution. This latter phenomenon, in damp conditions, may become less important due to a better voltage distribution. The noise level is generally greater than with dry insulators but, again, it is limited to frequencies up to a few megahertz.

When the surface of the insulator is heavily polluted and wet, the phenomenon is completely different, since radio noise is produced by current pulses which flow when sparking occurs across the dry bands that are created by heating due to the passage of leakage currents on the surface of the insulator. The amplitude and number of these pulses depend on the voltage stress across the insulating dry bands, on the insulator shape and dimensions, on the surface conductivity of the pollutant layer and on the characteristic of the material at the surface of the insulator. The cut-off frequency of the spectra relating to these impulses may reach a few tens of megahertz and therefore the radio noise may also affect television frequencies. With wet and polluted glass or porcelain insulators, the radio noise at the normal voltage stresses, that are imposed by dielectric withstand requirements, may reach much higher levels than in other conditions previously described.

These levels may be reduced, not only by reducing the voltage stress, but also by using insulators of special characteristics. For instance, insulators made of organic material, or glass or porcelain insulators coated with grease, prevent the formation of a continuous damp layer, and therefore of leakage currents and dry bands, due to the water repelling properties of the surface. Consequently, these are adequate solutions for reducing the noise level in wet and polluted conditions. However, such insulators may no longer be noise-free when aged and their surfaces become contaminated and hence more wettable. The semi-conducting

Copyrighted material licensed to BR Demo by Thomson Reuters (Scientific), Inc., subscriptions.techstreet.com, downloaded on Nov-28-2014 by James Madison. No further reproduction or distribution is permitted. Uncontrolled when print

glaze type of insulator is also a possible solution, as it is characterized by relatively low noise levels in polluted conditions, since the conducting glaze improves the control of voltage distribution and the heat caused by the current flow in the glaze maintains dry bands which are sufficiently wide to sustain the applied voltage without sparking.

6.2 Correlation between radio noise voltage and the corresponding field strength for distributed and individual sources

6.2.1 General

This subclause deals with the problem of the correlation between the radio noise voltages of a single source of noise as can be measured in the laboratory, and the radio noise field strength actually generated in service by that source alone, or by a number of similar sources distributed along a line or present in a substation.

Usually, a number of single sources, with similar characteristics, are distributed along a line, for example insulators and spacers, or are present in a substation, for example post insulators, clamps and joints. Occasionally, however, the radio noise may be caused by just one source, for example the noise produced by a defective insulator or a loose or faulty hardware on a line, the injected noise from a substation, or the commutation noise from an a.c./d.c. convertor.

A single source of radio noise, for example an insulator string, can be represented as an ideal current generator producing a noise current I and connected between the energized conductor and ground. As shown in 4.5 of CISPR/TR 18-2, this current can be measured directly in the laboratory by using an appropriate test circuit simulating the actual circuit in service and by connecting the object under test, which includes the noise source, to that circuit. Though the noise current is the parameter which is constant between service and laboratory conditions, the results of a laboratory measurement are usually expressed in terms of the voltage V across a resistance R of 300 Ω, corresponding to about half the surge impedance of a typical line taken as a reference. The relationship between the level of the noise voltage V, in dB(μV), and the level of the noise current I, in dB(μA), is given by the expression:

$$I = V - 20 \lg 300 = V - 49{,}5$$

Briefly reviewed below are methods and formulae for calculating the correlation between the above current level I and the level of the generated electric field strength E. These methods and formulae apply only to frequencies up to a few megahertz.

6.2.2 Semi-empirical approach and formula

6.2.2.1 Overview

The general approach for establishing a quantitative correlation between the radio noise current I and the corresponding radio noise field strength E includes the following steps:

a) Single noise source
   - Determination of the current I of the source, which can be obtained directly in the laboratory from measurement of the voltage V.
   - Calculation of the noise current in each phase for the section of the line for which the profile of the radio noise field is to be calculated. This step takes into account longitudinal attenuation as well as mutual coupling between phases.
   - On the basis of the radio noise currents in the above line section, calculation of the radio noise fields due to these currents at different lateral distances from the line.
   - For each lateral distance the aggregate field is obtained by the summation of the above fields.

b) Multiple noise sources

Copyrighted material licensed to BR Demo by Thomson Reuters (Scientific), Inc., subscriptions.techstreet.com, downloaded on Nov-28-2014 by James Madison. No further reproduction or distribution is permitted. Uncontrolled when print

– Repetition of the calculations described for the single source for each source present in the phase under consideration.

– Aggregation of the noise fields for each distance from the line, calculated separately for each source on the phase under consideration.

The above approach determines the electric field strength E_k due to the sources of noise that are present on phase *k* of a line or a substation. Calculations are repeated for each phase on which noise sources are present. The aggregate field strength level *E* at each lateral distance is obtained, according to the rule described in [1], in adding 0 dB to 1,5 dB to the highest value of the field strength level calculated for each phase at the particular lateral distance. In normal cases involving three-phase lines, with the same distributed sources on each phase, the correction derived from the above rule is generally lower than 1 dB and hence it can be neglected. The aggregate field strength level *E* can therefore be evaluated by considering the sources of noise on the nearest phase only.

6.2.2.2 Formulae

On the basis of the above approach, the following semi-empirical formulae can be obtained:

a) Single noise source

1) In the case of lines with only one conductor, for example a monopolar d.c. line, the electric field strength level $E(x)$, in dB(µV/m), at a longitudinal distance *x*, in kilometres, from the injection point of the noise source generating a noise current level *I*, in dB(µA), and at a given lateral distance *y*, in metres, from the line, can be expressed by the following formula:

$$E(x) = I + A - Bx + C \qquad (3)$$

where *A* takes into account the splitting of the injected current on either side of the injection point. It can be calculated by means of the formula

$$A = 20 \lg \frac{Z_1}{Z_1 + Z_2}$$

where Z_1 and Z_2 are the surge impedances of the two sections on either side of the injection point. In the most common case of a single source of noise on a long line, for example a defective insulator, $Z_1 = Z_2$ and then $A = -6$ dB.

Term *Bx* expresses the attenuation of the current along the line. Coefficient *B*, in practice, lies between 2 dB/km and 4 dB/km; an average value of 3 dB can be assumed for frequencies around 0,5 MHz.

C expresses the correlation between the strength of the noise field and the noise current in the section of the line where the field is to be calculated. It can be determined experimentally, but it can also be obtained by making use of the following formula (for the meaning of the symbols see Figure 8):

$$C = 20 \lg \left[60 \left(\frac{h}{h^2 + y^2} + \frac{h + 2P_g}{(h + 2P_g)^2 + y^2} \right) \right]$$

For a direct distance *D* from the conductor of 20 m, that is to say the CISPR position, the value of *C* lies between 7 dB and 12 dB.

2) In the case of three-phase lines, a similar semi-empirical formula can be used for the determination of the electric field strength level $E(x)$ produced by the nearest phase:

$$E(x) = I + A + F(x) + C \qquad (4)$$

The most important difference between the two cases represented by formulae (3) and (4) is that in the case of a three-phase line the longitudinal attenuation cannot be expressed by means of only one attenuation constant; in this case the definition of an attenuation function $F(x)$ is necessary. Figure 9 shows an average trend of this

Copyrighted material licensed to BR Demo by Thomson Reuters (Scientific), Inc., subscriptions.techstreet.com, downloaded on Nov-28-2014 by James Madison. No further reproduction or distribution is permitted. Uncontrolled when print

attenuation function, based on the results of experiments performed on high voltage and extra high voltage lines. The other symbols in formula (4) are the same as in formula (3) [41, 45, 46, 47, 48, 49, 50].

b) Multiple noise sources

1) In the case of lines with only one conductor, the electric field strength level E, due to multiple noise sources equally distributed along the conductor, can be expressed by the formula:

$$E = I + A - 10 \lg (\alpha s) + C \qquad (5)$$

A and C are the same as in formula (3);

s is the distance between sources at the line in metres;

α is the attenuation constant per metre, and is related to coefficient B of formula (3) by means of the relationship:

$$\alpha = (B/8{,}7) \times 10^{-3}$$

The range of values assumed by coefficient α per metre, corresponding to the range of B given in the preceding paragraph is between 250×10^{-6} and 450×10^{-6}. Formula (5) applies to lines of infinite length and for shorter lines appropriate corrections can be applied.

2) In the case of three-phase lines, the electric field strength level E, due to distributed sources of noise on the three phases, can be calculated as follows:

$$E = I + A + (D - 10 \lg (s/500)) + C \qquad (6)$$

where the term $(D - 10 \lg (s/500))$ takes into account the aggregation of the noise sources along the line on the basis of an average attenuation law given in Figure 9. Average values of D lie between 10 dB and 12 dB. Formula (6) also applies to lines of infinite length and for shorter lines appropriate corrections can be applied.

6.2.3 Analytical methods

The correlation between noise current and noise field can also be evaluated by means of analytical methods similar to those already described in the case of the corona effect on conductors (see 5.3). When the radio noise current I, generated by an individual source on a conductor and injected into the conductor, is known, the determination of the electric field strength E, produced at a given position with respect to the conductor, is carried out by considering, in the first place, the splitting of the current I between the two sections of line, as seen from the injection point. For example, in the case of a source of noise on a line of infinite length, the current propagating along the conductor is then calculated and, finally, the field produced by the current at a given position is evaluated.

In the case of lines with only one conductor, for example a monopolar d.c. line, the calculation process is relatively simple, as all it calls for is a knowledge of the attenuation constant as a function of the frequency and the resistivity of the soil.

In the case of lines with more than one conductor, three-phase a.c. lines, bipolar or homopolar d.c. lines, the calculation of propagation of the noise is less simple and is generally dealt with by modal analysis. The complete modal theory is relatively complex and various more or less simplified procedures have been developed [2, 3, 8, 42, 43, 44]. The principle, however, remains substantially the same and the actual system of radio noise currents, or voltages, is reduced to a few simple systems, characterized by simpler laws of propagation similar to those that exist for a system with only one conductor. It is then a question of applying similar calculations to each system and then aggregating the individual fields in order to determine the resultant field.

Copyrighted material licensed to BR Demo by Thomson Reuters (Scientific), Inc., subscriptions.techstreet.com, downloaded on Nov-28-2014 by James Madison. No further reproduction or distribution is permitted. Uncontrolled when print

Where several sources are distributed on one of the three phases, the calculation process is much the same as previously described for the single source. In this case, account has only to be taken of the aggregation of the various sources of noise which are usually assumed to be of the random type.

In the case of noise sources on all three phases, the calculation of the *E* field is carried out separately for the noise injected into each phase, and the total *E* field is obtained by the same processes as those described in 6.2.2.1.

6.2.4 Example of application

An example using the analytical method described above has been worked out with reference to a 420 kV line of infinite length having an average span length of 400 m and insulator strings producing a radio noise voltage, when referred to 300 Ω, of 49,5 dB(μV), that is, a radio noise current of 1 μA per string. These calculations have been performed by using suitable computing programs and the results are summarized in Figure 10, which also gives the data assumed in the calculations.

If the calculations are repeated using the semi-empirical formula (6), with reference to the CISPR position of 20 m from the nearest conductor and assuming an average value for *D* of 11 dB, the following value is obtained for the electric field strength level:

$$E = 0 - 6 + 11 - 10\,lg\,\frac{400}{500} + 20\,lg\,60\left(\frac{2\times 9}{20^2}\right) = \text{ 14,5 dB(μV/m)}$$

This is in good agreement with the value of 13,5 dB(μV/m) calculated by the analytical method (see Figure 10).

6.3 Influence of ambient conditions

Subclause 6.1 gives qualitative information on the effect of the ambient conditions; humidity, rain, fog, pollution, on the radio noise levels of insulators and hardware. This information is based essentially on a simplified analysis of the physical phenomena involved in the various situations. The knowledge of these physical phenomena is generally sufficient to establish qualitative variation laws of the radio noise levels as a function of the main parameters characterizing the surface conditions of the insulators and hardware.

On the other hand, some uncertainties still exist on the quantitative effects of these parameters. In particular some results of radio noise tests performed by different experimenters on lightly polluted insulators, especially in dry conditions, are not quite consistent. There is at present no agreed procedure for simulating in the laboratory the most common service conditions of lightly polluted insulators nor the implementation of any relevant test results as referred to in CISPR/TR 18-2.

The matter is under consideration and will be reviewed when the results of studies within CIGRÉ yield agreed and conclusive data.

7 Sparking due to bad contacts

7.1 Physical aspects of the radio noise phenomenon

Not bonded conducting parts of a power line or substation, or even such items as nearby metal fences or rain-water guttering, when in the strong electric field of high voltage power lines and associated equipment, can become electrically charged and the potential difference between adjacent conducting parts will increase even if both parts are floating, that is to say they are not connected to a line conductor or to earth.

Copyrighted material licensed to BR Demo by Thomson Reuters (Scientific), Inc., subscriptions.techstreet.com, downloaded on Nov-28-2014 by James Madison. No further reproduction or distribution is permitted. Uncontrolled when print

If the distance separating the conducting parts is small, the increasing field strength in the intervening space may reach the critical level and lead to a complete breakdown of the gap. Avalanche ionization initiates the development of an arc, gap discharge occurs, the potential difference across the gap then falls to a low level and the arc extinguishes. The whole sequence of events can be repeated when the parts become re-charged, as the space is once again electrically stressed and the next gap discharge takes place.

The repetition rate of this sequence depends on the charging and discharging time constants of the circuit and the value of the surrounding electric field, as well as on the length of the gap. Individual sparks can occur at many hundreds to a few thousands of times per second. The repetition rate is, however, at least one order of magnitude lower than the range of repetition rates of corona discharges.

The probability of a particular gap sparking over is, of course, greater around the peaks of the power frequency voltage. When the line voltage and consequently the field strength in the gap, exceeds a critical value, a train or burst of sparks is generated during each half-cycle.

The significant factor in the shape of the discharge pulse is its steep rise time and, consequently, a broad range of high frequencies is produced and emitted. A comparison between the frequency spectra of the radio noise field from corona and gap-type discharges, at a particular distance from the line, is shown in Figure 11. The emitted frequencies may extend to a few hundred megahertz. If the discharge process excites a hardware or component which is capable of oscillating at a particular frequency, due to its geometrical dimensions, energetic narrow-band radiation at this frequency may occur as the hardware or component acts as a tuned antenna. Therefore, gap-type discharges may cause interference to the reception of both a.m. radio signals and the vision signals of television. By contrast, f.m. radio, in the v.h.f. band, the audio signals of television are less likely to be affected by this type of interference.

Propagation along the line, with the associated electric and magnetic fields, and radiation are the routes by which the disturbing radio frequencies reach the receiving antenna. It has been observed, in practice, that noise at frequencies corresponding to the long and medium wave bands propagates some tens of kilometres along the line. At television and f.m. radio frequencies the propagation along the line is less important than radiation from the source. Line geometry, resistance of the underlying ground and the frequency are of major importance to propagation. For the higher frequencies, the attenuation along the line is greater and the distance of propagation is shorter.

Significant levels of the radio noise field are normally confined to the immediate vicinity of the line, possibly reaching out to a few hundred metres on either side. If, however, a resonant condition occurs in a hardware or component, a narrow band of radiation may be measured at distances of up to a few kilometres. A curve showing a typical relationship between field strength and distance is shown in Figure 12. The fluctuations are the result of the interaction of the direct wave with the ground-reflected wave.

7.2 Example of gap sources

Gap sources on overhead lines may be due to lightly weighted cap and pin insulators, where the weight of the insulator is insufficient to prevent the metal contact surfaces from oxidizing, or with corroded metal parts, or faulty joints. In the case of porcelain string insulator units, it has been found that sparks can be produced by discharges in small voids in the porcelain. Broken insulators, paint layers and even objects not forming part of a transmission line, such as nearby not bonded metal fences or gutters, may give rise to gap discharges.

Where wood poles are used for power lines, sparking may occur between items of metal hardware which can lead to severe interference to television reception. This usually occurs due to the shrinking or swelling of the wood with variations in the humidity. As the wood shrinks, nuts and bolts used to hold the cross-arms in place, or to fasten insulator pins to the pole or cross-arm, can become slightly loose. If any corrosion is present between the nut and bolt, or the washer if one is used, an imperfect contact results and sparking takes place.

Copyrighted material licensed to BR Demo by Thomson Reuters (Scientific), Inc., subscriptions.techstreet.com, downloaded on Nov-28-2014 by James Madison. No further reproduction or distribution is permitted. Uncontrolled when print

Another source of television interference from wood-pole lines can arise from the staples used to fasten the earth wire to the pole. As there are potential differences between sections of the pole, the staples may spark over to the earth wire, particularly if there is any corrosion between them.

Finally, the contact between a pin-type insulator and phase conductor can be a source of sparking at the tie-wire, where the conductor rests in the top groove, or at the stirrups in the side groove. The problem is the small, highly stressed, pockets of air between the conductor and the insulator that may spark over.

Care shall be taken both during the erection of the line to ensure good workmanship throughout and, in the subsequent maintenance, to ensure that any defects caused, for example by vandalism, are found and the necessary remedial action taken. Special attention should be given to the design and maintenance of equipment to ensure the durability and adequacy of contacts at, for example, air-break isolating switches, the flexible connections provided in the design of such switches, fuse-mounts and line taps.

Gap discharges are strongly influenced by the weather. It is only in dry weather that a small gap between, for example, two conductive parts provides insulation which can break down. In wet weather the gap may be bridged with water thereby establishing a conducting path. Therefore, interference caused by gap discharges is a phenomenon that is normally associated with fair weather and it is usually absent in wet weather. Consequently, this type of interference is often referred to as dry noise.

8 Special d.c. effects

8.1 General

High voltage d.c. transmission systems can generate radio noise in two quite different ways: firstly, by the normal operation of the main convertor valves, which may be of the mercury arc type or thyristors and, secondly, by corona discharge and associated phenomena on the high voltage equipment, busbars and overhead lines. It is therefore necessary to take into consideration:

a) the effect of d.c. corona;

b) the effect of valve firing.

Compared with high voltage a.c. transmission systems, the problem of radio noise from high voltage d.c. systems is not so important, as only relatively few are in operation throughout the world. Consequently, experience of radio interference problems associated with high voltage d.c. systems is less than that with high voltage a.c. systems. Most of the information on high voltage d.c. interference has been obtained from test lines and cages, and the remainder from existing systems.

High voltage d.c. transmission systems are at present operating at voltages up to ± 800 kV and, in the near future, even higher voltages will be used [57].

8.2 Effects of corona from conductors

Although the causes of radio noise from high voltage d.c. systems, due to corona discharges on line conductors, insulators and hardware, is the same as for a.c., there are some noticeable differences in the effects.

The physical aspects of a.c. corona were discussed in 5.1, but the corona mechanism with d.c. is different because:

a) a stationary ionization sheath is created around each conductor;

Copyrighted material licensed to BR Demo by Thomson Reuters (Scientific), Inc., subscriptions.techstreet.com, downloaded on Nov-28-2014 by James Madison. No further reproduction or distribution is permitted. Uncontrolled when print

b) a space charge is built up in the remaining space between the conductors and ground and between the conductors themselves.

The ionization acts partly as a shield, which modifies the electric field close to the conductor and, due to the space charge, the actual electric field differs markedly from the theoretical static field.

For an a.c. line, no stationary space charge exists and the ionization effects around the conductor act in a different manner.

Corona discharges are always initiated by collisions of free electrons with stable atoms. These electrons exist in the atmosphere under all normal conditions and move away from the negative conductor and towards the positive conductor. This leads to a significant difference between the two resulting forms of corona. Negative corona discharges occur at a high repetition frequency and moderate amplitude, whilst those near the positive conductor are less frequent and have much larger amplitude.

The radio noise characteristics: level, frequency, spectrum and lateral profile of a high voltage d.c. line are determined by:

– design parameters;
– line voltage, or conductor surface voltage gradient and polarity;
– weather conditions.

The subjective effects of a d.c. noise field are less than those from the field, of identical strength, from an a.c. line because of the different character of the noise.

Design parameters

Unlike a.c. lines, a d.c. line is normally either monopolar, with earth or sea/earth return, or bipolar, with single or bundle conductors. The insulator length and the pole spacing can be relatively small because the internal overvoltages are significantly lower than with a.c., due to rapid fault clearance by valve blocking, and usually the insulator length is determined more by pollution than by overvoltages.

Line voltage, or conductor surface voltage gradient and polarity

In the case of d.c. lines, the choice of the line voltage is influenced not only by economic reasons but also by the layout of the convertor stations and valves. Although there is no standardization of this voltage, d.c. lines at present in service usually operate between ± 200 kV and ± 800 kV. However, in the near future, the voltage level will be raised considerably. The voltage of any high voltage line has a most important influence on the generation of radio noise. This influence depends on the surface stress, or gradient, of the conductors. If, for an a.c. line, a gradient of E kV/cm r.m.s. is used, the comparable gradient for a d.c. line would then be $\sqrt{2}\,E$ kV/cm. The d.c. line will, however, produce a lower noise level than the a.c. line.

Disregarding the effects of ionization and space charge, the theoretical gradient can be calculated as for a.c. lines (Clause 5) and this value is also used for radio noise calculations. The influence of this gradient on the radio noise level was investigated on several test lines and the results show that over the range 20 kV/cm to 27 kV/cm the radio noise level increases at approximately 1,6 dB for each 1 kV/cm increment and above about 27 kV/cm the noise level increases at lower rate.

The lateral profile of a bipolar d.c. line, with corona-free earth wires, is nearly symmetrical about the positive conductor. This behaviour can be explained by the fact that the negative conductor produces a lower level of radio noise than the positive conductor, because of the different ionization mechanisms indicated in this subclause. With the same gradient for both conductors the difference in their radio noise level contributions is at least 6 dB.

Copyrighted material licensed to BR Demo by Thomson Reuters (Scientific), Inc., subscriptions.techstreet.com, downloaded on Nov-28-2014 by James Madison. No further reproduction or distribution is permitted. Uncontrolled when print

Hence the contribution from the negative conductor to the aggregate radio noise level of a bipolar line may be considered to be negligible. For a negative monopolar line, the noise level may be even 20 dB lower than for the same line with positive polarity.

Weather conditions

It is well known that the radio noise level from a.c. lines is significantly influenced by the weather conditions. Between fair weather and heavy rainfall this level may increase by up to 25 dB but in the case of d.c. lines the noise level actually reduces in rain.

Thus the highest radio noise level of a d.c. line normally occurs under conditions of fair weather. At the beginning of rainfall and for dry snow precipitation, this level may rise for a short time but when the conductors are fully wet it will decrease by up to 10 dB and in some cases even more. The level may also be influenced by the line configuration and the voltage gradient and the above remarks apply to bipolar and to positive monopolar lines. However, the 80 %/80 % criteria, discussed in 4.3 of CISPR/TR 18-2, are still valid.

As an explanation of this difference in behaviour, when compared with a.c. lines, various hypotheses could be given, but they still have to be proven and further investigations are necessary.

Another area where the performance of d.c. lines differs from a.c. lines is the influence of wind. Some investigations have indicated that for a wind direction from the negative to the positive conductor the radio noise level increases with wind speeds above 3 m/s from 0,3 dB to 0,5 dB for each 1 m/s increment. For a wind direction from the positive to the negative conductor this effect is significantly lower.

Furthermore, the long-term radio noise level of a d.c. line is influenced by seasonal effects; in summer the level is normally higher than in winter by approximately 5 dB. This may be caused by insects and airborne particles on the conductor surface, or by the absolute humidity of the air.

Frequency spectrum

In the case of a.c. lines, the radio noise spectrum is one of the main characteristics of a high voltage line. The frequency spectrum for d.c. lines seems to show a similar shape over the long and medium wave broadcast bands but further investigations should be made.

Subjective effects

Investigations have shown that for d.c. lines, a lower signal-to-noise ratio (SNR) may be acceptable than for a.c. lines given in 4.3 of CISPR/TR 18-2. For a particular reading on a CISPR measuring receiver, the subjective annoyance of a d.c. line could be less than for an a.c. line by as much as 10 dB.

Calculation of the radio noise level due to conductor corona

The radio noise level of a.c. lines, due to conductor corona, can be calculated by using analytical methods or experimental formulae. Both are based on the results of many measured values derived from test lines, test cages and operational lines. In the case of d.c. lines, experience is relatively scanty, the data coming almost entirely from test facilities.

The analytical methods that can be applied to d.c. lines are similar, in principle, to those described in Clause 5 for a.c. lines. Obviously, in this case, use shall be made of the excitation function results (see 5.2) for measurements on d.c. test lines or cages, and account should be taken of the propagation characteristics of d.c. lines.

Copyrighted material licensed to BR Demo by Thomson Reuters (Scientific), Inc., subscriptions.techstreet.com, downloaded on Nov-28-2014 by James Madison. No further reproduction or distribution is permitted. Uncontrolled when print

As for a.c. lines different empirical formulae for the calculation of the radio noise level for d.c. lines have been evolved. Based on extensive measurements on lines [55], with various configurations, the following formula is suggested for a bipolar line:

$$E = 38 + 1{,}6\,(g_{max} - 24) + 46 \lg r + 5 \lg n + \\ + \Delta E_f + 33 \lg \frac{20}{D} + \Delta E_w \quad \text{in dB(µV/m)}$$

where

E is the level of the radio noise field strength in dB(µV/m);

g_{max} is the maximum surface gradient of the line, in kV/cm;

r is the radius of conductor or subconductor, in cm;

n is the number of subconductors;

D is the direct distance between antenna and nearest conductor, in m;

ΔE_w is the correction for different weather condition, in dB;

ΔE_f is the correction for different measurement frequency, in dB (see below).

The value g_{max} is calculated as for a.c. lines. The first line of the formula gives the level for the CISPR reference frequency of 0,5 MHz and for the CISPR position, i.e. at a direct distance of 20 m from the nearest conductor in fair weather, when ΔE_f, $\lg \frac{20}{D}$ and ΔE_w are all zero.

The above formula is basically intended to be used for bipolar lines. It can also be used for positive monopolar lines if the correct conductor voltage gradient is applied. For the same applied pole voltage, the noise will be lower than on the bipolar line by 3 dB to 6 dB. Regarding bipolar transmission lines, built as two separate monopolar lines, the monopolar character will dominate if the pole distance is greater than about 20 m.

Measurements have shown that the rate of lateral attenuation for d.c. lines is similar to that for a.c. lines. Over the frequency range 0,4 MHz to 1,6 MHz and for a distance of around $\frac{300}{2\pi f}$ m, where f is to be taken as the numerical value of the frequency, in MHz, the following approximate formula will give satisfactory results:

$$\frac{E_2}{E_1} = \left(\frac{D_1}{D_2}\right)^{1,65}$$

where

E_2 and E_1 are the noise field strength values at the direct distances D_2 and D_1, respectively; and

E_1 and D_1 are the reference values.

For the direct distance D_0 of 20 m from the nearest conductor and using logarithmic terms, this formula may also be written as:

$$E_2 = E_1 + 33 \lg \frac{20}{D_2}$$

The distance expression $33 \lg \frac{20}{D_2}$ is an approximation which tends to give a low correction up to about 100 m and high correction beyond this distance.

Copyrighted material licensed to BR Demo by Thomson Reuters (Scientific), Inc., subscriptions.techstreet.com, downloaded on Nov-28-2014 by James Madison. No further reproduction or distribution is permitted. Uncontrolled when print

A considerable variation in the measured results of the frequency spectrum at different locations has so far been obtained, particularly at low frequencies. However, the frequency spectrum shown in Figure B.12 and discussed in 4.3.2, which is valid for a.c. lines, seems also to constitute a good average relationship for d.c. lines and it is, therefore, suggested that this spectrum be used until more reliable material is available. The correction according to this spectrum can be written:

$$\Delta E_f = 5\ (1 - 2(\lg 10 f)^2) \quad \text{in dB}$$

where f is the numerical value of the measurement frequency, in MHz.

This expression can be used from 0,15 MHz up to about 3 MHz.

For a negative monopolar line, the radio noise level from the pole conductor itself is normally low but, if an earth wire is used, the earth wire will act as a positive conductor and the noise level can be calculated as above.

8.3 Radio noise due to insulators, hardware and substation equipment

There is a lack of information concerning the radio noise level produced by insulators, hardware and substation equipment. Available experience indicates, however, that there will be no significant difference from the equivalent level of a.c. lines given in Clause 7.

Under dry weather conditions, the radio noise level produced by conductor corona may dominate for the higher voltage gradients. However, the radio noise level of a d.c. line conductor decreases when the conductor is wetted, and this is in contrast to the level produced by the line insulators, as the leakage current on these insulators is determined by the ohmic resistance of the pollution. From service experience it is known that, even in districts with a relatively low level of industrial pollution, the surface of d.c. insulators becomes polluted in a relatively short time. When this polluted surface becomes wet, partial discharges occur which may cause a relatively high increase in the radio noise level. Hence it is possible that the difference found in the reduction of the noise level from d.c. lines, under some conditions (see under weather conditions, above), may be influenced by the behaviour of the polluted insulators. For confirmation of this assumption, more information is necessary.

8.4 Valve firing effects

As well as overhead lines, underground cables and substations, high voltage d.c. transmission systems include convertor stations with their valve equipment. These valves can generate radio noise by their special operational performance, as they are acting as very fast switches.

A convertor group normally comprises six valves fired cyclically at the power frequency and a complete convertor installation may be made up of several such convertors. Each time a valve is fired the voltage across it collapses and a wide spectrum of radio noise is generated extending from very low frequencies to a few megahertz depending on the physical dimensions of the connections. Because of lumped and distributed capacitances and inductances in the associated connections and equipment, local loops may resonate and this will produce peaks at certain frequencies.

This radio noise may be emitted directly from the valves and associated equipment comprising, in this instance, mainly the feeders and the busbars of the convertor station. These busbars will often be of considerable length and well able to act as efficient radiators. The convertor will be, of course, connected to incoming and outgoing a.c. and d.c. circuits and these may both be of overhead line construction. The radio noise will be guided and emitted from such overhead lines.

Copyrighted material licensed to BR Demo by Thomson Reuters (Scientific), Inc., subscriptions.techstreet.com, downloaded on Nov-28-2014 by James Madison. No further reproduction or distribution is permitted. Uncontrolled when print

With any suppression measures, the radio noise level could be intolerable and it is, therefore, necessary to reduce this level to an acceptable value. This can be achieved by different methods which depend on the valve type and the technical installation of the substation.

In most of the earlier operational high voltage d.c. schemes, mercury valves were used. The technical layout of this valve type requires a hall which protects the valves against environmental influences and makes it possible to keep temperature limits within a specified range. By electromagnetic screening of these halls the radio noise level outside can be reduced considerably. Using solid metal sheets or wire mesh, an attenuation value of 40 dB to 50 dB for frequencies between 0,15 MHz and 5 MHz is possible. To reduce the noise passing through the valve hall bushings, filters should be installed in all outgoing lines and the filtering of the d.c. lines shall be especially effective. The convertor transformers, between the valve group and the a.c. lines, and the filter circuits on the a.c. side, may reduce the possible conduction of radio noise from the convertor station to these a.c. lines.

In the case of thyristor valves the radio noise problem may be somewhat less severe. Thyristor valves, when fired, may have a voltage collapse time of up to 25 µs, compared with 1 µs for mercury-arc valves. One reason for this is the use of damping circuits within the thyristor valve. With such a long voltage collapse time, it may not be necessary to screen the valve, hall, and radio noise filters may be simpler or even unnecessary.

A possible solution for reducing direct radiation from a valve is the installation of the thyristor valve within a steel tank which acts as an effective screen. Care should be taken that the tank does not radiate as a dipole or resonator.

The further development of high voltage d.c. convertor stations will tend towards more compact layouts with shorter connections between valve groups, convertor transformers and substations. This will have a favourable influence on the reduction of radio noise from convertor stations.

Generally, it is possible to reduce the radio noise produced by convertor valves and their auxiliaries to an acceptable level. The costs of such a reduction largely depend on the valve type and the convertor station design.

Copyrighted material licensed to BR Demo by Thomson Reuters (Scientific), Inc., subscriptions.techstreet.com, downloaded on Nov-28-2014 by James Madison. No further reproduction or distribution is permitted. Uncontrolled when print

9 Figures

This clause contains the figures referred to elsewhere in this technical report.

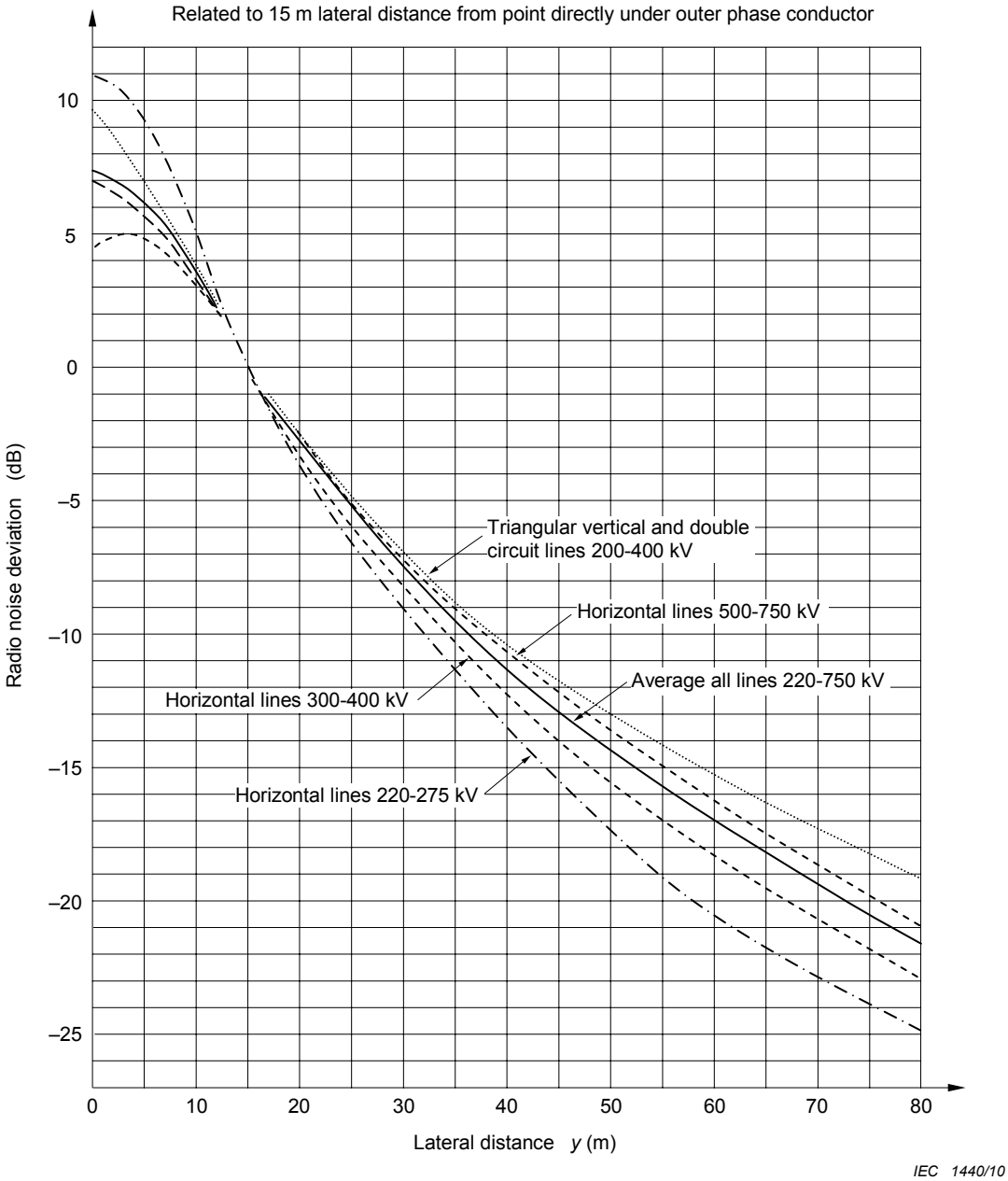

Figure 1 – Typical lateral attenuation curves for high voltage lines, normalized to a lateral distance of y_0 = 15 m, distance in linear scale

Copyrighted material licensed to BR Demo by Thomson Reuters (Scientific), Inc., subscriptions.techstreet.com, downloaded on Nov-28-2014 by James Madison. No further reproduction or distribution is permitted. Uncontrolled when print

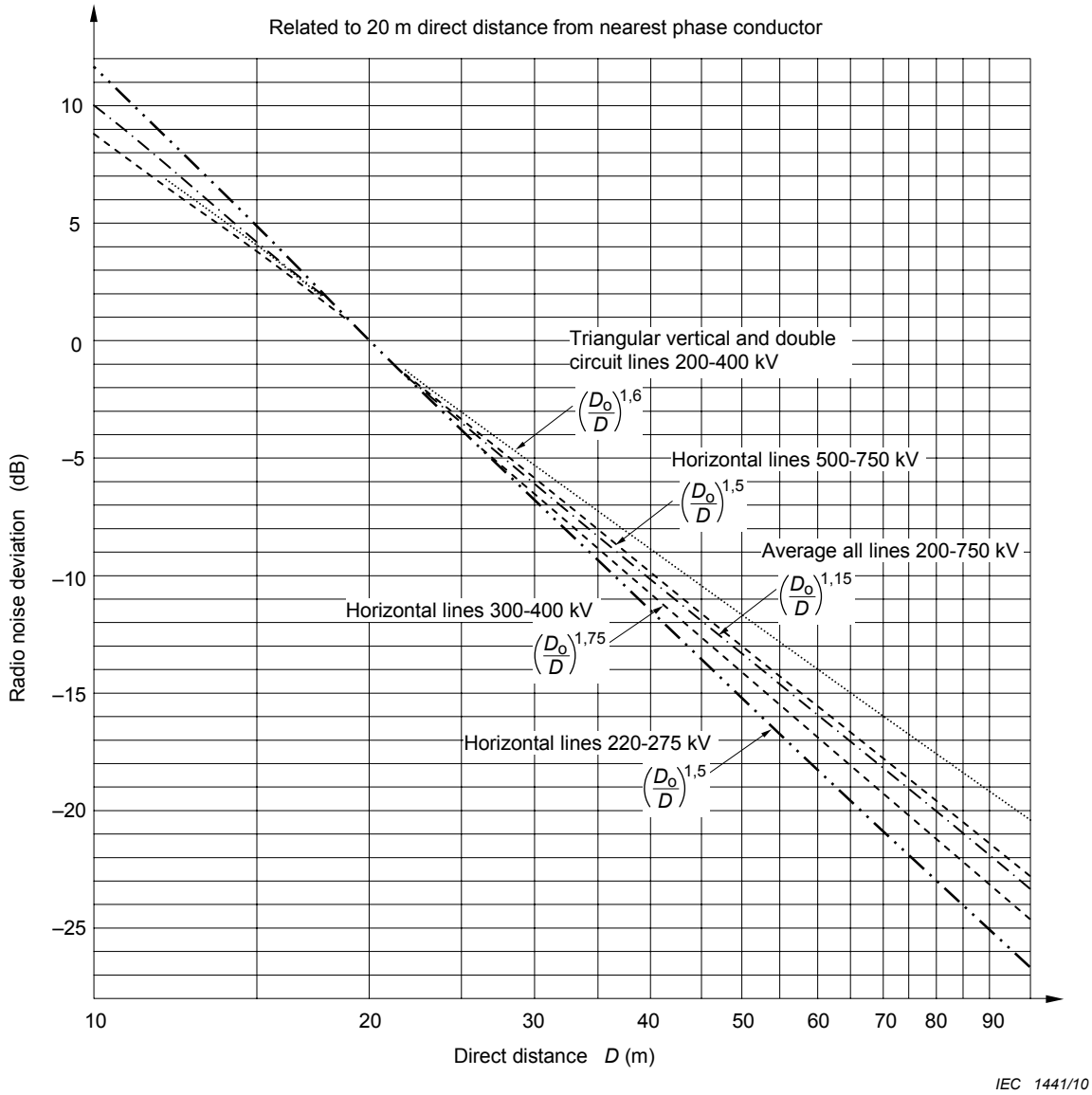

Figure 2 – Typical lateral attenuation curves for high voltage lines, normalized to a direct distance of D_0 = 20 m, distance in logarithmic scale

Copyrighted material licensed to BR Demo by Thomson Reuters (Scientific), Inc., subscriptions.techstreet.com, downloaded on Nov-28-2014 by James Madison. No further reproduction or distribution is permitted. Uncontrolled when print

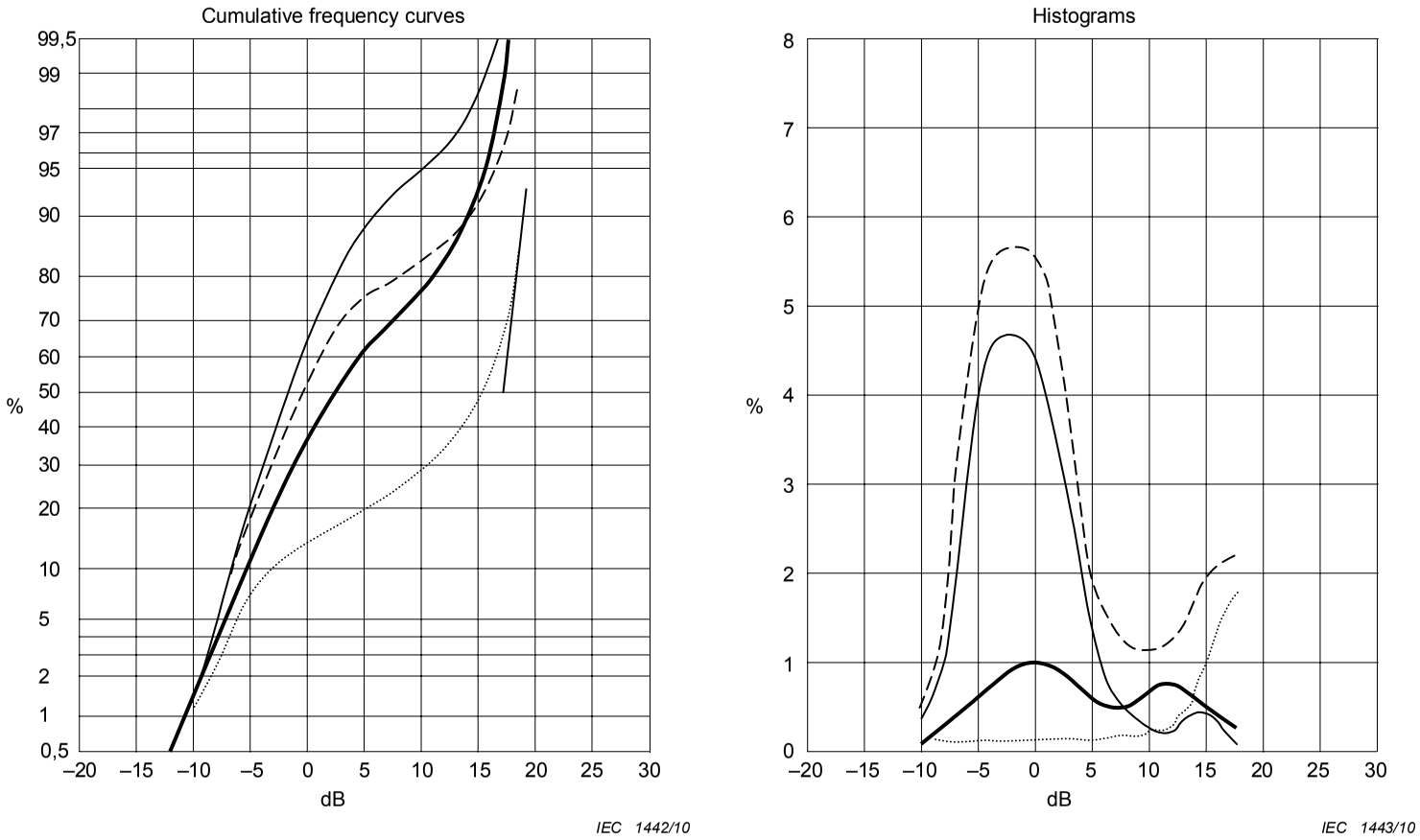

– – – – – -100 % overall ——— 66 % fair weather ━━━ 21 % immediately before and after rain ····· 13 % rain

Relative radio-noise levels: dB(µV/m) 50 %, all weathers

420 kV line – Single 50 mm conductor – Voltage gradient 15 kV/cm – ITALY

Figure 3a **Figure 3b**

Figure 3 – Examples of statistical yearly distributions of radio-noise levels recorded continuously under various overhead lines

Copyrighted material licensed to BR Demo by Thomson Reuters (Scientific), Inc., subscriptions.techstreet.com, downloaded on Nov-28-2014 by James Madison. No further reproduction or distribution is permitted. Uncontrolled when print

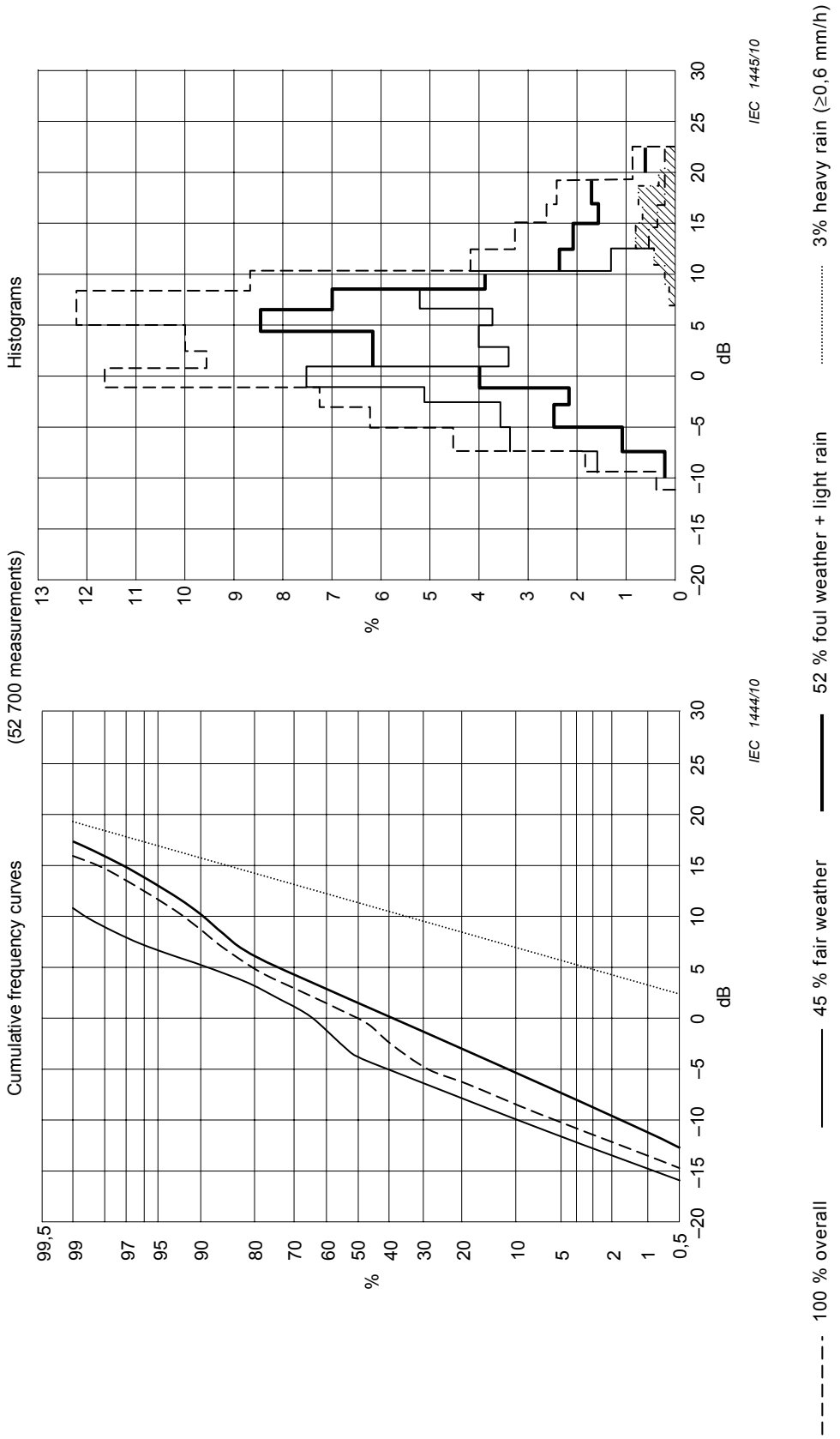

Relative radio-noise levels: dB/µV/m) 50 %, all weathers

400 kV line GÉNISSIAT-ALBERTVILLE – 2 × 26,4 mm conductors – FRANCE

Figure 4a **Figure 4b**

Figure 4 – Examples of statistical yearly distributions of radio-noise levels recorded continuously under various overhead lines

Copyrighted material licensed to BR Demo by Thomson Reuters (Scientific), Inc., subscriptions.techstreet.com, downloaded on Nov-28-2014 by James Madison. No further reproduction or distribution is permitted. Uncontrolled when print

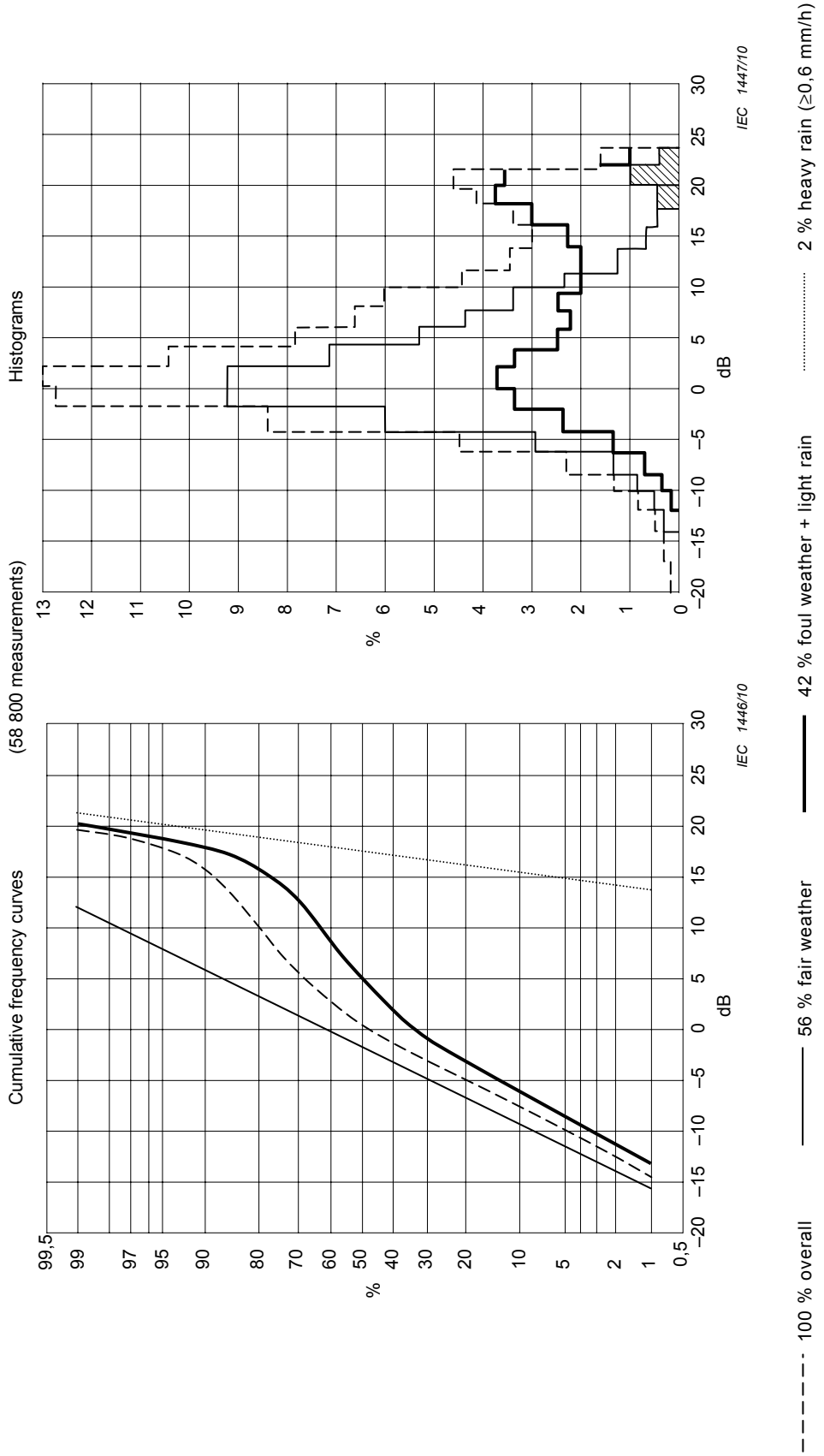

Relative radio-noise levels: dB(µV/m) 50 %, all weathers

Experimental line (1,2 km long) at 750 kV – France

Figure 5a **Figure 5b**

Figure 5 – Example of statistical yearly distributions of radio-noise levels recorded continuously under various overhead lines

Copyrighted material licensed to BR Demo by Thomson Reuters (Scientific), Inc., subscriptions.techstreet.com, downloaded on Nov-28-2014 by James Madison. No further reproduction or distribution is permitted. Uncontrolled when print

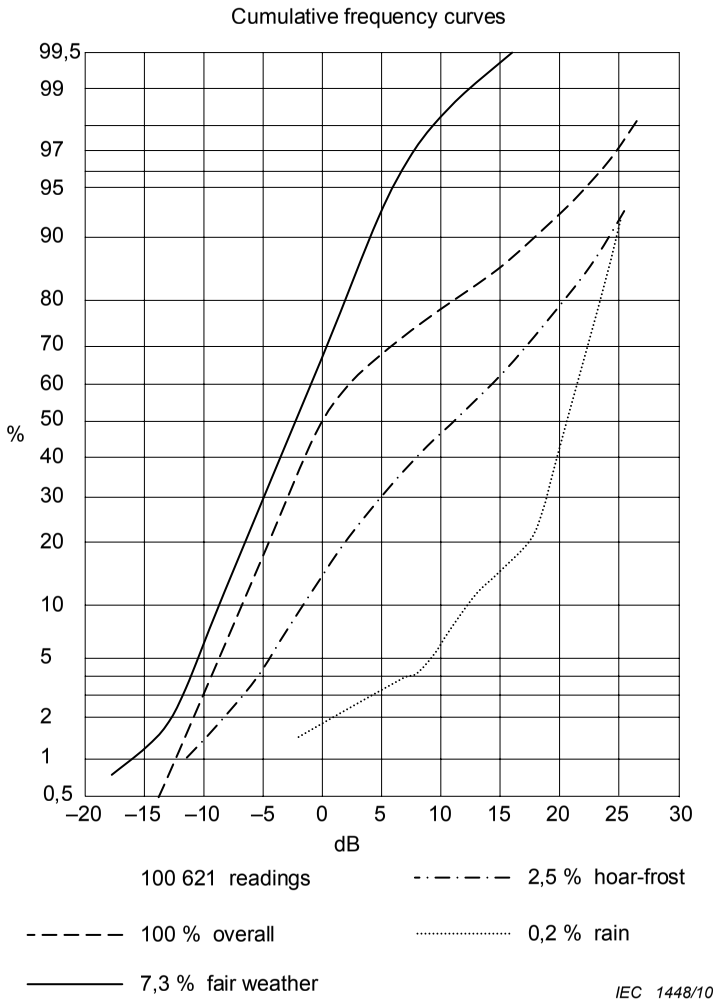

Figure 6a

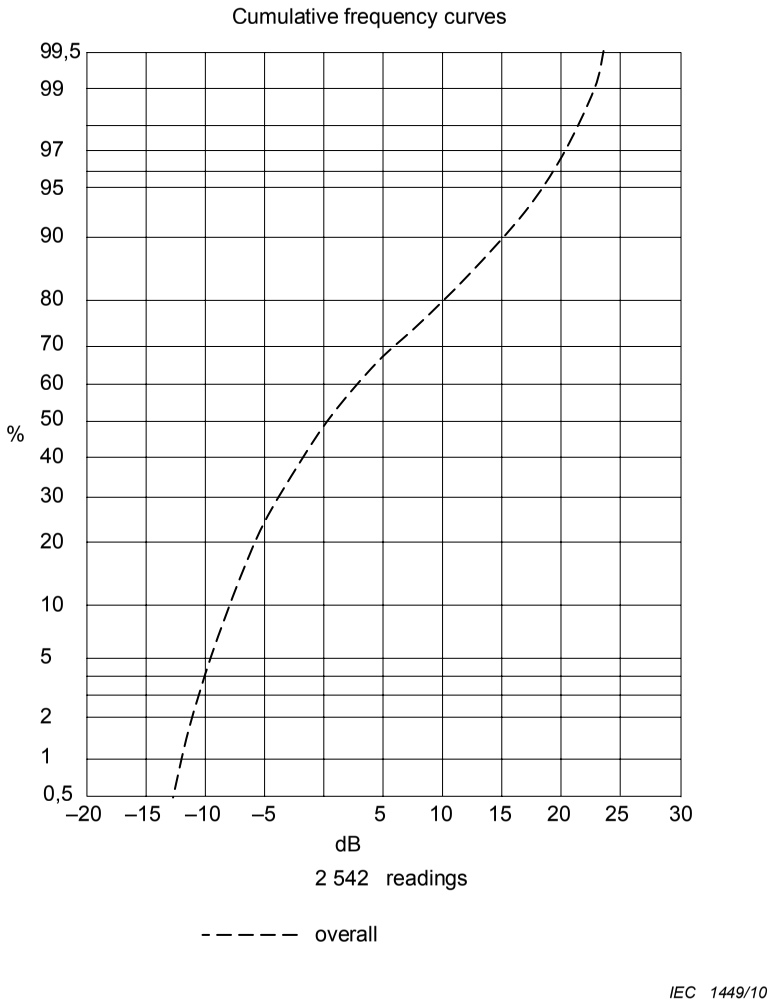

Figure 6b

Relative radio-noise levels: dB(µV/m) 50 %, all weathers

450 kV line – SWEDEN – Conductor 2 × 593 mm2, ACSR

Line 525 kV – UNITED STATES OF AMERICA

Figure 6 – Examples of statistical yearly distributions of radio-noise levels recorded continuously under various overhead lines

Copyrighted material licensed to BR Demo by Thomson Reuters (Scientific), Inc., subscriptions.techstreet.com, downloaded on Nov-28-2014 by James Madison. No further reproduction or distribution is permitted. Uncontrolled when print

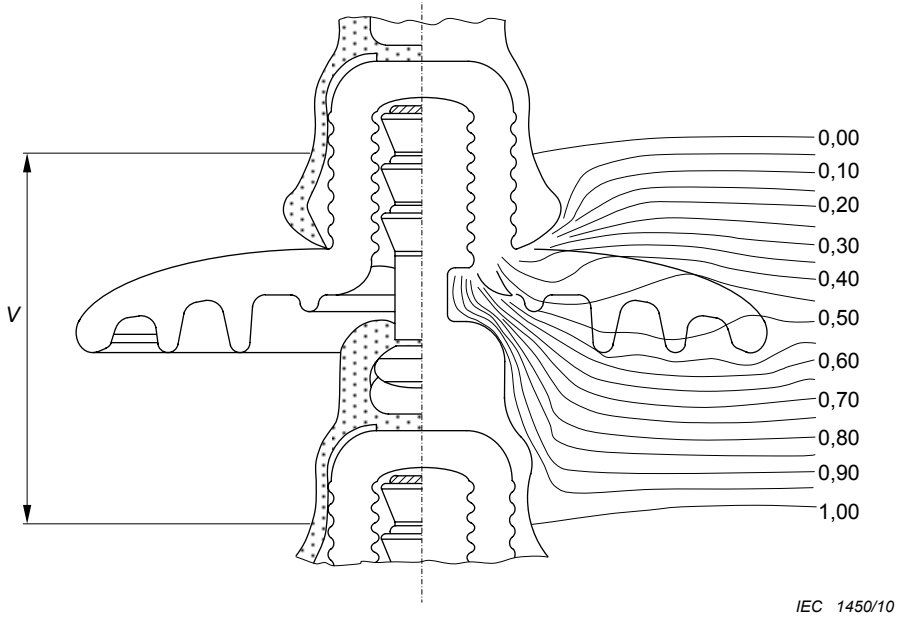

Source : The diagram is drawn from the report: L. Paris, M. Sforzini: *L'isolamento delle linee a 370 kV: criteri di progetto dedotti da una serie di prove comparative*. Rendiconti della LXV Riunione Annuale dell'AEI, Palermo, 1964 [58].

Figure 7 – Equipotential lines for clean and dry insulation units

Copyrighted material licensed to BR Demo by Thomson Reuters (Scientific), Inc., subscriptions.techstreet.com, downloaded on Nov-28-2014 by James Madison. No further reproduction or distribution is permitted. Uncontrolled when print

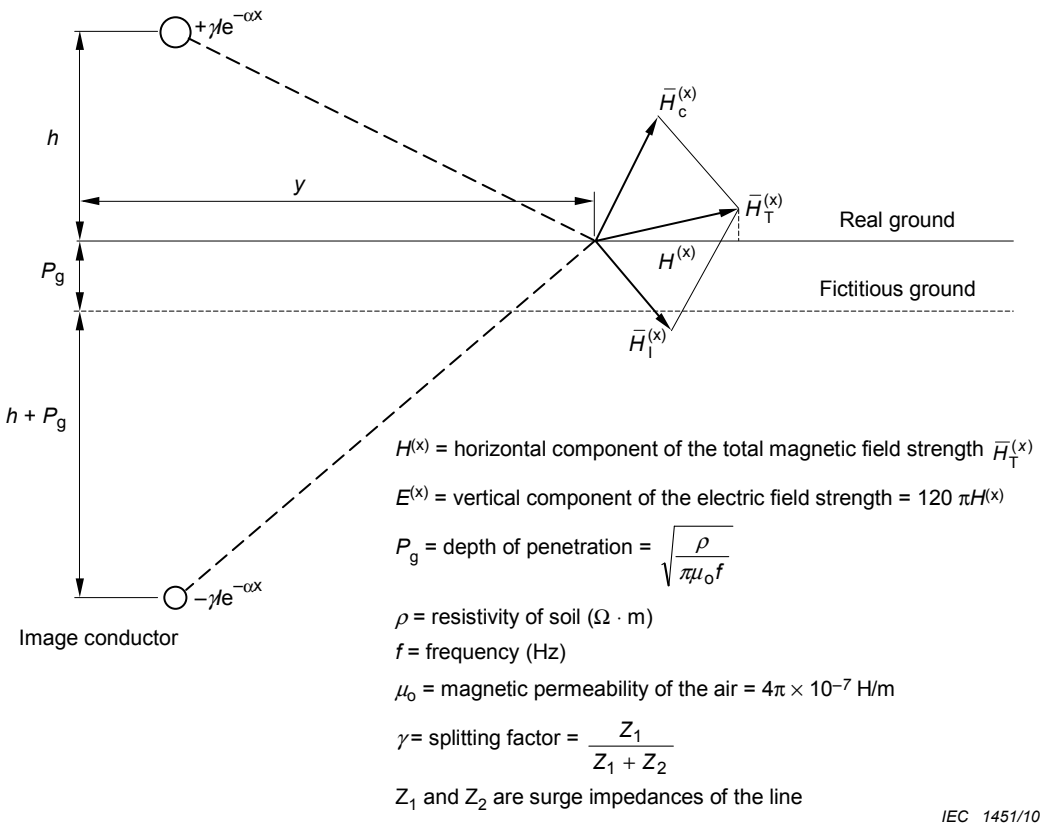

Figure 8 – Determination of the magnetic field strength from a perpendicular to a section of a line, at a distance *x* from the point of injection of noise current *I*

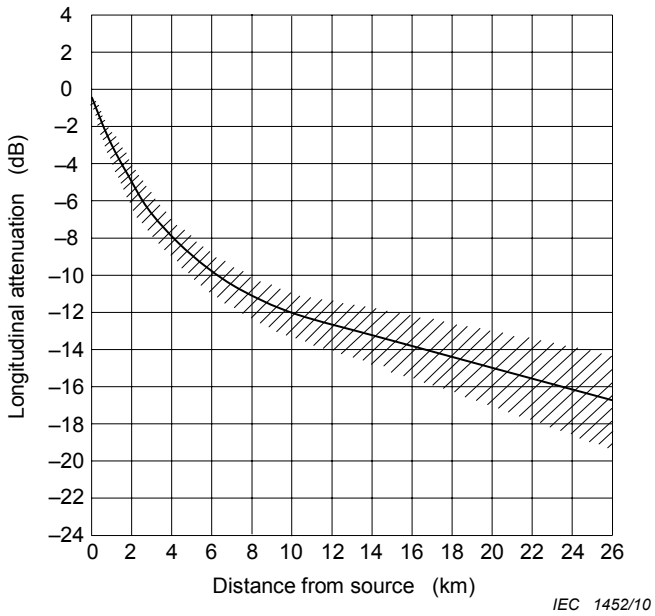

Figure 9 – Longitudinal noise attenuation versus distance from noise source (from test results of various experiments frequencies around 0,5 MHz)

Copyrighted material licensed to BR Demo by Thomson Reuters (Scientific), Inc., subscriptions.techstreet.com, downloaded on Nov-28-2014 by James Madison. No further reproduction or distribution is permitted. Uncontrolled when print

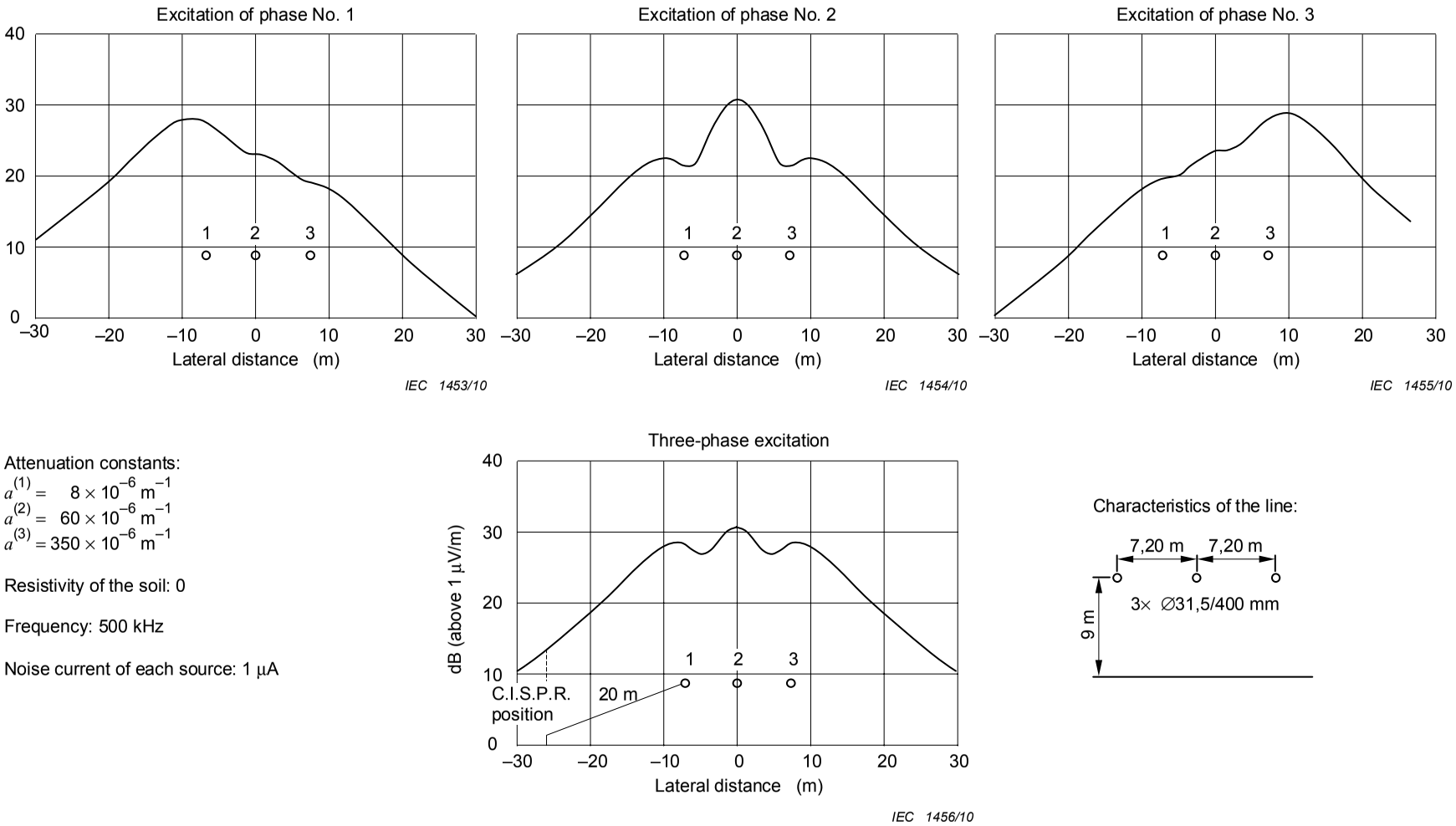

Figure 10 – Lateral profile of the radio noise field strength produced by distributed discrete sources on a 420 kV line of infinite length

Copyrighted material licensed to BR Demo by Thomson Reuters (Scientific), Inc., subscriptions.techstreet.com, downloaded on Nov-28-2014 by James Madison. No further reproduction or distribution is permitted. Uncontrolled when print

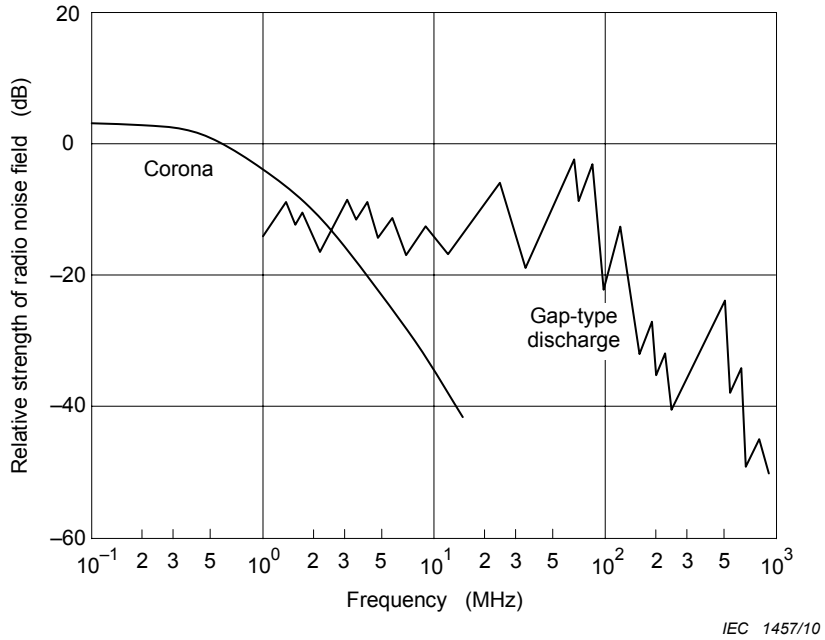

Figure 11 – Example of relative strength of radio noise field as a function of frequency

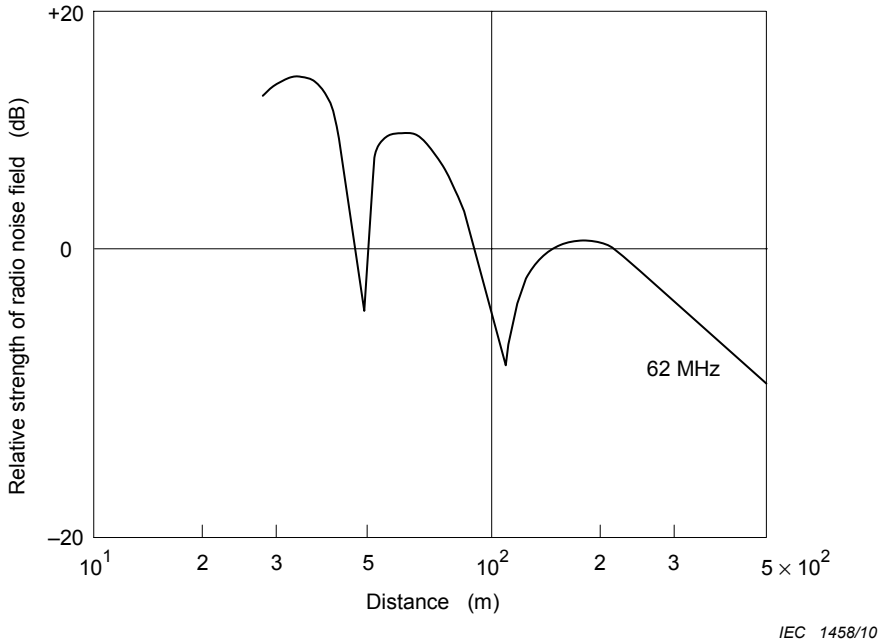

Figure 12 – Example of relative strength of radio noise field as a function of the distance from the line

Copyrighted material licensed to BR Demo by Thomson Reuters (Scientific), Inc., subscriptions.techstreet.com, downloaded on Nov-28-2014 by James Madison. No further reproduction or distribution is permitted. Uncontrolled when print

Annex A
(informative)

Calculation of the voltage gradient at the surface of a conductor of an overhead line

Various methods are available for the calculation of the voltage gradient at the surface of a conductor of an overhead line. All these methods give very similar results for both non-bundle conductors and symmetrical bundles consisting of a small number of subconductors; up to three or four. For bundles with a greater number of subconductors and for asymmetrical bundles the most suitable methods are those based on the principle of successive images [A.1]. With the advent of the digital computer, extensive use is now made of calculation programs based on these methods. For the majority of line configurations, that is where the height of the conductors above ground and the spacing between phases or poles is large compared with the conductor diameter or bundle dimensions and the subconductor spacing is large compared with the subconductor diameter, a single-image method can be used.

A further approximation to this approach is to calculate the charge on each conductor or subconductor, adopting the Maxwell potential coefficient method, and then to compute the voltage gradient at the surface of the conductor or subconductor considering only the charge on the conductor under consideration. In the case of a conductor bundle, it may be represented by an equivalent single conductor which has the same capacitance as the bundle. For single conductors and symmetrical bundles with a small number of subconductors, very simple formulae can be used for the determination of the voltage gradient from the charge.

The average gradient, g_{av}, is obtained by applying Gauss' theorem, from which the electric field strength at the surface of a conductor is equal to the surface charge density σ divided by the permittivity ε_o:

$$g_{av} = \frac{\sigma}{\varepsilon_o} = \frac{q}{\varepsilon_o \, n \, \pi \, d} \qquad \text{(A.1)}$$

where

q is the surface charge per unit length;

n is the number of subconductors in the bundle;

d is the diameter of subconductor, in centimetres;

$\varepsilon_o = \dfrac{1}{3\pi \times 10^9}$, is the permittivity of free space, in farads per metre.

In the case of a single phase line with earth return or a monopolar d.c. line, the calculation of the charge q as a function of the applied voltage U is very simple since the capacitance per unit length C is given by:

$$C = \frac{2 \, \pi \, \varepsilon_o}{\ln \dfrac{2h}{r_{eq}}}$$

where

h is the height of the conductor above ground in centimetres. Usually an average height is used and it is found by taking the conductor height at the tower, or the mean of the heights at the two towers of the span if the heights differ, and subtracting 2/3 of the sag at the lowest point of the conductor;

r_{eq} is the radius of conductor or radius of bundle equivalent conductor in centimetres;

Copyrighted material licensed to BR Demo by Thomson Reuters (Scientific), Inc., subscriptions.techstreet.com, downloaded on Nov-28-2014 by James Madison. No further reproduction or distribution is permitted. Uncontrolled when print

$r_{eq} = \frac{d}{2}$ in the case of a single conductor;

$r_{eq} = \frac{b}{2}\sqrt[n]{\frac{nd}{b}}$ in the case of a conductor bundle;

where b is the pitch-circle diameter of the subconductors.

Then

$$g_{av} = \frac{q}{\pi\varepsilon_o nd} = \frac{CU}{\pi\varepsilon_o nd} = \frac{U}{\frac{nd}{2}\ln\frac{2h}{r_{eq}}} \qquad \text{(A.2)}$$

To obtain g_{av} in kilovolts per centimetres, U shall be expressed in kilovolts and, in the case of a.c. lines, r.m.s. values are usually used.

In the general case of multiphase lines or multipole d.c. lines the calculation of the charges on each conductor or bundle requires the solution of the following set of equations:

$$[p] \times [q] = [U] \qquad \text{(A.3)}$$

where $[q]$ and $[U]$ are the one-column matrices of charges and voltages on the conductors or bundles and [p] is the square matrix of the potential coefficient of multiconductor configuration:

$$p_{ii} = \frac{1}{2\pi\varepsilon_o}\ln\frac{2h_i}{r_{eqi}}$$

$$p_{ij} = \frac{1}{2\pi\varepsilon_o}\ln\frac{D'_{ij}}{D_{ij}}$$

where

D_{ij} is the distance between conductors or bundles i and j;

D'_{ij} is the distance between conductor or bundle i and ground image of conductor or bundle j.

As regards the matrix of voltages, the following elements are to be considered for the following practical cases:

a) Single-circuit three-phase lines

$$[U] = \begin{bmatrix} U_1 \\ U_2 \\ U_3 \end{bmatrix} = U\begin{bmatrix} 1 \\ a \\ a^2 \end{bmatrix} \text{ with } a = -\frac{1}{2} + \frac{1}{2}j\sqrt{3}$$

where U is the modulus of the phase-to-earth voltage of the line. The above matrix refers to lines without an earth wire or wires. To take into account the presence of earth wires, the voltages, which are equal to zero on these wires, have to be inserted into the voltage matrix. The order of the matrix is increased but this does not present a great problem in the solution of the equations (A.3). However, it is possible, by dividing the matrix of potential coefficients into submatrices relating to phase conductors and earth wires and coupling matrices, to reduce the matrix order to hat for a line without earth wires. The presence of the earth wires increases the voltage gradient at the conductors but, with usual configurations, this increase is relatively small: 1 % to 3 %.

Copyrighted material licensed to BR Demo by Thomson Reuters (Scientific), Inc., subscriptions.techstreet.com, downloaded on Nov-28-2014 by James Madison. No further reproduction or distribution is permitted. Uncontrolled when print

b) Multi-circuit three-phase lines

In this case the voltage matrix [*U*] includes a series of elements which takes into account all the phase conductors or bundles and, when present, the earth wires of the line. As an example, the voltage matrix of a double-circuit three-phase line with two earth wires is an eight-order column matrix. The corresponding potential coefficient matrix is an eight-order square matrix, the inversion of which requires the use of a suitable computer. However, a sufficient range of computer capabilities now exists for the calculation of the voltage gradient of any type of multicircuit three-phase line.

It should be noted that the relative positions of the corresponding phases in the different circuits affect the charges on the conductors and it is important to take them into account when calculating the gradients of a multicircuit line. For example, the flat formations of two circuits defined by 1, a, a^2 and 1, a, $\underline{a}^2$ will result in higher gradients that the configuration 1, a, a^2 and a^2, a, 1.

c) Bipolar d.c. lines

$$[U] = \begin{bmatrix} U_1 \\ U_2 \end{bmatrix} = U \begin{bmatrix} 1 \\ -1 \end{bmatrix}$$

where U is the value of the pole-to-earth voltage.

The presence of earth wires can be taken into account in the same way as for a.c. three-phase lines.

The voltage gradient derived from formula (A.1) is an average value g_{av} around the circumference of the conductor or subconductor, in as much as it is calculated on the basis of the average charge density on the conductor:

$$\left(\sigma = \frac{q}{n \pi d} \right)$$

For single conductors this charge density can be considered uniform around the circumference and, therefore, the gradient is assumed to be constant. For the subconductors in a bundle, the charge density is not uniform, due to the mutual shielding effect of the subconductors, the charge density and consequently the gradient, is larger towards the exterior and smaller towards the interior of the bundle.

A simplified approach to obtain the variation of this gradient around the circumference is given by the following formula:

$$g_\theta = g_{av} \left(1 + \frac{(n-1)\, d}{b} \cos\theta \right)$$

where θ is the angle between:

– the radius from the centre of a subconductor to a chosen point on the surface of the subconductor;

– the line passing through the centre of the bundle and the point where the maximum gradient occurs on the same subconductor.

In particular, the maximum gradient g_{max} is given by:

$$g_{max} = g_{av} \left(1 + \frac{(n-1) d}{b} \right)$$

Copyrighted material licensed to BR Demo by Thomson Reuters (Scientific), Inc., subscriptions.techstreet.com, downloaded on Nov-28-2014 by James Madison. No further reproduction or distribution is permitted. Uncontrolled when print

Reference document:

[A.1] IEEE Corona and Field Effects sub-committee Report – Radio Noise Working Group: *A survey of Methods for Calculating Transmission Line Conductor Surface Voltage Gradients*, IEEE Trans. on Power Apparatus and System, vol. PAS-98, No. 6, Nov./Dec. 1979, pp. 1996-2014.

Copyrighted material licensed to BR Demo by Thomson Reuters (Scientific), Inc., subscriptions.techstreet.com, downloaded on Nov-28-2014 by James Madison. No further reproduction or distribution is permitted. Uncontrolled when print

Annex B
(informative)

Catalogue of profiles of radio noise field due to conductor corona for certain types of power line

The appearance of a given line in the catalogue does not purport that this line generates an acceptable radio noise level.

Table B.1 – List of profiles

(These profiles refer to the middle of the spans and the levels are related to the voltage given at the top of each figure)

		Figures	Origin
I.	*225 kV lines*	B.1	
	Triangular formation of conductors	B.2	
	Float formation	B.3	Ref. [8]
	Arched formation	B.4	
	Flat (wide formation)	B.5	
II.	*345 kV lines*		
	Vertical formation of Double circuit	B.6	
III.	*362 kV lines*		
	Flat formation	B.7	Ref. [35, 39]
IV.	*380 kV lines*		
	Flat formation	B.8	Ref. [8]
	Arched formation	B.9	Ref. [8]
V.	*525 kV lines*		
	Flat formation	B.10	Ref. [35, 39]
VI.	*750 kV lines*		
	Arched formation	B.11	Ref. [8]
VII.	*765 kV lines*		
	Flat formation	B.12	Ref. [35, 39]
VIII.	*765 kV lines*		
	Vertical formation of Double circuit	B.13	Ref. [56]

Corrections:

I.	Frequency	B.14	Ref. [8]
II.	Weather categories	B.15	Ref. [8]

Copyrighted material licensed to BR Demo by Thomson Reuters (Scientific), Inc., subscriptions.techstreet.com, downloaded on Nov-28-2014 by James Madison. No further reproduction or distribution is permitted. Uncontrolled when print

225 kV line

Frequency 0,5 MHz	Conductors				Maximum gradients			
h average 15 m *h* min. 11 m	Number of conductors	Phase spacing S	Radius of bundle R	Radius of conductor r	Phase 1	Phase 2	Phase 3	Level correction
		m	mm	mm	kVeff./cm	kVeff./cm	kVeff./cm	dB
	1	–	–	13,2	15,40	15,05	14,60	0
	1	–	–	15,5	13,45	13,15	12,75	–6,4
	1	–	–	16,2	12,95	12,55	12,30	–8,0

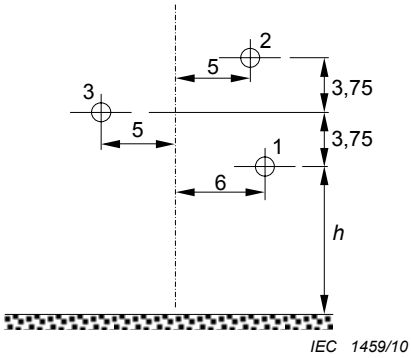

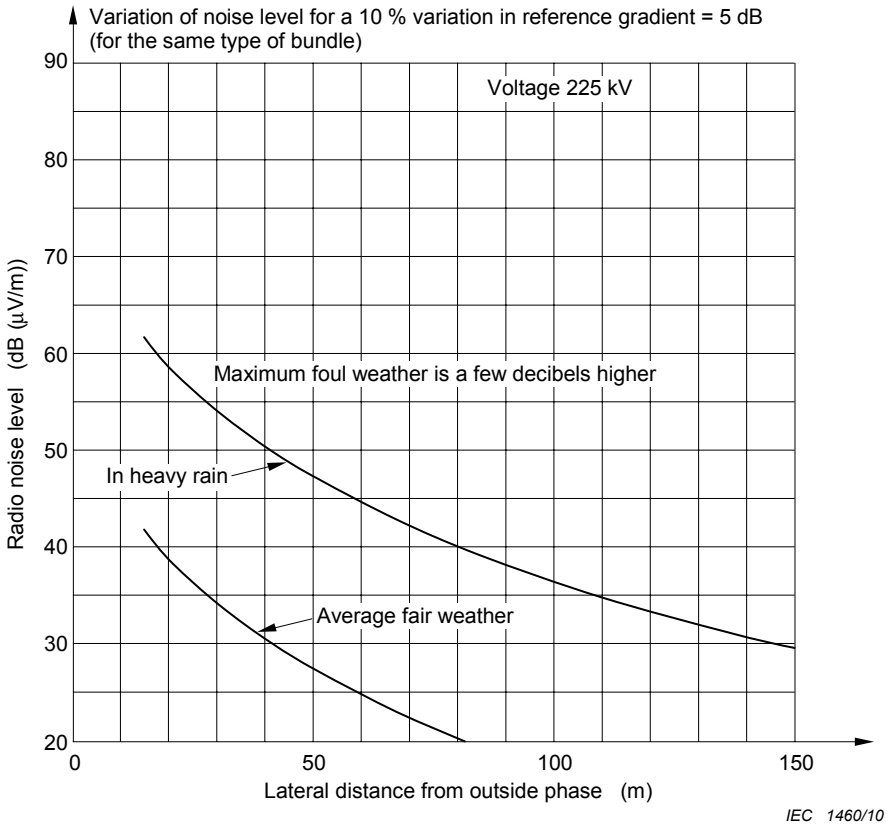

Figure B.1 – Triangular formation (1)

Copyrighted material licensed to BR Demo by Thomson Reuters (Scientific), Inc., subscriptions.techstreet.com, downloaded on Nov-28-2014 by James Madison. No further reproduction or distribution is permitted. Uncontrolled when print

225 kV line

Frequency 0,5 MHz	Conductors				Maximum gradients			
h average 15 m *h* min. 11 m	Number of conductors	Phase spacing S m	Radius of bundle R mm	Radius of conductor r mm	Phase 1 kVeff./cm	Phase 2 kVeff./cm	Phase 3 kVeff./cm	Level correction dB
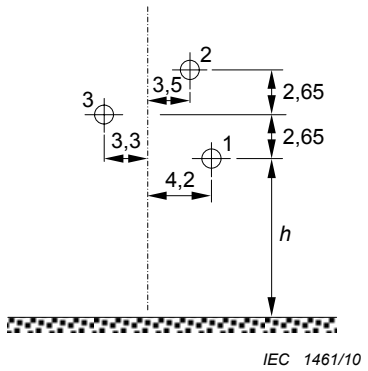	1	–	–	13,2	16,15	16,00	15,45	0
	1	–	–	15,5	14,15	14,00	13,50	–6
	1	–	–	16,2	13,65	13,50	13,00	–7,6

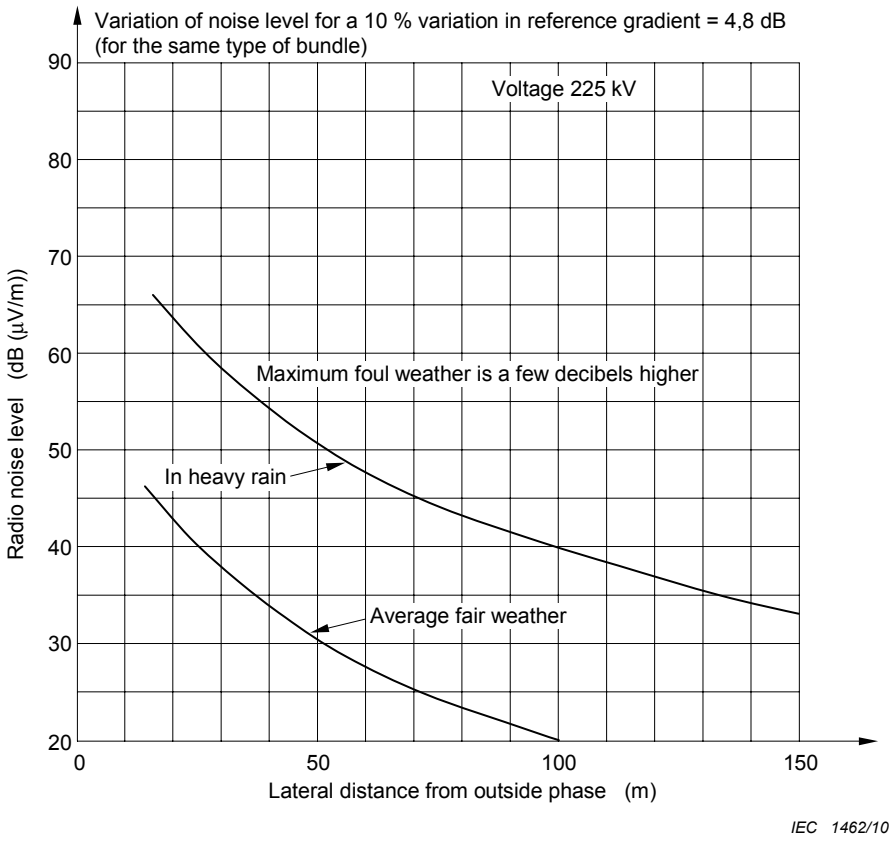

Figure B.2 – Triangular formation (2)

Copyrighted material licensed to BR Demo by Thomson Reuters (Scientific), Inc., subscriptions.techstreet.com, downloaded on Nov-28-2014 by James Madison. No further reproduction or distribution is permitted. Uncontrolled when print

225 kV line

Frequency 0,5 MHz	Conductors				Maximum gradients			
h average 15 m *h* min. 11 m 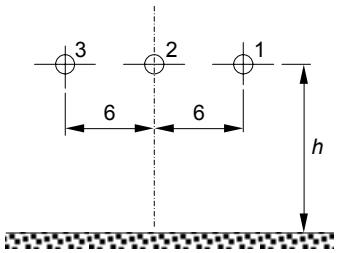 	Number of conductors	Phase spacing S m	Radius of bundle R mm	Radius of conductor r mm	Phase 1 kVeff./cm	Phase 2 kVeff./cm	Phase 3 kVeff./cm	Level correction dB
	1	–	–	13,2	15,35	16,40	15,35	0
	1	–	–	15,5	13,40	14,35	13,40	–6
	1	–	–	16,2	12,90	13,85	12,90	–7,5

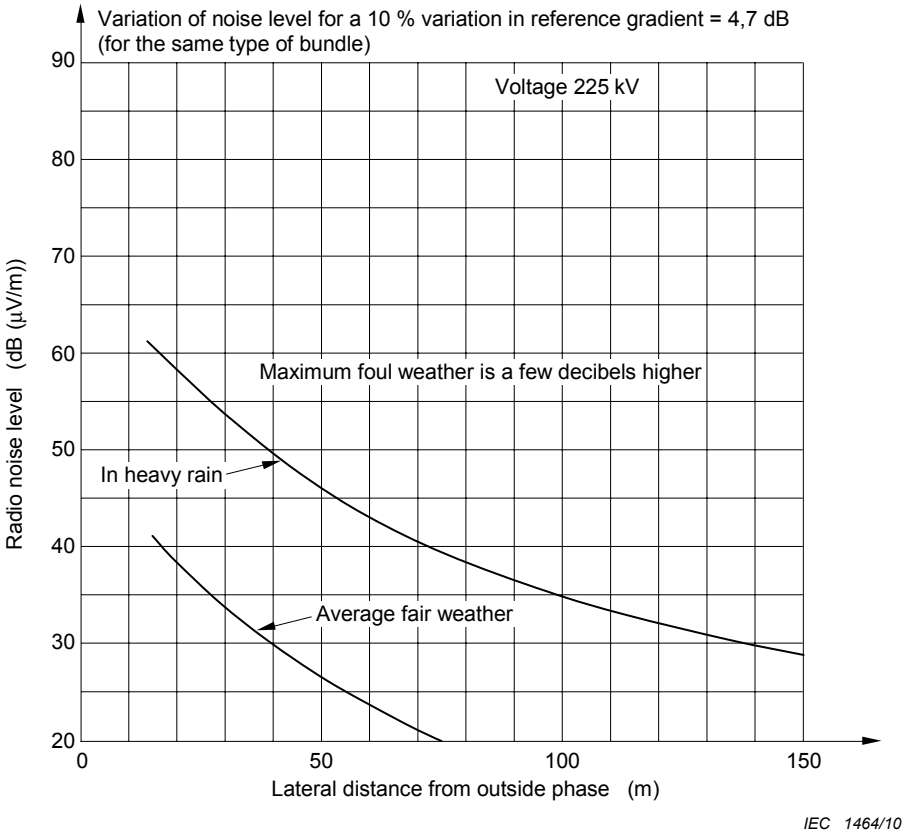

Figure B.3 – Flat formation

Copyrighted material licensed to BR Demo by Thomson Reuters (Scientific), Inc., subscriptions.techstreet.com, downloaded on Nov-28-2014 by James Madison. No further reproduction or distribution is permitted. Uncontrolled when print

225 kV line

Frequency 0,5 MHz	Conductors				Maximum gradients			
h average 15 m *h* min. 11 m 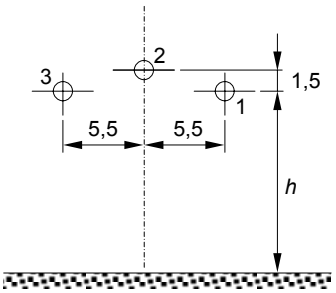 IEC 1465/10	Number of conductors	Phase spacing S m	Radius of bundle R mm	Radius of conductor r mm	Phase 1 kVeff./cm	Phase 2 kVeff./cm	Phase 3 kVeff./cm	Level correction dB
	1	5,5	–	13,2	15,55	16,45	15,55	0
	1	5,5	–	15,5	13,60	14,40	13,60	–6
	1	5,5	–	16,2	13,10	13,90	13,10	–7,6

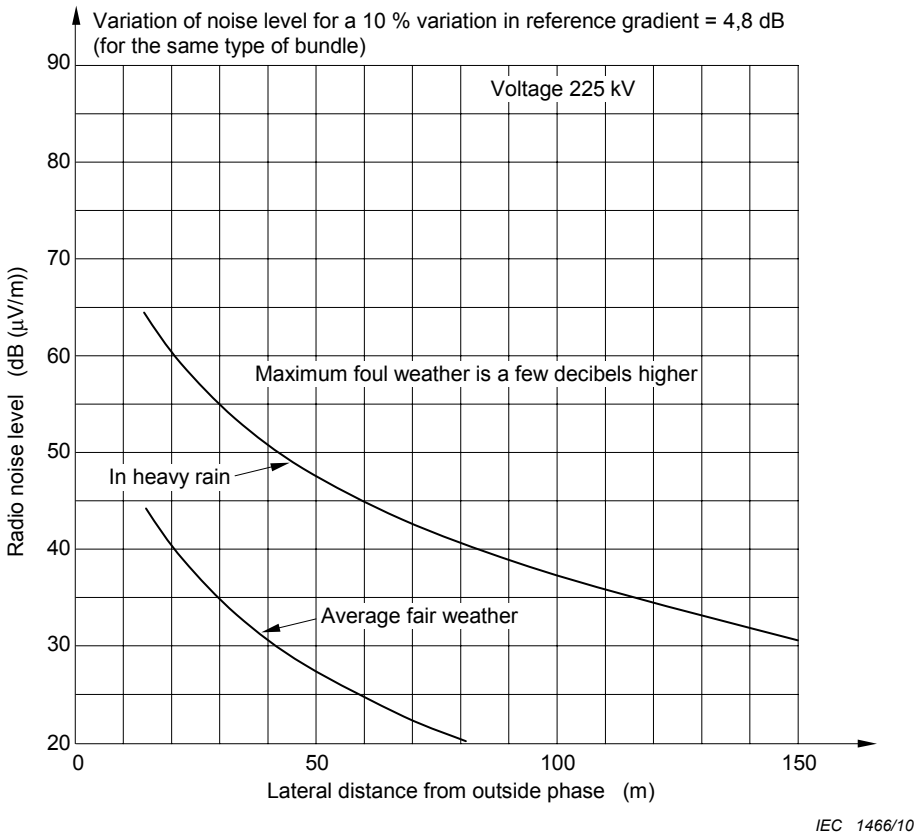

Figure B.4 – Arched formation

Copyrighted material licensed to BR Demo by Thomson Reuters (Scientific), Inc., subscriptions.techstreet.com, downloaded on Nov-28-2014 by James Madison. No further reproduction or distribution is permitted. Uncontrolled when print

225 kV line

Frequency 0,5 MHz	Conductors				Maximum gradients			
h average 15 m *h* min. 11 m 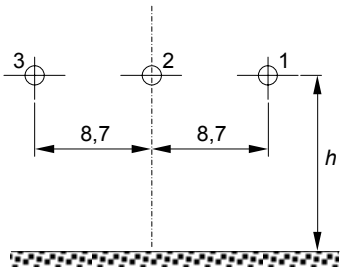 IEC 1467/10	Number of conductors	Phase spacing S m	Radius of bundle R mm	Radius of conductor r mm	Phase 1 kVeff./cm	Phase 2 kVeff./cm	Phase 3 kVeff./cm	Level correction dB
	1	8,7	–	13,2	14,60	15,45	14,60	0
	1	8,7	–	15,5	12,75	13,50	12,75	–6,3
	1	8,7	–	16,2	12,30	13,00	12,30	–8,0

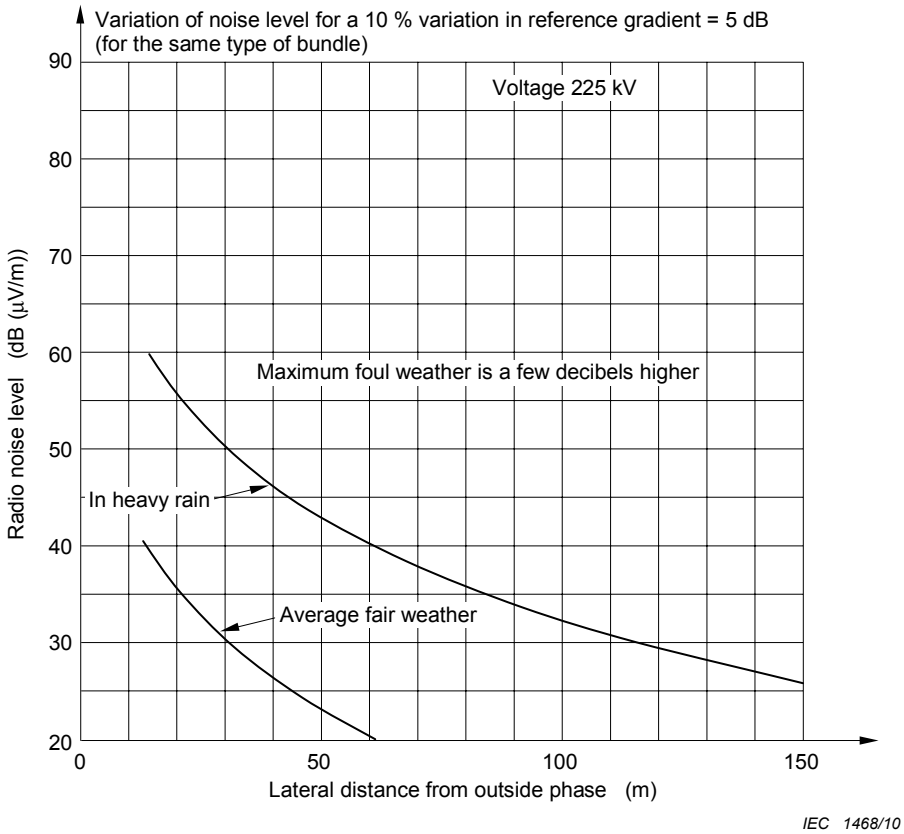

Figure B.5 – Flat wide formation

Copyrighted material licensed to BR Demo by Thomson Reuters (Scientific), Inc., subscriptions.techstreet.com, downloaded on Nov-28-2014 by James Madison. No further reproduction or distribution is permitted. Uncontrolled when print

345 kV line, Double circuit

Frequency 0,5 MHz	Conductors				Maximum gradients						
h average 20,5 m *h* min. 18 m 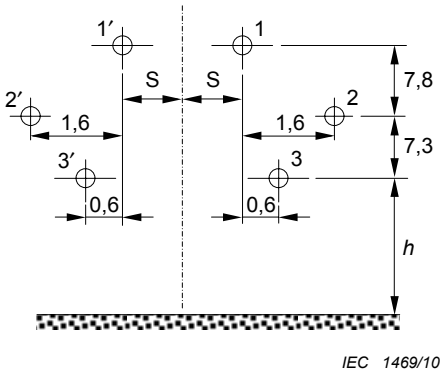 	Number of conductors	Phase spacing S	Radius of bundle R	Radius of conductor r	Phase 1	Phase 1′	Phase 2	Phase 2′	Phase 3	Phase 3′	Level correction
		m	mm	mm	kVeff./cm		kVeff./cm		kVeff./cm		dB
	4	7,6	200	14,8	10,24		10,85		10,18		0

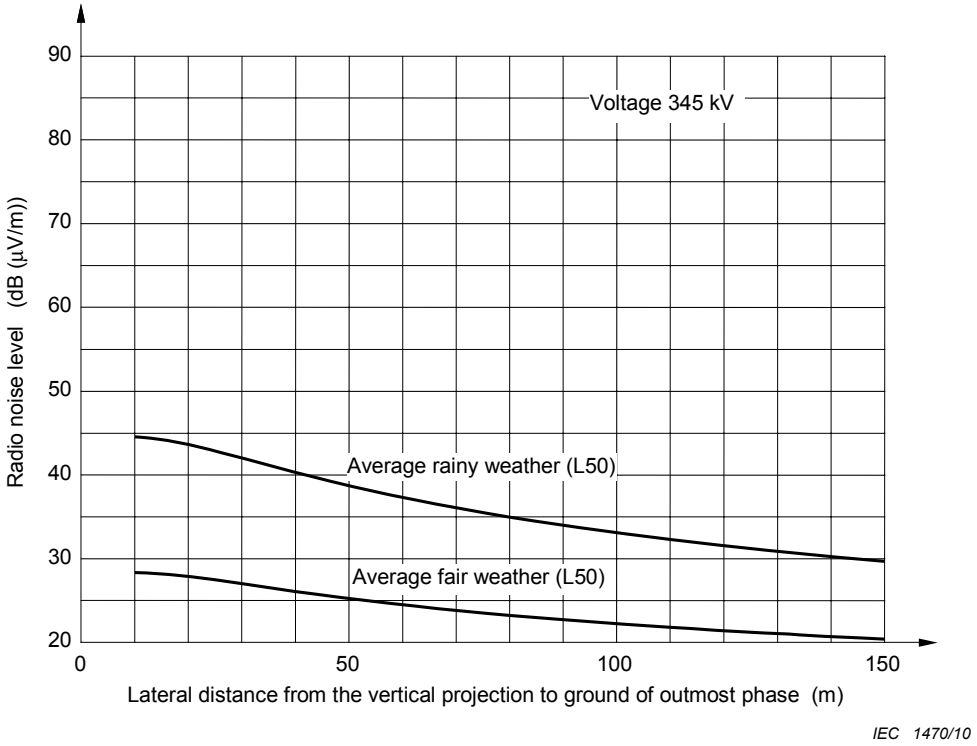

Figure B.6 – Vertical formation (480 (Rail) X 4B)

Copyrighted material licensed to BR Demo by Thomson Reuters (Scientific), Inc., subscriptions.techstreet.com, downloaded on Nov-28-2014 by James Madison. No further reproduction or distribution is permitted. Uncontrolled when print

362 kV line

Frequency 0,5 MHz	Conductors				Maximum gradients			
h average 14 m *h* min. 10 m 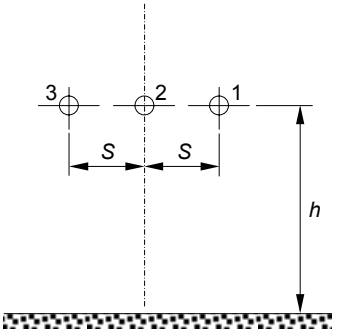 	Number of conductors	Phase spacing S m	Radius of bundle R mm	Radius of conductor r mm	Phase 1 kVeff./cm	Phase 2 kVeff./cm	Phase 3 kVeff./cm	Level correction dB
	1	9,75	–	20,35	16,1	17,0	16,1	0
	2	9,0	–	13,4	16,7	17,8	16,7	–4

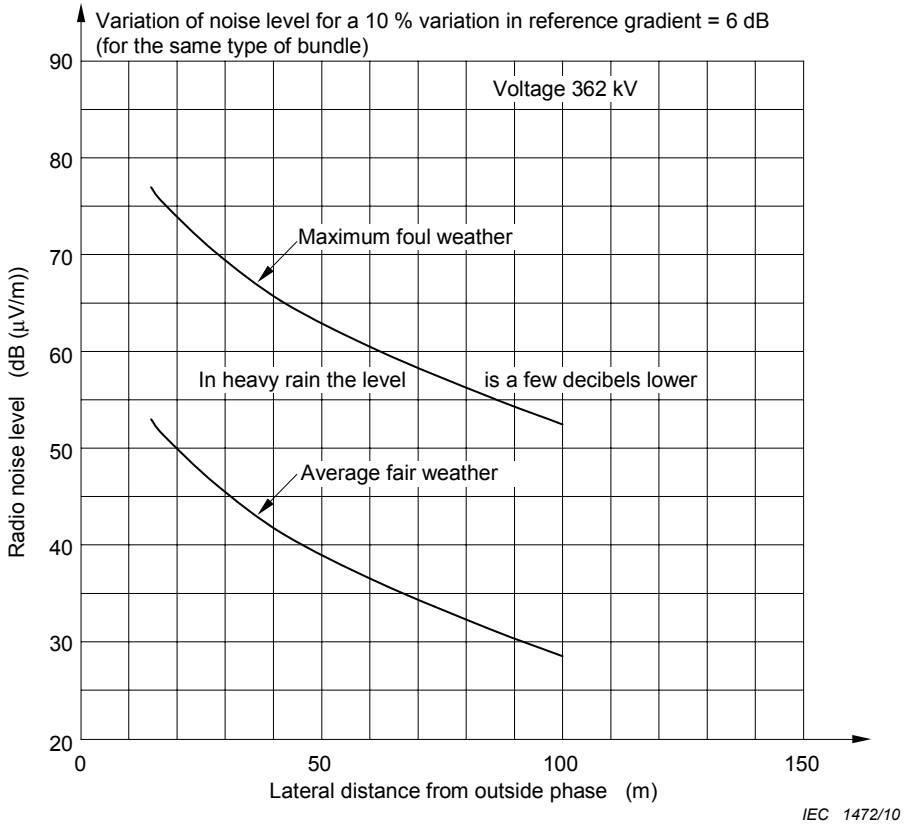

Figure B.7 – Flat formation

Copyrighted material licensed to BR Demo by Thomson Reuters (Scientific), Inc., subscriptions.techstreet.com, downloaded on Nov-28-2014 by James Madison. No further reproduction or distribution is permitted. Uncontrolled when print

380 kV line

Frequency 0,5 MHz	Conductors				Maximum gradients			
h average 16 m *h* min. 12 m 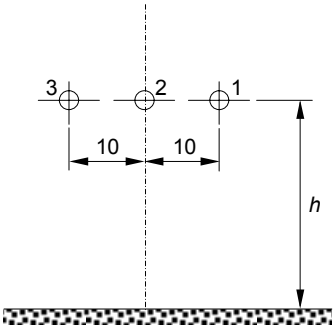 	**Number of conductors**	**Phase spacing S** m	**Radius of bundle R** mm	**Radius of conductor r** mm	**Phase 1** kVeff./cm	**Phase 2** kVeff./cm	**Phase 3** kVeff./cm	**Level correction** dB
	2	10,0	200	13,2	17,20	18,50	17,20	0
	2	10,0	200	15,5	15,05	16,20	15,05	–5,5
	2	10,0	200	16,2	14,50	15,60	14,50	–7,0
	2	10,0	–	22,4	15,50	16,40	15,50	+6,5

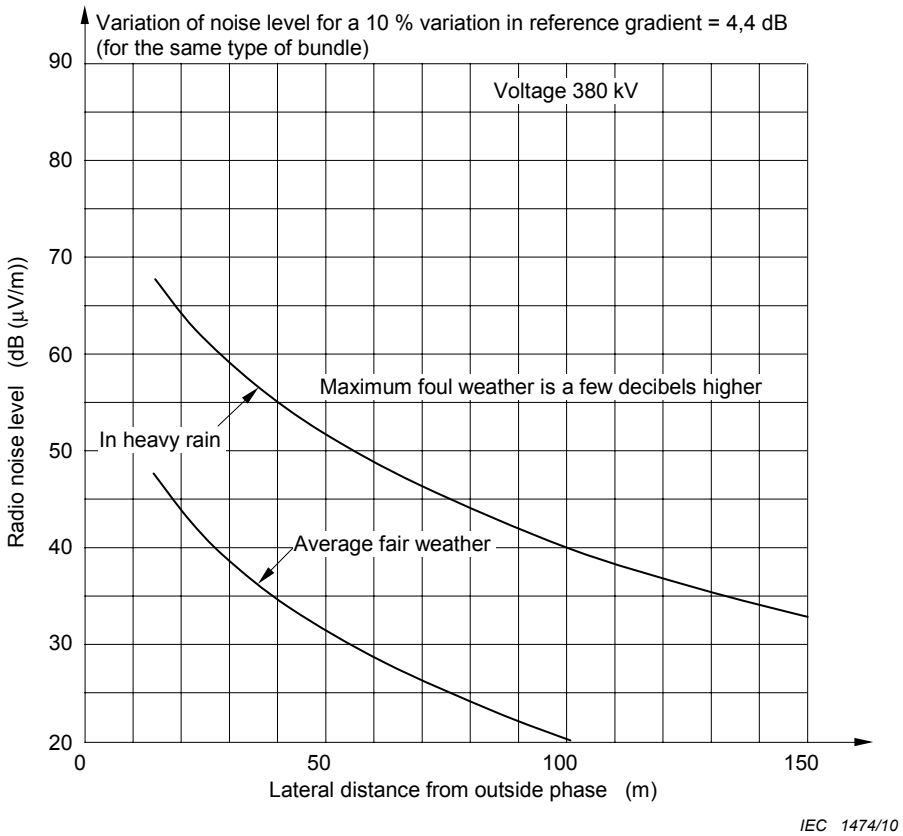

Figure B.8 – Flat formation

Copyrighted material licensed to BR Demo by Thomson Reuters (Scientific), Inc., subscriptions.techstreet.com, downloaded on Nov-28-2014 by James Madison. No further reproduction or distribution is permitted. Uncontrolled when print

380 kV line

Frequency 0,5 MHz	Conductors				Maximum gradients			
h average 16 m *h* min. 12 m	Number of conductors	Phase spacing S m	Radius of bundle R mm	Radius of conductor r mm	Phase 1 kVeff./cm	Phase 2 kVeff./cm	Phase 3 kVeff./cm	Level correction dB
	2	10,00	200	13,2	17,20	18,00	17,20	0
	2	10,00	200	15,5	15,05	15,75	15,05	–5,5
	2	10,00	200	16,2	14,60	15,30	14,60	–6,7
	1	10,00	–	22,4	15,50	16,00	15,50	+6,7

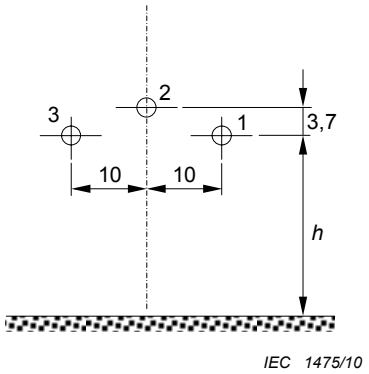

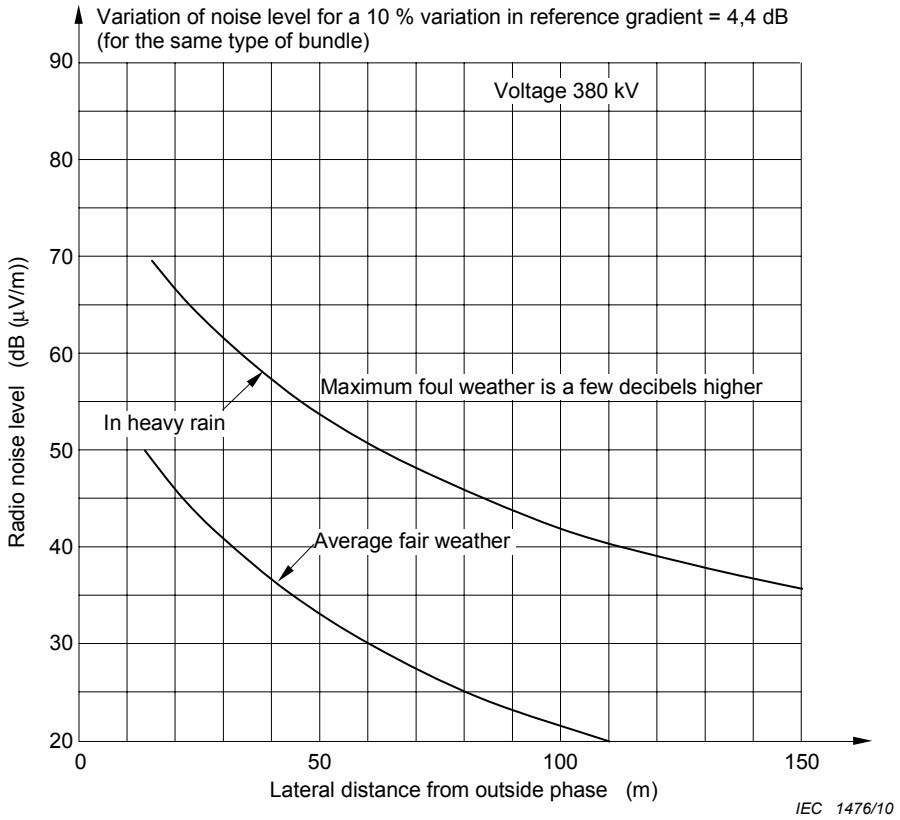

Figure B.9 – Arched formation

Copyrighted material licensed to BR Demo by Thomson Reuters (Scientific), Inc., subscriptions.techstreet.com, downloaded on Nov-28-2014 by James Madison. No further reproduction or distribution is permitted. Uncontrolled when print

525 kV line

Frequency 0,5 MHz	Conductors				Maximum gradients			
h average 17 m *h* min. 12 m 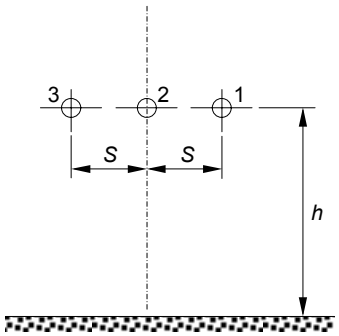 	Number of conductors	Phase spacing S m	Radius of bundle R mm	Radius of conductor r mm	Phase 1 kVeff./cm	Phase 2 kVeff./cm	Phase 3 kVeff./cm	Level correction dB
	4	12,2	323	10,80	17,9	19,3	17,9	0
	3	9,2	264	14,80	17,3	19,0	17,3	+1
	2	9,1	229	20,95	16,5	17,9	16,5	+7

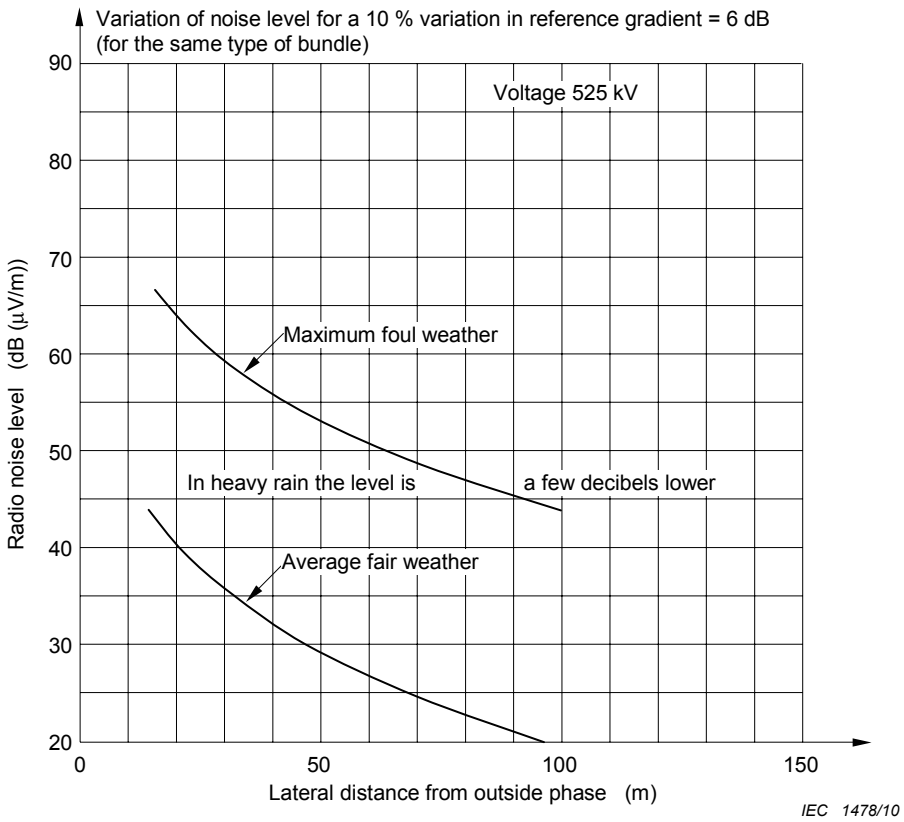

Figure B.10 – Flat formation

Copyrighted material licensed to BR Demo by Thomson Reuters (Scientific), Inc., subscriptions.techstreet.com, downloaded on Nov-28-2014 by James Madison. No further reproduction or distribution is permitted. Uncontrolled when print

750 kV line

Frequency 0,5 MHz	Conductors				Maximum gradients			
h average 18 m *h* min. 14 m 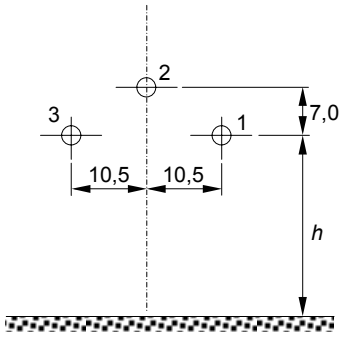 	Number of conductors	Phase spacing S m	Radius of bundle R mm	Radius of conductor r mm	Phase 1 kVeff./cm	Phase 2 kVeff./cm	Phase 3 kVeff./cm	Level correction dB
	4	10,5	212	15,5	18,30	17,00	18,30	0
	4	10,5	212	18,95	15,70	14,60	15,70	–4,9
	4	10,5	323	15,5	18,40	17,05	18,40	+0,8
	4	10,5	323	18,95	15,65	14,50	15,65	–4,7

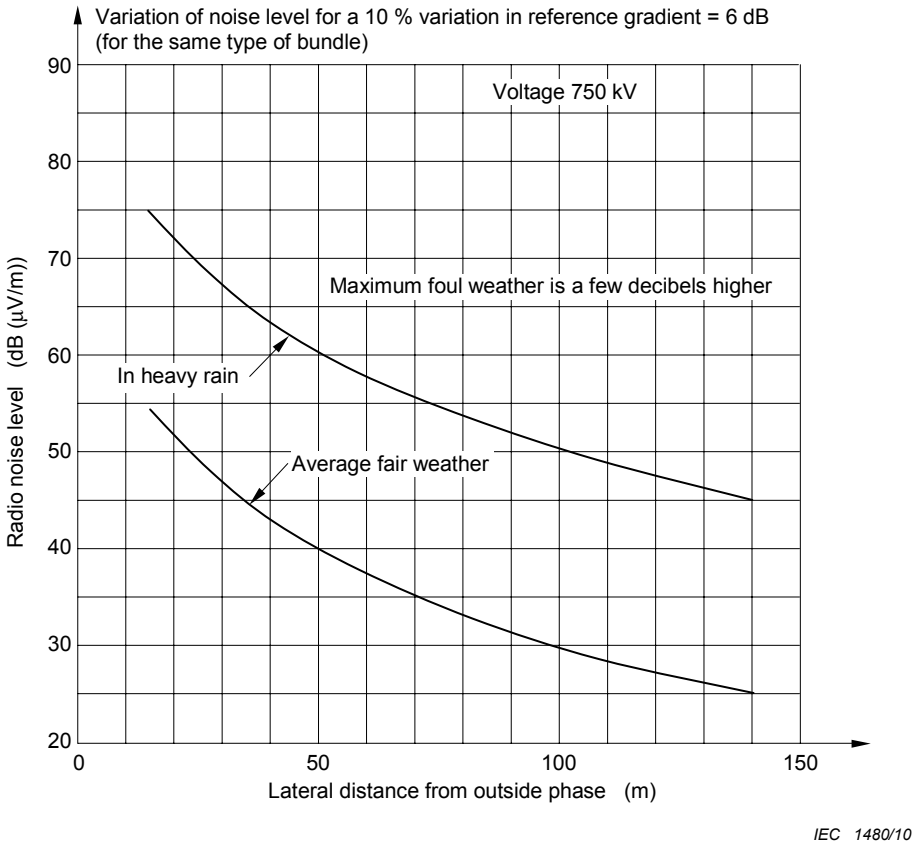

Figure B.11 – Arched formation

Copyrighted material licensed to BR Demo by Thomson Reuters (Scientific), Inc., subscriptions.techstreet.com, downloaded on Nov-28-2014 by James Madison. No further reproduction or distribution is permitted. Uncontrolled when print

765 kV line

Frequency 0,5 MHz	Conductors				Maximum gradients			
h average 18 m *h* min. 14 m 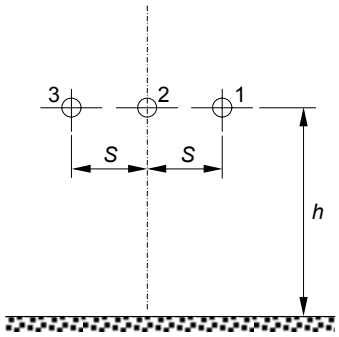 IEC 1481/10	Number of conductors	Phase spacing S m	Radius of bundle R mm	Radius of conductor r mm	Phase 1 kVeff./cm	Phase 2 kVeff./cm	Phase 3 kVeff./cm	Level correction dB
	4	15,2	323	17,55	16,9	18,0	16,9	0
	4	13,7	323	15,19	19,2	20,6	19,2	+6,0

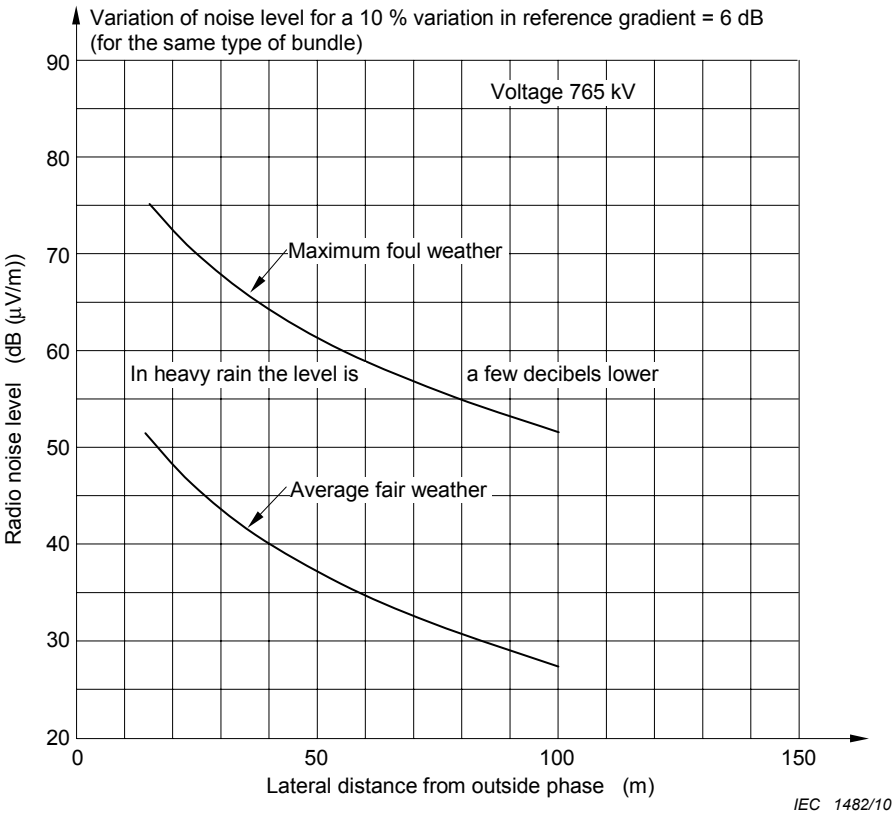

Figure B.12 – Flat formation

Copyrighted material licensed to BR Demo by Thomson Reuters (Scientific), Inc., subscriptions.techstreet.com, downloaded on Nov-28-2014 by James Madison. No further reproduction or distribution is permitted. Uncontrolled when print

765 kV line, Double circuit

Frequency 0,5 MHz	Conductors				Maximum gradients						
h average 31 m *h* min.28 m	Number of conductors	Phase spacing S	Radius of bundle R	Radius of conductor r	Phase 1	Phase 1'	Phase 2	Phase 2'	Phase 3	Phase 3'	Level correction
		m	mm	mm	kVeff./cm		kVeff./cm		kVeff./cm		dB
	6	13,5	400	15,2	16,24		16,49		15,91		0

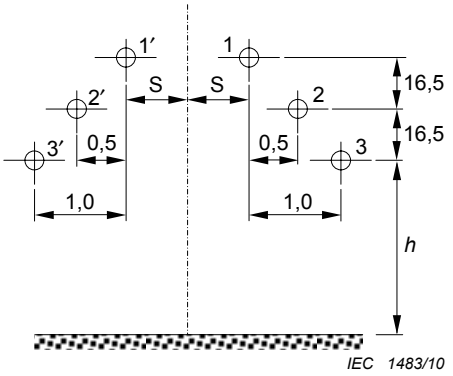

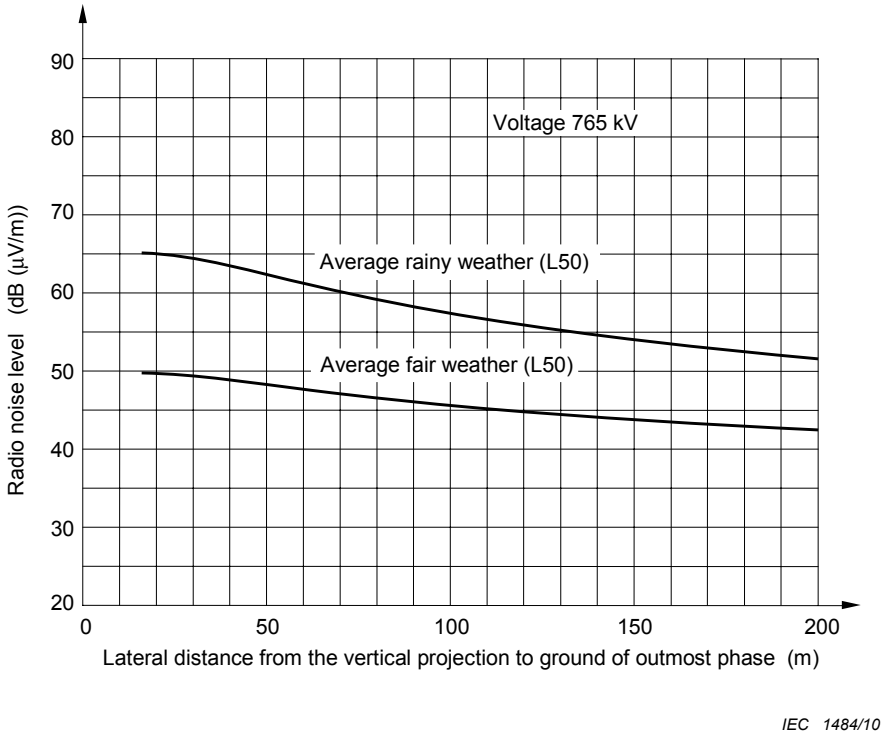

Figure B.13 – Vertical formation (480 (Cardinal) X 6B)

Copyrighted material licensed to BR Demo by Thomson Reuters (Scientific), Inc., subscriptions.techstreet.com, downloaded on Nov-28-2014 by James Madison. No further reproduction or distribution is permitted. Uncontrolled when print

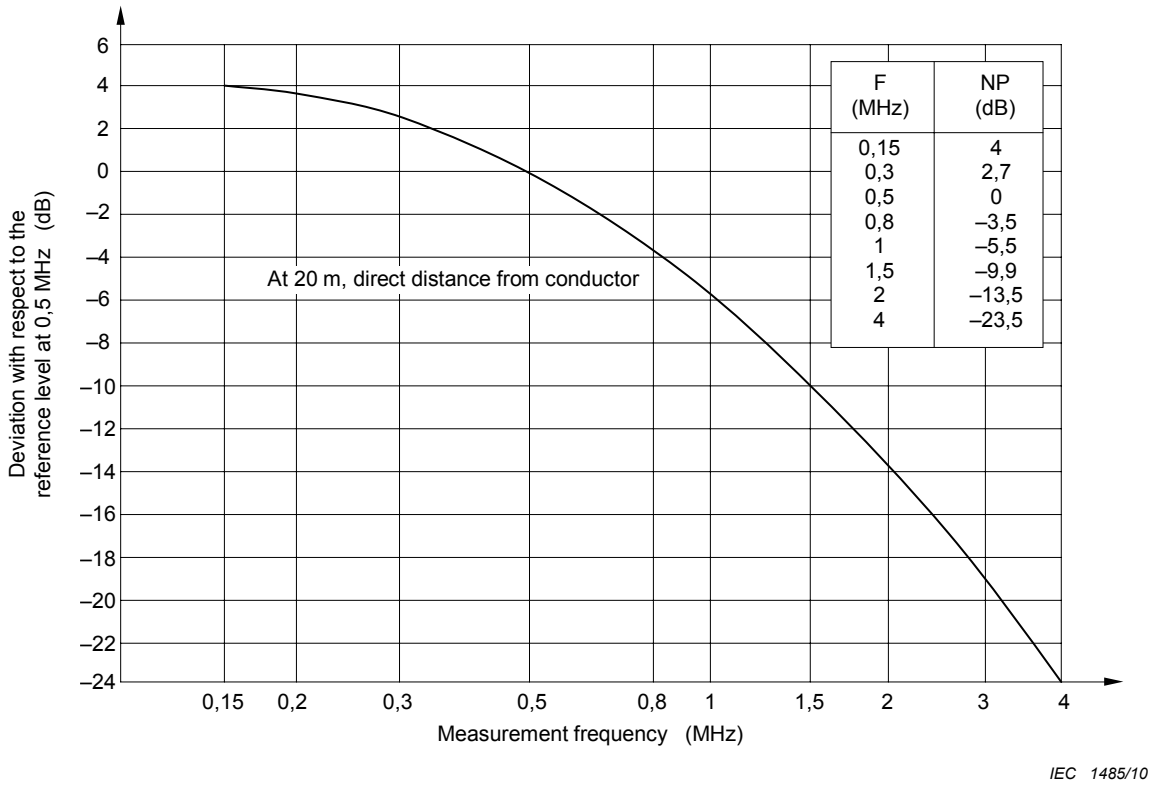

Figure B.14 – Typical frequency spectra for the radio noise fields of high voltage power lines

Copyrighted material licensed to BR Demo by Thomson Reuters (Scientific), Inc., subscriptions.techstreet.com, downloaded on Nov-28-2014 by James Madison. No further reproduction or distribution is permitted. Uncontrolled when print

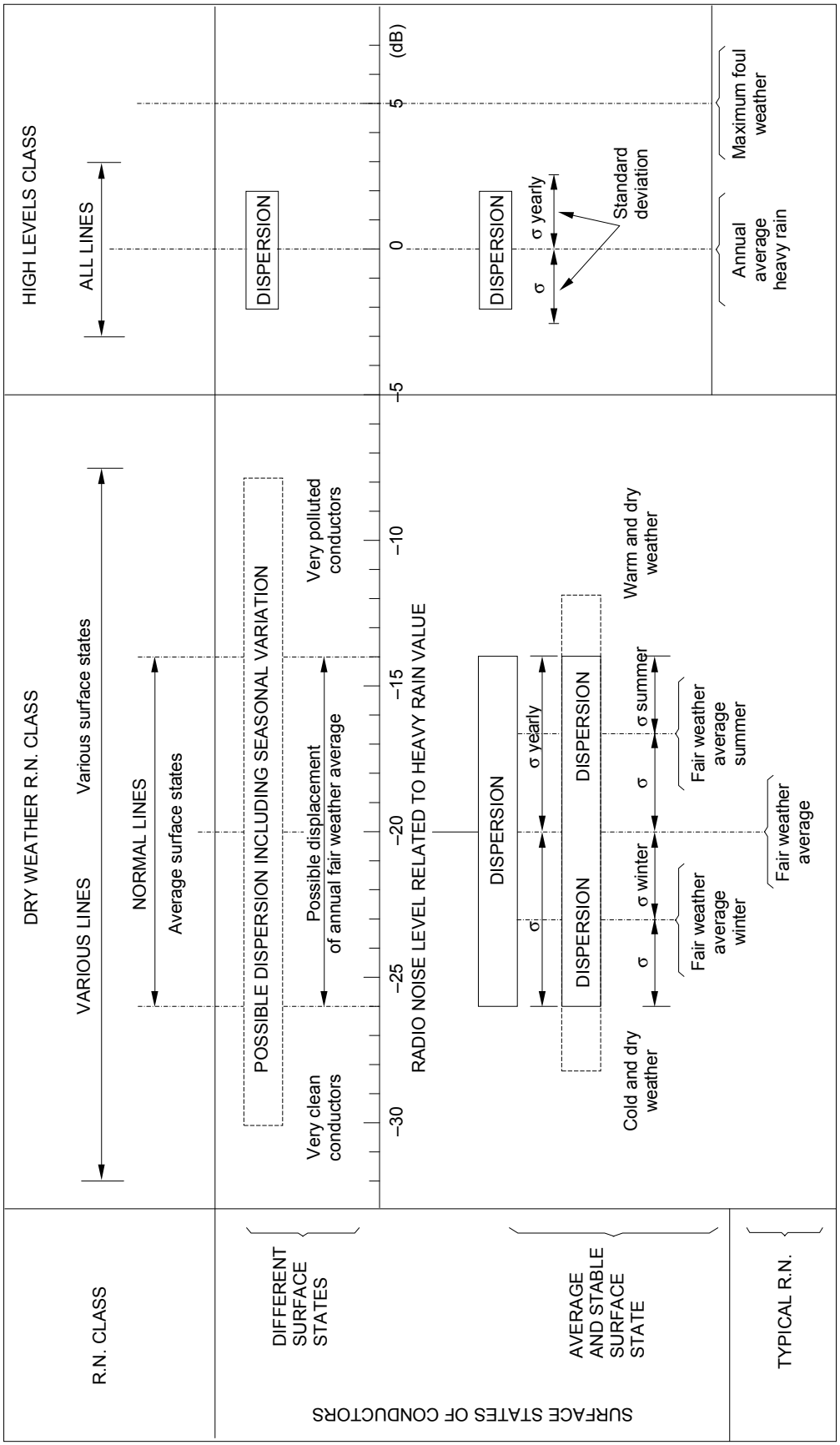

NOTE Daily dry weather variations are not included in this graph.

Figure B.15 – Prediction of radio noise level of a transmission line for various types of weather

Copyrighted material licensed to BR Demo by Thomson Reuters (Scientific), Inc., subscriptions.techstreet.com, downloaded on Nov-28-2014 by James Madison. No further reproduction or distribution is permitted. Uncontrolled when print

Annex C
(informative)

Summary of the catalogue of radio noise profiles according to the recommendations of the CISPR

Figure No.	Voltage kV	Configuration	Noise field at the reference distance D_o = 20 m [a]		Exponent [b] n
			Heavy rain dB(µV/m)	Dry weather dB(µV/m)	
B.1	225	Triangular	52-60	32-40	–1,65
B.2	225	Triangular	54-62	34-42	–1,65
B.3	225	Flat	52-59	32-39	–1,65
B.4	225	Arched	54-60	34-40	–1,7
B.5	225	Flat, wide	49-57	29-37	–1,7
B.6	345	Vertical 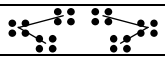	43 [d]	27 [d]	–
B.7	362 [c]	Flat	68-72	48-52	–1,6
B.8	380	Flat	59-66	39-46	–1,7
B.9	380	Arched	60-67	40-47	–1,75
B.10	525 [c]	Flat 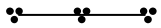	63-70	43-50	–1,55
B.11	750	Arched	69-75	49-55	–1,65
B.12	765 [c]	Flat 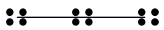	71-77	51-57	–1,55
B.13	765	Vertical 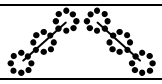	64-65 [d]	49-50 [d]	–

Underlined values, as e.g. 52-60 dB(µV/m), are basic values. Dotted underlined values, as e.g. 34-42 dB(µV/m), are derived values.

[a] Interpolated value from profiles of Figures B.1 to B.13. The range (52-60 dB(µV/m) for example) takes into account the various diameters of conductors and bundle dimensions.

[b] Exponent of attenuation versus distance D

$$\frac{E}{E_o}(\mu\text{V/m}) = \left(\frac{D}{D_o}\right)^n$$

$$E\ (\text{dB}\mu\text{V/m}) = E_0(\text{dB}\mu\text{V/m}) + 20\ n\ \lg \frac{D}{D_o}$$

D is the direct distance in metres between the nearest conductor and the antenna of the radio noise meter. The average value of n is very close to –1,65. So the formula $E = E_0 - 33 \lg \frac{D}{D_o}$ can be considered as valid for all the lines.

[c] The noise values are related to the maximum voltage of the line (as specified by the IEC).

[d] Noise field at the lateral distance y_0 = 15 m.

Copyrighted material licensed to BR Demo by Thomson Reuters (Scientific), Inc., subscriptions.techstreet.com, downloaded on Nov-28-2014 by James Madison. No further reproduction or distribution is permitted. Uncontrolled when print

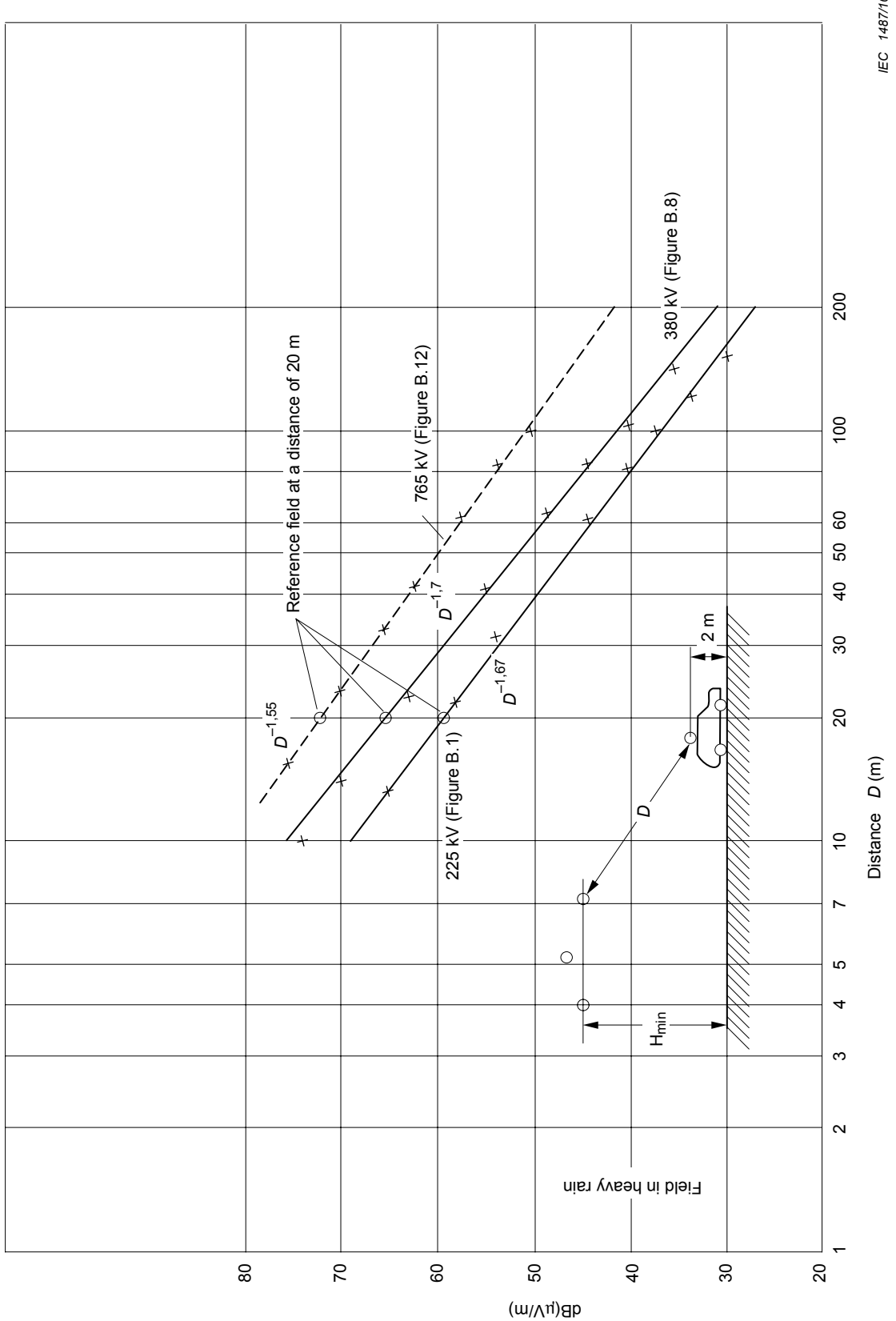

Figure C.1 – Examples of transformations of the profiles of Figures B.1 to B.13 using the direct distance of 20 m as reference

Copyrighted material licensed to BR Demo by Thomson Reuters (Scientific), Inc., subscriptions.techstreet.com, downloaded on Nov-28-2014 by James Madison. No further reproduction or distribution is permitted. Uncontrolled when print

Bibliography

[1] *Interference Produced by Corona Effect of Electric Systems* (Description of Phenomena, Practical Guide for Calculation), International Conference on Large High Voltage Electric Systems (CIGRÉ), Paris 1974.

[2] D.E. Hedman: *Propagation on Overhead Transmission Lines*, IEEE Transactions of PAS, vol. 84, March 1964, pp. 200-211.

[3] F.L. Taylor, C.J. Crockford, R.V. Nicolson: *Investigation of radio noise from existing lines and equipment to aid in the design of future extra-high voltage lines*, IEEE PAS, August 1957, pp. 436-445.

[4] C. Gary, M Moreau: *Predetermination of the Radio Noise Level under Rain of an Extra-High Voltage Line*, IEEE Transactions (Power Apparatus and Systems), vol. PAS-88, pp. 653-660, May 1969.

[5] G.W. Juette, L.E. Zaffanella: *Radio Noise Currents and Audible Noise on Short Sections of UHV Bundle Conductors*, IEEE Transactions (Power Apparatus and Systems), vol. PAS-89, No. 5, pp.902-913, May/June 1970.

[6] N. Giao Trinh, P. Sarma Maruvada, B. Poirier: *A comparative Study of the Corona Performances of Conductor Bundles for 1 200 kV Transmission Lines*, IEEE Transactions, vol. PAS-93, May/June 1974, pp. 940-949.

[7] G.W. Juette, L.E. Zaffanella: *Radio Noise, Audible Noise and Corona Loss of EHV and UHV Transmission Lines under Rain: Predetermination based on Cage Test*, IEEE Transactions, Vol. PAS-89, Nov./Dec. 1970, pp. 1168-1178.

[8] M.R. Moreau, C.H. Gary: *Predetermination of the Radio Interference Level of High Voltage Transmission Lines*, Parts I and II, IEEE Transactions, vol. PAS-91, pp.284-304, Jan./Feb. 1972.

[9] N.G. Trinh, P.S. Maruvada: *A Method of Predicting the Corona Performance of Conductor Bundles Based on Cage Test Results*, IEEE Transactions, vol. PAS-96, pp. 312-325, Jan./Feb. 1977.

[10] G.D. Lippert, W.E. Pakala, S.C. Barlett, C.D. Fahrnkoft: *Radio Influence Tests in Field and Laboratory – 500 kV Test Project of American Gas and Electric Company*, AIEE Transactions, vol. 70, Part I, pp. 251-269, 1951.

[11] L.M. Robertson, W.E. Pakala, E.R. Taylor, Jr.: *Leadville High Altitude Extra-High-Voltage Test Project: Part III – Radio Influence Investigations*, AIEE Transactions (Power Apparatus and Systems), vol. 80, pp.732-743, Dec. 1961.

[12] J. Reichman, J.R. Leslie*: A Summary of Radio Interference Studies Applied to EHV lines*, IEEE Transactions (Power Apparatus and Systems), vol. 83, No. 3, pp.223-228, March 1964.

[13] J.J. LaForest, C.B. Lindh, D.D. McCarthy, F. Olsen, M.W. Schultz, Jr.: *Radio Noise and Corona Loss Results from Project EHV*, IEEE Transactions on Power Apparatus and Systems, vol. 82, pp.735-750.

[14] V.L. Chartier, D.F. Shankle, N. Kolcio: *The Apple Grove 750 kV Project – Statistical Analysis of Radio Influence and Corona Loss Performance of Conductors at 775 kV*, IEEE Transactions (Power Apparatus and Systems), vol. 89, May/June 1970.

Copyrighted material licensed to BR Demo by Thomson Reuters (Scientific), Inc., subscriptions.techstreet.com, downloaded on Nov-28-2014 by James Madison. No further reproduction or distribution is permitted. Uncontrolled when print

[15] E.R. Taylor, Jr., W.E. Pakala, N. Kolcio*: The Apple Grove 750 kV – 515 kV Radio Influence and Corona Loss Investigation*, IEEE Transactions (Power Apparatus and Systems), vol. PAS-84, No. 7, pp. 561-573, July 1965,

[16] Y. Sawada: *Calculating Method of Radio Noise Level and Its Application to Design of AC power Transmission Line*, IEEE Transactions on Power Apparatus and Systems, vol. 89, pp. 844-853, May/June 1970.

[17] M. Magnien, J. Clade, C. Gary: *The Electricité de France Test Station for Corona Studies on Future EHV Lines*, CIGRÉ, 1966, Paper No. 427.

[18] N. Knudsen, H. Bergwvist, P. Forsgren: *Results from 3-Year Operation of the HVDC Test Station in Anneberg,* CIGRÉ Report, No. 31-04, 1970.

[19] F.W. Hirsch, E. Schafer: *Progress Report on the HVDC Test Line of the 400 kV-Forschungsgemeinschaft: Corona Losses and Radio Interference*, IEEE Transactions on Power Apparatus and Systems, vol. 88, pp. 1061-1069,July 1969.

[20] E.H. Gehrig, A.C. Peterson, C.F. Clark, T.C: Redmour: *BPA's 1100 kV DC Test Project, Part II, Radio Interference and Corona Loss*, IEEE Transactions on Power Apparatus and Systems, vol. 86, March 1967.

[21] N. Knudsen: *Corona Loss and Radio Interference Measurements at High Voltage AC on Test Lines in Sweden*, Paper No. 411, CIGRÉ, 1964.

[22] R. Bartenstein, G. Lesch: *Measurements of Corona Losses and Interference Levels at the 400 kV Research Station in Mannheim – Rheinau (Germany) with Special Reference to Bundle Conductors*, CIGRÉ Report, No. 402, 1956.

[23] R. Keitley, *et al.*: *Corona Power Loss and Radio Interference Measurement at 400 kV and 750 kV on the Leatherhead Experimental Line*, CIGRÉ Paper, No. 419, 1966.

[24] J.G. Anderson, J.M. Schamberger: *UHV Transmission Research Results from Project UHV*, 1968-1969, CIGRÉ Paper, No. 31-07, August 1970.

[25] M.G. Comber, J.R. Doyle, H.M. Schneider, L.E. Zaffanella: *Three-phase Test Facilities at EPRI's Project UHV.*

[26] R.M. Morris, B. Rakoshdas: *An Investigation of Corona Loss and Radio Interference from Transmission Line Conductors at High Direct Voltages*, IEEE Transactions on Power Apparatus and Systems, vol. 83, pp. 5-16, January 1964.

[27] S.A. Annestrand, G.A. Parks, D.E. Perry: *Bonneville Power Administration's 1200 kV Transmission Line Project*, CIGRÉ Paper, No. 31-09, 1978.

[28] P.S. Maruvada, N.G. Trinh, D. Dallaire, N. Rivest: *Corona Performance of a Conductor Bundle for Bipolar HVDC Transmission at ±750 kV*, IEEE Transactions on Power Apparatus and Systems, vol. 96, pp. 1872-1881, Nov./Dec. 1977.

[29] Y. Sawada, T. Sasano, Y. Sunaga, T. Tsurzura: *The Radio Interference Characteristics of Four and Three-Conductor Bundles of HVDC Line: Shiobara 600 kV Laboratory*, IEEE Transactions on Power Apparatus and Systems, vol. 96, 1901-1907, Nov./Dec. 1977.

[30] E. Bagala, F. Galli, C. Malaguti, L. Paris, M. Sforzini, M. Valtorta: *Italian 1000 kV Project and Related Test Facilities*, CIGRÉ Report 31.16, 1978.

Copyrighted material licensed to BR Demo by Thomson Reuters (Scientific), Inc., subscriptions.techstreet.com, downloaded on Nov-28-2014 by James Madison. No further reproduction or distribution is permitted. Uncontrolled when print

[31] J.J. Clade, C.H. Gary, M.R. Moreau: *Usage and Checking of the Theoretical Relations Between Fields, Currents, and Excitation Functions in Radio Frequencies in the Case of Short Test Lines*, IEEE Transactions on Power Apparatus and Systems, vol. 88, pp. 1501-1511, October 1969.

[32] C.W. Helstrom: *The Spectrum of Corona near a Transmission Line*, AIEE Transactions, Part III (Power Apparatus and Systems), vol. 80, Dec. 1961, pp. 831-837.

[33] C.R. Bond, W.E. Pakala, R.E. Graham, J.E. O'Heill: *Experimental Comparisons of Radio Influence Fields from Short and Long Transmission Lines*, IEEE Transactions on Power Apparatus and Systems, vol. 82, April 1963, pp. 175-185.

[34] Report of Working Group 1 of CIGRÉ Study Committee 36: *Comparison of Radio Noise Prediction Methods with CIGRÉ-IEEE Survey Results*, CIGRÉ-Electra, No. 22, May 1972.

[35] CIGRÉ-IEEE Committee Report: *Comparison of Radio Noise Prediction Methods with CIGRÉ-IEEE Survey Results*, IEEE Transactions on PAS, May/June 1973, vol. 92, pp.1029-1042.

[36] Report by the Swedish National Committee on *Recordings of Radio Interference from a 400 kV Power Line*, TELE (English edition), vol. 26, No. 2, 1974, pp. 14-21, published by the Swedish Telecommunications Administration.

[37] R. Cortina, W. Serravalli, M. Sforzini. *Radio Interference Long-Term Recording on a 420 kV Operating Line*, IEEE Transactions on PAS, vol 89, May/June 1970, pp.881-892.

[38] R. Bartenstein, E. Schafer: *Continuous Measurements of the High Frequency Interference Level of HV Transmission Lines and their Statistical Evaluation*, Paper 409, CIGRÉ, 1962.

[39] *CIGRÉ-IEEE Survey on Extra High Voltage Transmission Radio Noise*, CIGRÉ SC36-WG 01 and IEEE Radio Noise Subcommittee WG01, IEEE Trans PAS, May/June 1973, vol. 92, pp. 1019-1028.

[40] *A Survey of Methods for Calculating Transmission Line Conductor Surface Voltage Gradients*, IEEE Corona and Field Effects Sub-Committee Report, IEEE Transactions on Power Apparatus and Systems, vol. PAS-98, Nov./Dec. 1979, pp. 1996-2014.

[41] L. Paris, M. Sforzini: *RI Problems in HV Line Design*, IEEE Transactions on PAS, April 1968.

[42] *Transmission line reference books, 340 kV and above*, Electric Power Research Institute, 1975.

[43] M.C. Perz: *Propagation analysis of HV currents and voltages on lossy power lines*, IEEE Transactions on PAS, Nov./Dec. 1973.

[44] G.N. Juette, G.M. Roe: *Modal Components in Multiphase Transmission Line Radio Noise Analysis*, IEEE Transactions on PAS, Mar./Apr. 1971.

[45] J. Meyer de Stadelhofen, W. Walter: *Contribution relative à l'estimation du pouvoir radioperturbateur de lignes à très haute tension*, Bulletin Technique PTT, N 11-1957.

[46] W. Serravalli, M. Sforzini: *Il radiodisturbo prodotto di linee ad alta tensione, alcuni risultati di indagini sperimentali*, Rendiconti AEI di Palermo, 1964, Report No. 113.

Copyrighted material licensed to BR Demo by Thomson Reuters (Scientific), Inc., subscriptions.techstreet.com, downloaded on Nov-28-2014 by James Madison. No further reproduction or distribution is permitted. Uncontrolled when print

[47] G.E. Adams, T.W. Liao, M.G. Poland, F.J. Trebby: *Radio noise propagation and attenuation tests on Bonneville Power Administration McNary-Ross 345 kV line*, AIEE Transactions, Part III, vol. 78, June 1959, pp. 380-388.

[48] L.O. Barthold, J.J. La Forest, R.H. Schlomann, F.J. Trebby: *Radio noise attenuation and field factor measurements on the American Electric Power Corporation Breed-Olive 345 kV line*, AIEE Transactions, Part III, vol. 79, June 1960, pp.303-309.

[49] J. Davey, H.L. Deloney, J.J. La Forest: *Effect of station radio noise sources on transmission line noise levels, Experimental results*, IEEE Transactions on PAS, vol. 86, No. 8, August 1967, pp. 1007-1011.

[50] P.B. Barber, J.M. Cranmer, E.M. Dembinski, J.S.T. Looms*: Measurements of acoustic and radio noise from UK transmission lines*, CIGRÉ Report 36-05, 1972.

[51] H. Witt: *Insulation Levels and Corona Phenomena on HVDC Transmission Lines*, Techn Dr dissertation Gothenburg (Sweden) 1961.

[52] E.H. Gehrig, A.C. Peterson, C.F. Clark, T.C. Rednour: *Bonneville Power Administration's 1100 kV direct current test project, Radio Interference and Corona Loss*, IEEE Transactions PAS, vol. 36, No. 3, March 1967.

[53] Stig A. Annestrand: *Radio Interference from HVDC Convertor Stations*, IEEE Transactions on PAS, vol. 91, No. 3, May/June 1972.

[54] G.L. Reiner, E.H. Gehrig: *Celilo-Sylmar ±400 kV line RI Correlation with Short Test Line,* IEEE Transactions on Power Apparatus and Systems, vol. PAS 96, No. 3, May/June 1977.

[55] *Transmission Line Reference Book HV DC TO + 600 kV*, published by Electric Power Research Institute, 3412 Hillview Avenue, Palo Alto, CA 94304.

[56] Jeong-Boo Kim, Dong-Il Lee, Koo-Yong Shin, Hee-Sung Ahn, Kwang-Ho Yang: *Electromagnetic Interference from A Three Phase Double Circuit 765-kV Test Line*, IEEE Transactions on Power Delivery, Vol.14, No.1, January 1999.

[57] Jian Tang, Rong Zeng, Hongbin Ma, Jinliang He, Jie Zhao, Xiaolin Li, and Qi Wang: *Analysis of Electromagnetic Interference on DC Line From Parallel AC Line in Close Proximity*, IEEE Transactions on Power Delivery, Vol.22, No.4, October 2007.

[58] L. Paris, M. Sforzini: *L'isolamento delle linee a 370 kV: criteri di progetto dedotti da una serie di prove comparative*. Rendiconti della LXV Riunione Annuale dell'AEI, Palermo, 1964.

[59] CISPR/TR 18-3:2010, *Radio interference characteristics of overhead power lines and high-voltage equipment – Part 3: Code of practice for minimizing the generation of radio noise*

Copyrighted material licensed to BR Demo by Thomson Reuters (Scientific), Inc., subscriptions.techstreet.com, downloaded on Nov-28-2014 by James Madison. No further reproduction or distribution is permitted. Uncontrolled when print

Copyrighted material licensed to BR Demo by Thomson Reuters (Scientific), Inc., subscriptions.techstreet.com, downloaded on Nov-28-2014 by James Madison. No further reproduction or distribution is permitted. Uncontrolled when print

Copyrighted material licensed to BR Demo by Thomson Reuters (Scientific), Inc., subscriptions.techstreet.com, downloaded on Nov-28-2014 by James Madison. No further reproduction or distribution is permitted. Uncontrolled when print

INTERNATIONAL
ELECTROTECHNICAL
COMMISSION

3, rue de Varembé
PO Box 131
CH-1211 Geneva 20
Switzerland

Tel: + 41 22 919 02 11
Fax: + 41 22 919 03 00
info@iec.ch
www.iec.ch

Copyrighted material licensed to BR Demo by Thomson Reuters (Scientific), Inc., subscriptions.techstreet.com, downloaded on Nov-28-2014 by James Madison. No further reproduction or distribution is permitted. Uncontrolled when print